





Generalised analytical results on n -ejection-collision orbits in the RTBP. Analysis of bifurcations

T. M-Seara , M. Ollé , Ó. Rodríguez*, J. Soler 

Abstract In the planar circular restricted three-body problem and for any value of the mass parameter $\mu \in (0, 1)$ and $n \geq 1$, we prove the existence of four families of n -ejection-collision (n -EC) orbits, that is, orbits where the particle ejects from a primary, reaches n maxima in the (Euclidean) distance with respect to it and finally collides with the primary. Such EC orbits have a value of the Jacobi constant of the form $C = 3\mu + Ln^{2/3}(1 - \mu)^{2/3}$, where $L > 0$ is big enough but independent of μ and n . In order to prove this optimal result, we consider Levi-Civita's transformation to regularize the collision with one primary and a perturbative approach using an ad hoc small parameter once a suitable scale in the configuration plane and time has previously been applied. This result improves a previous work where the existence of the n -EC orbits was stated when the mass parameter $\mu > 0$ was small enough. Moreover, for decreasing values of C , there appear some bifurcations which are first numerically investigated and afterwards explicit expressions for the approximation of the bifurcation values of C are discussed. Finally, a detailed analysis of the existence of n -EC orbits when $\mu \rightarrow 1$ is also described. In a natural way Hill's problem shows up. For this problem, we prove an analytical result on the existence of four families of n -EC orbits and numerically we describe them as well as the appearing bifurcations.

1 Introduction

This paper studies the existence of ejection-collision orbits in the planar circular Restricted three-body problem (RTBP), which describes the motion of a particle (of neglectible mass) under the attraction of two point massive bodies P_1 and P_2 , called primaries, restricted to circular orbits around their common center of mass. Introducing a rotating system of coordinates that rotates with the primaries, and using suitable units of length, time and mass, an autonomous system of four ODEs of first order are derived, depending on a unique parameter $\mu \in (0, 1)$, in such a way that the primaries have masses $1 - \mu$ and μ respectively. Such system of ODEs has the well known Jacobi first integral (equal to C along each solution) and is a regular system everywhere except when the particle collides with each of the primaries.

n -ejection-collision orbits (n -EC orbits from now on) are orbits which eject from a primary reaches n maxima in the distance with respect to it and finally collides with the primary (see Definition 4.a). From a physical point of view, for instance taking the earth and the moon as primaries, we may think of an n -EC orbit as that described by a satellite ejecting from the earth, reaching a maximum distance away from the earth followed by a passage close to the earth, repeating this motion n times and finally landing on earth at the n -th close approach. Since the n -EC orbits are the main target of this paper and collisions between the particle and one primary lead to singularities in the system of ODEs, some kind of regularization, that transforms the original system to a new one which is regular at collisions, is necessary. Among the different possible choices, ranging from local to global regularizations (see [6, 8, 27, 28]) we will use along the paper the (local) Levi-Civita regularization [14], because it is conceptually simple, suitable for our theoretical purposes and efficient for numerical simulations.

*oscar.rodiguez@upc.edu

40 The main analytical result of this paper is Theorem 1, where we prove that there exists an \hat{L} such that
 41 for $L \geq \hat{L}$ and for any value of $\mu \in (0, 1)$, $n \in \mathbb{N}$ and the Jacobi constant $C = 3\mu + Ln^{2/3}(1 - \mu)^{2/3}$,
 42 there exist four n -EC orbits, and we characterize them.

43 This improves a recent result (see [21]) where the existence of four n -EC orbits ejecting (and colliding)
 44 from the *big* primary (of mass $1 - \mu$) is proved but only for small enough $\mu > 0$.

45 To prove this main result we first consider a weaker version in Theorem 2 where we show that
 46 for all $n \in \mathbb{N}$, there exists a $\hat{K}(n)$ such that for $K \geq \hat{K}(n)$ and for any value of $\mu \in (0, 1)$ and
 47 $C = 3\mu + K(1 - \mu)^{2/3}$, there exist four n -EC orbits. This weaker version also improves the result of [21]
 48 since we cover *any* value of μ so we can eject from (and collide with) any of the primaries, irrespective
 49 of its mass. Another improvement is the proof's approach. In the previous paper a perturbative
 50 approach for small enough $\mu > 0$ and big enough C was considered. There, the authors computed the
 51 series expansion, with respect to the mass parameter μ , of the ejection (collision) manifold. So the
 52 explicit analytical expansion, up to certain order, of this manifold integrated up to a suitable Poincaré
 53 section Σ (maximum distance to the ejecting primary) was obtained. For suitable number of crossings
 54 with Σ , i for the ejection manifold and j for the collision one (with $i + j = n + 1$), the resulting two
 55 curves C_i^+ and C_j^- were computed. Achieving such curves required some technicalities, in particular,
 56 the computation of terms up to order 9 (at least) in such expansions and the expressions of them in
 57 the usual polar coordinates (instead of the initial angle θ_0). The application of the Implicit Function
 58 Theorem (IFT) to analyze the intersection of both curves gave rise to the existence of four n -EC orbits
 59 for any n , C big enough and $\mu > 0$ small enough.

60 In this paper, the perturbative approach considers a suitable small parameter, related with the inverse
 61 of the Jacobi constant, regardless of the value of μ . Moreover, instead of computing the *two* curves
 62 C_i^+ and C_j^- , we consider the angular momentum at the n -th passage with the minimum distance to
 63 the primary (the particle ejected from). We characterize an n -EC orbit by the zero value of that
 64 angular momentum. This strategy to use the angular momentum simplifies the computations in three
 65 directions: first only expansions up to order 6 are required, second obtaining just one function instead
 66 of two different curves, and third the parametrization of the angular momentum directly in terms of
 67 θ_0 (thus avoiding the technical issue of the transformation to usual polar coordinates).

68 The second part of the paper focuses on the bifurcations that may appear when doing the continuation
 69 of families of n -EC orbits. It is clear that, given any value of $\mu > 0$, and fixed n , we can continue
 70 the four families of n -EC orbits for C big enough, from the IFT. According to previous papers ([22,
 71 21]) we will name such families as α_n , β_n , δ_n and γ_n . However, as long as C decreases, the IFT does
 72 not apply and bifurcations may appear for suitable values of C . We analyze such bifurcations from
 73 the analytical expressions obtained in the series expansions for order higher than 6. A rich variety of
 74 bifurcations show up. They are discussed and numerically described.

75 Precisely the results derived from this numerical exploration provides inspiration to obtain the main
 76 result: an explicit expression of the bifurcating value of C as $\hat{C} = 3\mu + \hat{L}n^{2/3}(1 - \mu)^{2/3}$, i.e. we prove
 77 that $\hat{K}(n) = \hat{L}n^{2/3}$.

78 Finally, taking $\mu \rightarrow 1$ gives rise to the Hill problem. Quite naturally the same kind of proof developed
 79 previously applies to the Hill problem. So as a corollary we obtain an analytical result that establishes
 80 the existence of four families of n -EC in this problem. Moreover the existence of the successive
 81 bifurcations when decreasing C for all $n \in [1, 100]$ are also numerically discussed.

82 Concerning previous published results on this subject for the circular planar RTBP, we distinguish
 83 between analytical and numerical results. Focusing on the theoretical analysis of n -EC orbits, only
 84 the case for $n = 1$ is considered in Llibre [15], Chenciner and Llibre [5] and Lacomba and Llibre [13].
 85 The general case $n \geq 1$ is studied in [21], but for small enough values of $\mu > 0$. Regarding a numerical
 86 approach, and for $n = 1$, we mention the papers by Bozis [2], Hénon [9, 10], where the authors
 87 compute some particular EC orbits that naturally appear when doing the continuation of families of

88 periodic orbits. For the general case $n \geq 1$, we mention Ollé, Rodriguez and Soler papers [22, 23],
 89 where the authors compute and analyze the continuation of families of n -EC orbits for $n = 1, \dots, 25$
 90 and discuss the advantages and disadvantages of Levi-Civita's versus McGehee's [16] regularization.
 91 Very recently, Ollé, Rodriguez and Soler [24] analyze the global behavior of the whole set of ejection
 92 orbits and the dynamical consequences resulting from the interaction between ejection orbits and the
 93 Lyapunov periodic orbit around the collinear equilibrium point L_1 . In particular infinitely many (in a
 94 chaotic way) EC orbits show up. Finally we mention a recent preprint that studies ejection-collision
 95 orbits between the two primaries [4].

96 We remark that the EC orbits appear quite naturally in astronomical applications. Let us mention
 97 that EC orbits allow to explain a mechanism of transfer of mass in binary star systems (see [11, 17, 26,
 98 29]), to describe regions of capture of irregular moons by giant planets ([1]) or to discuss temporary
 99 capture ([25]). Other applications include the probability of crash motion (see [18, 19]) or the role of
 100 ejection orbits to explain a mechanism for ionization in atomic problems (see [3, 20]).

101 The paper is organized as follows: In Section 2 we recall some basics of the RTBP, we introduce
 102 the Levi-Civita coordinates and the new normalized variables that will become useful to prove the
 103 existence of the n -EC orbits for any value of $\mu > 0$. Section 3 recalls the topics described in Section
 104 2 but for the Hill problem. In Section 4 we state the two main theorems, Theorem 1 and Theorem 2,
 105 concerning the existence of n -EC orbits in the RTBP. We provide the analytical proof of Theorem 2
 106 in Section 5. Section 6 is devoted to numerically analyse the bifurcations of families of n -EC orbits
 107 in the RTBP. In Section 7 we provide the analytical proof of Theorem 1. Section 8 is devoted to the
 108 Hill problem.

109 Finally, we observe that all the numerical computations have been done using double precision and the
 110 numerical integration of the systems of ODE rely on an own implemented Runge-Kutta (7)8 integrator
 111 with an adaptive step size control described in [7] and a Taylor method implemented on a robust, fast
 112 and accurate software package in [12]. The absolute and relative tolerances used with the numerical
 113 integrators are 10^{-16} and the tolerances used in the Newton methods are in the range 10^{-15} to 10^{-14} .

114 2 The planar RTBP and the Levi Civita regularization

115 As mentioned in the Introduction, we consider the RTPB. In the rotating (synodical) system, the
 116 primaries with mass $1 - \mu$ and μ , $\mu \in (0, 1)$, have positions $P_1 = (\mu, 0)$ and $P_2 = (\mu - 1, 0)$ respectively,
 117 and the period of their motion will be 2π . In such context, the equations of motion for the particle in
 118 the rotating system are given by

$$\begin{cases} \ddot{x} - 2\dot{y} = \Omega_x(x, y), \\ \ddot{y} + 2\dot{x} = \Omega_y(x, y), \end{cases} \quad (1)$$

119 where $\dot{} = d/dt$ and

$$\begin{aligned} \Omega(x, y) &= \frac{1}{2}(x^2 + y^2) + \frac{1 - \mu}{\sqrt{(x - \mu)^2 + y^2}} + \frac{\mu}{\sqrt{(x - \mu + 1)^2 + y^2}} + \frac{1}{2}\mu(1 - \mu) \\ &= \frac{1}{2} [(1 - \mu)r_1^2 + \mu r_2^2] + \frac{1 - \mu}{r_1} + \frac{\mu}{r_2}, \end{aligned} \quad (2)$$

120 with $r_1 = \sqrt{(x - \mu)^2 + y^2}$ and $r_2 = \sqrt{(x - \mu + 1)^2 + y^2}$. So, the equations become singular when r_1
 121 or $r_2 \rightarrow 0$.

122 The main properties of this system used later on are the following (see [28] for details):

123 1. There exists a first integral, defined by

$$C = 2\Omega(x, y) - \dot{x}^2 - \dot{y}^2, \quad (3)$$

124 and known as Jacobi integral.

125 2. System (1) has the symmetry

$$(t, x, y, \dot{x}, \dot{y}) \rightarrow (-t, x, -y, -\dot{x}, \dot{y}). \quad (4)$$

126 A geometrical interpretation of it is that given an orbit in the configuration space (x, y) , the
127 symmetrical orbit with respect to the x axis will also exist.

128 3. The simplest solutions are 5 equilibrium points: the so called collinear ones L_i , $i = 1, 2, 3$, and
129 the triangular ones L_i , $i = 4, 5$. On the plane (x, y) , $L_{1,2,3}$ are located on the x axis, with
130 $x_{L_2} < \mu - 1 < x_{L_1} < \mu < x_{L_3}$ and $L_{4,5}$ forming an equilateral triangle with the primaries. C_{L_i}
131 will stand for the value of C at L_i , $i = 1, \dots, 5$.

132 4. Depending on the value of the Jacobi constant C , the particle can move on specific regions of
133 the plane (x, y) , called Hill regions and defined by

$$\mathcal{R}(C) = \{(x, y) \in \mathbb{R}^2 \mid 2\Omega(x, y) \geq C\}. \quad (5)$$

134 In order to deal with the singularity of the primary $P_1 = (\mu, 0)$ ($r_1 = 0$) we will consider the Levi-Civita
135 regularization (see [28]). The well known transformation of coordinates and time is given by:

$$\begin{cases} x = \mu + u^2 - v^2, \\ y = 2uv, \\ \frac{dt}{ds} = 4(u^2 + v^2), \end{cases}$$

136 and we remark that, taking $\mu \in (0, 1)$ we are regularizing the big primary (if $\mu \in (0, 1/2]$) or the
137 small one (if $\mu \in [1/2, 1)$). In this new system of coordinates, the solutions of system (1) with Jacobi
138 constant equal to C satisfy:

$$\begin{cases} u'' - 8(u^2 + v^2)v' = (4\mathcal{U}(u^2 + v^2))_u \\ \quad = 4\mu u + 16\mu u^3 + 12(u^2 + v^2)^2 u + \frac{8\mu u}{r_2} - \frac{8\mu u(u^2 + v^2)(u^2 + v^2 + 1)}{r_2^3} - 4Cu, \\ v'' + 8(u^2 + v^2)u' = (4\mathcal{U}(u^2 + v^2))_v \\ \quad = 4\mu v - 16\mu v^3 + 12(u^2 + v^2)^2 v + \frac{8\mu v}{r_2} - \frac{8\mu v(u^2 + v^2)(u^2 + v^2 - 1)}{r_2^3} - 4Cv, \\ C' = 0 \end{cases} \quad (6)$$

139 where $' = d/ds$, Ω_x and Ω_y are the partial derivatives with respect to x and y respectively and

$$\mathcal{U} = \frac{1}{2} \left[(1 - \mu)(u^2 + v^2)^2 + \mu((1 + u^2 - v^2)^2 + 4u^2v^2) \right] + \frac{1 - \mu}{u^2 + v^2} + \frac{\mu}{r_2} - \frac{C}{2}.$$

140 with $r_2 = \sqrt{(1 + u^2 - v^2)^2 + 4u^2v^2}$.

141 The system of ODEs is now regular everywhere except at the collision with the primary P_2 ($r_2 = 0$).

142 We observe that when studying the system of ODEs (6), a value of a Jacobi constant C is fixed. Thus
143 to take an initial condition of this system, we will take $(u(0), v(0), u'(0), v'(0), C(0))$. Nevertheless,
144 along the paper, we will actually study system (6) removing the last equation in C , and we will consider
145 the corresponding solution for a fixed C and initial condition simply given by $(u(0), v(0), u'(0), v'(0))$.

146 In this new system of variables, the previous properties of the RTBP are translated as:

147 1. Jacobi Integral:

$$u'^2 + v'^2 = 8(u^2 + v^2)\mathcal{U}, \quad (7)$$

148 which is regular at the collision with the primary P_1 . In particular (see [28]), the velocity at the
149 position of the first primary ($u = 0, v = 0$) satisfies:

$$u'^2 + v'^2 = 8(1 - \mu), \quad (8)$$

and therefore the velocities at the collision lie in a circle of radius $\sqrt{8(1 - \mu)}$.

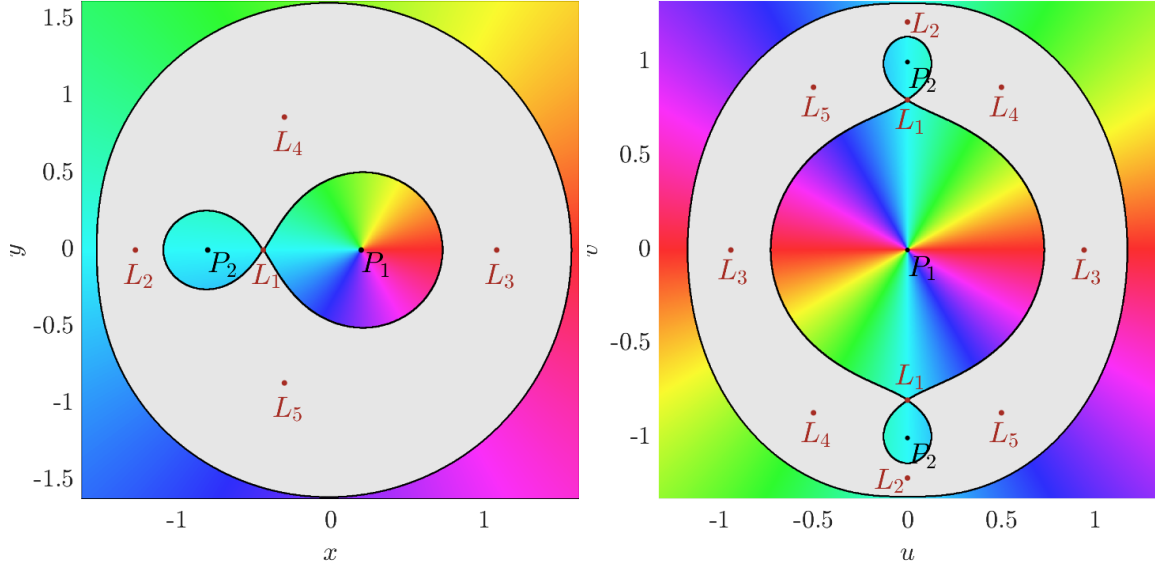


Figure 1: Levi-Civita transformation. Hill's region for $\mu = 0.2$ and C_{L_1} . Left. Synodic (x, y) coordinates. Right. Levi-Civita ones (u, v) . The gradient of colours represents the angle with respect to the position of the first primary in the original (x, y) synodical coordinates. In grey the forbidden region.

150

2. As the Levi-Civita transformation duplicates the configuration space (see Figure 1) the equations of motion satisfy two symmetries, (9a) as a consequence of the duplication of space and (9b) due to (4):

$$(s, u, v, u', v') \rightarrow (-s, u, -v, -u', v'), \quad (9a)$$

$$(s, u, v, u', v') \rightarrow (-s, -u, v, u', -v'). \quad (9b)$$

151 3. The equilibrium points are now duplicated and they are located on the plane (u, v) . In particular,
152 the collinear points now are located in the u axis and in the v axis. See Figure 1.

153 4. Similarly, given a value of the Jacobi constant C , the Hill's region in variables (u, v) now becomes

$$\mathcal{R}(C) = \{(u, v) \in \mathbb{R}^2 \mid (u^2 + v^2)\mathcal{U} \geq 0\}. \quad (10)$$

154 In particular we will consider values of the Jacobi constant $C \geq C_{L_1}$, the value of the Jacobi
155 constant associated to the equilibrium point L_1 . In this way, it will be enough to regularize only
156 the position of P_1 because the Hill's region associated to these values of C avoids collisions with
157 the second primary (assuming the particle moves in a neighbourhood of P_1), see Figure 1).

3 The Hill problem and the Levi-Civita regularization

The *Hill problem* is a simplified limiting case of the RTBP that allows to study the vicinity of the small primary when this mass tends to 0 (when mass parameter μ is very small or very close to 1). We can obtain easily the equation of Hill problem making a translation of the small primary (denoted by P_h) to the origin, and rescaling the coordinates by a factor $\mu^{1/3}$ if $\mu \rightarrow 0$ or $(1 - \mu)^{1/3}$ if $\mu \rightarrow 1$.

For our purpose we will consider this second case, so the first step is to introduce new variables (x_h, y_h) defined by the relation

$$x = \mu + (1 - \mu)^{1/3}x_h, \quad y = (1 - \mu)^{1/3}y_h.$$

In this way the expression (2) becomes

$$\frac{1}{(1 - \mu)^{2/3}} \left(\Omega(x, y) - \frac{3}{2} \right) = \frac{3}{2}x_h^2 + \frac{1}{\sqrt{x_h^2 + y_h^2}} + \mathcal{O}\left((1 - \mu)^{1/3}\right), \quad (11)$$

and taking the limit $\mu \rightarrow 1$ we obtain the Hill's potential

$$\Psi(x_h, y_h) = \frac{3}{2}x_h^2 + \frac{1}{\sqrt{x_h^2 + y_h^2}}. \quad (12)$$

Thus the equations of motion are given by

$$\begin{cases} \ddot{x}_h - 2\dot{y}_h = \Psi_{x_h}(x_h, y_h), \\ \ddot{y}_h + 2\dot{x}_h = \Psi_{y_h}(x_h, y_h). \end{cases} \quad (13)$$

The Hill problem also has some interesting properties for our purposes:

1. The system (13) has a first integral defined by

$$K = 2\Psi(x_h, y_h) - \dot{x}_h^2 - \dot{y}_h^2, \quad (14)$$

where K is related with the Jacobi integral by:

$$C = 3\mu + (1 - \mu)^{2/3}K + \mathcal{O}(1 - \mu). \quad (15)$$

2. The equations (13) not only inherit the symmetry of the problem, that is a symmetry with respect to the x_h -axis, but also has an extra one with respect to the y_h -axis. In this way the system (13) has the symmetries:

$$(t, x_h, y_h, \dot{x}_h, \dot{y}_h) \rightarrow (-t, x_h, -y_h, -\dot{x}_h, \dot{y}_h), \quad (16a)$$

$$(t, x_h, y_h, \dot{x}_h, \dot{y}_h) \rightarrow (-t, -x_h, y_h, \dot{x}_h, -\dot{y}_h). \quad (16b)$$

3. The Hill problem only preserves two equilibrium points, which are those that are in the vicinity of the small primary P_h . That is L_1 and L_2 if we consider $\mu \rightarrow 0$ or L_1 and L_3 if $\mu \rightarrow 1$. For historical consistency, we will call these equilibrium points L_1 and L_2 , which have positions $(\pm 1/3^{1/3}, 0)$ (see Figure 2) and we will denote by $K_L = 3^{4/3}$ the value of K at L_1 and L_2 .
4. In a similar way, from the first integral and taking into account that $2\Psi(x_h, y_h) - K \geq 0$, given a value of K , the motion can only take place in the Hill's region defined by

$$\mathcal{R}_h(K) = \{(x_h, y_h) \in \mathbb{R}^2 \mid 2\Psi(x_h, y_h) \geq K\}. \quad (17)$$

We notice that, similarly as we do in the RTBP, we will consider values of $K \geq K_L$ to guarantee that if the particle starts in a region around P_h , it will always remain there.

179 In order to regularize the Hill problem we only have to consider the Levi-Civita regularization

$$\begin{cases} x_h = u_h^2 - v_h^2, \\ y_h = 2u_h v_h, \\ \frac{dt}{ds} = 4(u_h^2 + v_h^2), \end{cases}$$

180 and the system (13) becomes:

$$\begin{cases} u_h'' - 8(u_h^2 + v_h^2)v_h' = (4\mathcal{U}_h(u_h^2 + v_h^2))_{u_h} \\ \quad = -4K u_h + 12(2(u_h^4 - 2u_h^2 v_h^2 - v_h^4) + (u_h^2 + v_h^2)^2) u_h, \\ v_h'' + 8(u_h^2 + v_h^2)u_h' = (4\mathcal{U}_h(u_h^2 + v_h^2))_{v_h} \\ \quad = -4K v_h + 12(2(v_h^4 - 2u_h^2 v_h^2 - u_h^4) + (u_h^2 + v_h^2)^2) v_h, \end{cases} \quad (18)$$

181 with

$$\mathcal{U}_h = \frac{3(u_h^2 - v_h^2)^2}{2} + \frac{1}{u_h^2 + v_h^2} - \frac{K}{2}. \quad (19)$$

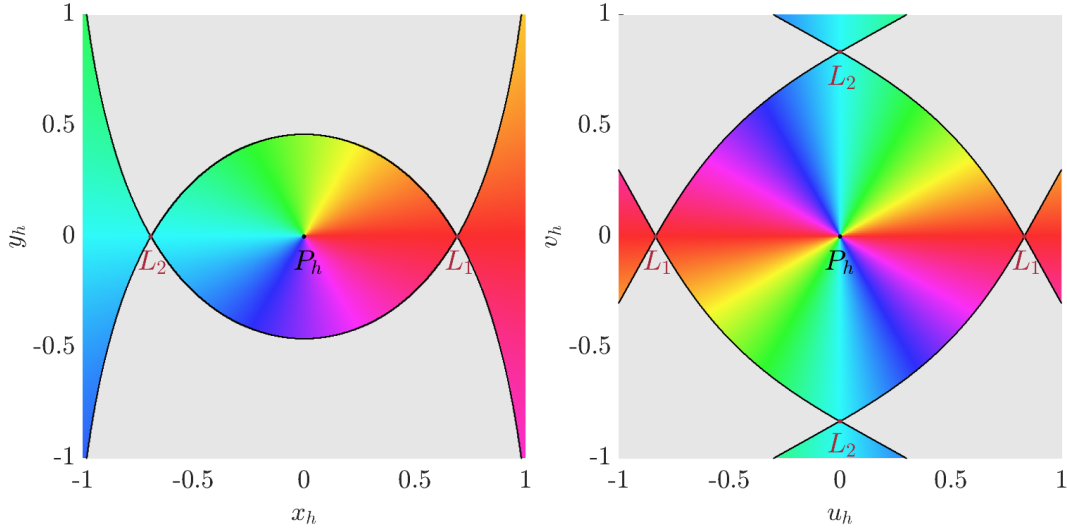


Figure 2: Levi-Civita transformation. Hill's region for $K = K_L = 3^{4/3}$. Left. Synodic (x_h, y_h) coordinates. Right. Levi-Civita ones (u_h, v_h) . The gradient of colours represents the angle with respect to the position of the first primary in the original (x_h, y_h) synodical coordinates. In grey the forbidden region.

182 Under this transformation the previous properties of the Hill problem are translated as:

183 1. The first integral of (18) is given by

$$u_h'^2 + v_h'^2 = 8(u_h^2 + v_h^2)\mathcal{U}_h, \quad (20)$$

184 which is regular at the collision with P_h . In particular the velocity at the position of the primary
185 $(u_h = 0, v_h = 0)$ satisfies

$$u_h'^2 + v_h'^2 = 8. \quad (21)$$

2. As the transformation duplicates the configuration space (see Figure 2), the equation (18) has an extra symmetry:

$$(s, u_h, v_h, u_h', v_h') \rightarrow (-s, u_h, -v_h, -u_h', v_h'), \quad (22a)$$

$$(s, u_h, v_h, u_h', v_h') \rightarrow (-s, -u_h, v_h, u_h', -v_h'), \quad (22b)$$

$$(s, u_h, v_h, u_h', v_h') \rightarrow (-s, v_h, u_h, -v_h', -u_h'). \quad (22c)$$

- 186 3. For the same reason, the equilibrium points are duplicated, and we have $L_1 = (\pm 3^{-1/6}, 0)$ and
187 $L_2 = (0, \pm 3^{-1/6})$.
- 188 4. In a similar way, depending on the value of K we can define the valid region of motion (see
189 Figure 2) in the plane (u_h, v_h) as:

$$\mathcal{R}(K) = \{(u_h, v_h) \in \mathbb{R}^2 \mid (u_h^2 + v_h^2)\mathcal{U}_h \geq 0\}. \quad (23)$$

190 4 n -EC orbits in the RTBP and main theorems

191 In this paper we will focus on a specific type of EC orbits, the n -EC orbits, formally defined as

192 **Definition 4.a.** *We call n -ejection-collision orbit of a primary, simply noted by n -EC orbit, to the*
193 *orbit that the particle describes when ejects from a primary and reaches n times a relative maximum*
194 *in the distance with respect to this primary before colliding with it.*

195 As we will consider any value of $\mu \in (0, 1)$ we will study only the n -EC orbits associated to the first
196 primary P_1 . Notice that from relation (8) it is easy to compute the initial conditions of the ejection
197 orbits (and the collision orbits):

$$(0, 0, 2\sqrt{2(1-\mu)} \cos \theta_0, 2\sqrt{2(1-\mu)} \sin \theta_0), \quad \theta_0 \in [0, 2\pi) \quad (24)$$

198 and we can compute the manifold of the ejection (collision) orbits integrating forward (backward) in
199 time. Observe that in this case it is enough to consider a value of $\theta_0 \in [0, \pi)$ due to the duplication
200 of the configuration plane.

201 **Remark.** In general the n -EC orbits are not periodic or part of a periodic orbit. The angle of ejection
202 θ_0 is usually different than the collision θ_f . However, it can happen that some n -EC orbits are periodic
203 (or part of a periodic orbit) as we will see below.

204 Concerning the existence of n -EC orbits, we mentioned above that in [21], the existence of four n -EC
205 orbits ejecting from (and colliding with) the big primary for any $n \geq 1$, given C big enough and $\mu > 0$
206 small enough, was proved. The proof was based on a perturbative approach in μ and assuming that
207 the orbits ejected from the big primary of mass $1 - \mu$.

208 The first goal of this paper is to improve this previous result and prove the existence of four n -EC
209 orbits ejecting from (and colliding with) the big or small primary, for any $n \geq 1$ given and C big
210 enough. So any value of the mass parameter $\mu \in (0, 1)$ is possible in this context.

211 For analytical and numerical purposes, though, we will use a characterization for an EC orbit, based
212 upon the zero value of its angular momentum, defined from now on as $M := U\dot{V} - V\dot{U}$ (for some
213 suitable variables (U, V) to be defined later), at a minimum distance with the primary the particle
214 ejected from (see Lemma 1 below). So in order to obtain an n -EC orbit, for $n \geq 1$, $\mu \in (0, 1)$ and C
215 given, first we will compute the corresponding ejection solution for each initial condition (that is, for
216 each value θ_0). Second we will determine the precise time $\tau^* = \tau^*(\theta_0)$ when the particle reaches the
217 n -th minimum in the distance to P_1 . At time τ^* we will compute the value of the angular momentum
218 that is, $(U\dot{V} - V\dot{U})(\tau^*)$. Varying $\theta_0 \in [0, \pi)$ we will obtain the corresponding angular momentum,
219 that will denote by $M(n, \theta_0) = (U\dot{V} - V\dot{U})(\tau^*)$ (overlooking the additional dependence on μ). The
220 zeros of $M(n, \theta_0) = 0$ will provide us with the precise values of θ_0 such that the corresponding ejection
221 orbit is precisely an n -EC orbit. Just to show this idea, we plot in Figure 3 left the behaviour of the
222 angular momentum $M(1, \theta_0)$ for $\mu = 0.1$ and $C = 5$. In the right figure we plot the corresponding
223 ejection orbits for three chosen values of θ_0 : the red one and green one plotted for a range of time
224 $[0, \tau^* + \delta]$ (a small suitable $\delta > 0$) to see the change of sign in the angular momentum (shown in the
225 zoom area) and the blue one which is a 1-EC orbit.

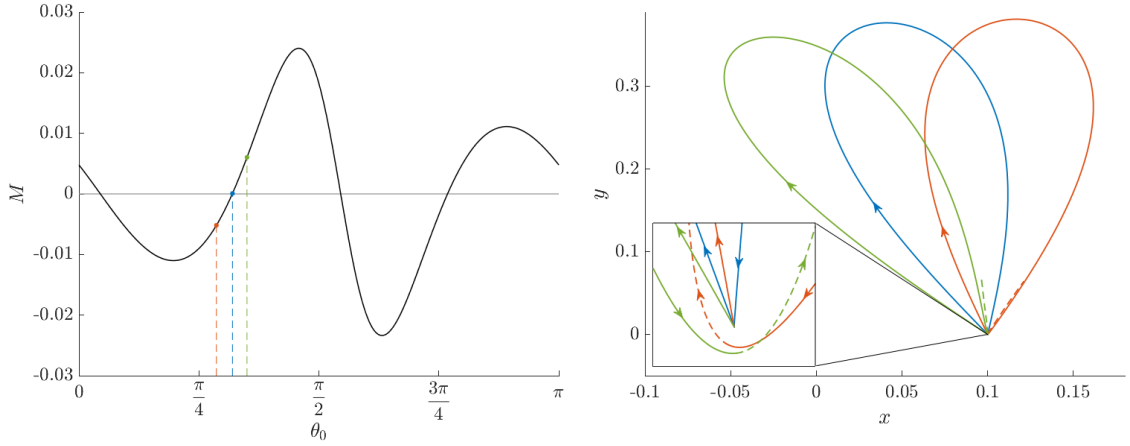


Figure 3: $n = 1$, $\mu = 0.1$ and $C = 5$. Left. Angular momentum $M(1, \theta_0)$. Right. Three ejection orbits corresponding to the initial values of θ_0 labelled in colours on the left plot. The blue orbit is precisely a 1-EC orbit.

226 Now, we proceed to state the main result of this paper about the existence, the number and the
 227 characteristics of the n -ejection-collision orbits for any value of the mass parameter and $n \in \mathbb{N}$, for
 228 sufficiently restricted Hill regions (i.e. C big enough).

229 **Theorem 1.** *There exists an \hat{L} such that for $L \geq \hat{L}$ and for any value of $\mu \in (0, 1)$, $n \in \mathbb{N}$ and*
 230 *$C = 3\mu + Ln^{2/3}(1 - \mu)^{2/3}$, there exist four n -EC orbits, which can be characterized by:*

- 231 • *Two n -EC orbits symmetric with respect to the x axis.*
- 232 • *Two n -EC orbits, one symmetric of the other with respect to the x axis.*

233 In order to prove Theorem 1 we will first state a weaker version of this theorem, Theorem 2, but
 234 the proof of this second version will provide light on the approach, mainly a suitable scaling in the
 235 configuration variables, time and the Jacobi constant C , used to prove the more optimal result in
 236 Theorem 1.

237 **Theorem 2.** *For all $n \in \mathbb{N}$, there exists a $\hat{K}(n)$ such that for $K \geq \hat{K}(n)$ and for any value of*
 238 *$\mu \in (0, 1)$ and $C = 3\mu + K(1 - \mu)^{2/3}$, there exist four n -EC orbits, which can be characterized in the*
 239 *same way as in Theorem 1.*

240 We remark that, in Theorem 2, we have a uniform constant $K = K(n)$ for any value of $\mu \in (0, 1)$.
 241 This implies that when $\mu \rightarrow 1$ the value of the Jacobi constant (for which Theorem 2 holds) tends
 242 to 3, as C_{L_1} does as well. Precisely, and as shown in the proof of Theorem 2, the expansion of C_{L_1}
 243 was the inspiration to choose a suitable scaling in the variables, time and C . Finally in Theorem 1 an
 244 expression for $K(n)$ as $Ln^{2/3}$ is provided.

5 Proof of Theorem 2

In order to prove Theorem 2, let us fix $C \geq C_{L_1}$ and consider the following change of variables and time:

$$\begin{cases} u = \sqrt{\frac{2(1-\mu)}{C-3\mu}}U, \\ v = \sqrt{\frac{2(1-\mu)}{C-3\mu}}V, \\ \tau = 2\sqrt{C-3\mu}s, \end{cases} \quad (25)$$

that corresponds to the change that normalizes the linear term of (6) and the initial condition of the ejection orbits. Denoting by $\dot{} = \frac{d}{d\tau}$ the new time derivative the system (6) transforms to the following:

$$\begin{cases} \ddot{U} = -\frac{(C-\mu)U}{C-3\mu} + \frac{8(1-\mu)(U^2+V^2)\dot{V}}{(C-3\mu)^{3/2}} + \frac{12(1-\mu)^2(U^2+V^2)^2U}{(C-3\mu)^3} + \frac{8\mu(1-\mu)U^3}{(C-3\mu)^2} \\ \quad + \frac{2\mu U}{(C-3\mu)R_2} - \frac{4\mu(1-\mu)U(U^2+V^2)[2(1-\mu)(U^2+V^2) + (C-3\mu)]}{(C-3\mu)^3R_2^3}, \\ \ddot{V} = -\frac{(C-\mu)V}{C-3\mu} - \frac{8(1-\mu)(U^2+V^2)\dot{U}}{(C-3\mu)^{3/2}} + \frac{12(1-\mu)^2(U^2+V^2)^2V}{(C-3\mu)^3} - \frac{8\mu(1-\mu)V^3}{(C-3\mu)^2} \\ \quad + \frac{2\mu V}{(C-3\mu)R_2} - \frac{4\mu(1-\mu)V(U^2+V^2)[2(1-\mu)(U^2+V^2) - (C-3\mu)]}{(C-3\mu)^3R_2^3}, \end{cases} \quad (26)$$

where $R_2 = \sqrt{1 + \frac{4(1-\mu)(U^2-V^2)}{C-3\mu} + \frac{4(1-\mu)^2(U^2+V^2)^2}{(C-3\mu)^2}}$.

It is important to remark that the properties (7), (8), (10) are preserved (translated to the new variables), and so are the symmetries obtained in the Levi-Civita regularization, i. e.:

$$(\tau, U, V, \dot{U}, \dot{V}) \rightarrow (\tau, -U, -V, -\dot{U}, -\dot{V}), \quad (27a)$$

$$(\tau, U, V, \dot{U}, \dot{V}) \rightarrow (-\tau, -U, V, \dot{U}, -\dot{V}). \quad (27b)$$

At this point, the two main ideas to prove the theorem are: (i) a perturbative approach taking $\delta = 1/\sqrt{C-3\mu}$ as a small parameter, and (ii) the requirement of the angular momentum to be zero at a minimum distance with the primary the particle ejected from.

First of all we observe that the functions $1/R_2$ and $1/R_2^3$ are analytic for U, V bounded, $0 \leq \mu \leq 1$, and δ small enough. In fact, the expansions of $1/R_2$ and $1/R_2^3$ are of the form:

$$\begin{aligned} \frac{1}{R_2} &= 1 - 2(1-\mu)(U^2 - V^2)\delta^2 + 8(1-\mu)^2(11(U^2 - V^2)^2 - 4U^2V^2)\delta^4 + \sum_{k \geq 3} (1-\mu)^k P_{2k}(U, V)\delta^{2k}, \\ \frac{1}{R_2^3} &= 1 - 6(1-\mu)(U^2 - V^2)\delta^2 + \sum_{k \geq 2} (1-\mu)^k Q_{2k}(U, V)\delta^{2k}, \end{aligned} \quad (28)$$

where $P_{2k}(U, V)$ and $Q_{2k}(U, V)$ are polynomials sum of monomials of degree $2k$.

257 So if we expand the system (26) with respect to δ we obtain:

$$\left\{ \begin{array}{l} \ddot{U} = -U + 8(1-\mu)(U^2 + V^2)\dot{V}\delta^3 + 12(1-\mu)^2 [2\mu(U^4 - 2U^2V^2 - V^4) + (U^2 + V^2)^2] U\delta^6 \\ \quad + \mu \sum_{k \geq 4} (1-\mu)^{k-1} \bar{P}_{2k-1}(U, V)\delta^{2k}, \\ \ddot{V} = -V - 8(1-\mu)(U^2 + V^2)\dot{U}\delta^3 + 12(1-\mu)^2 [2\mu(V^4 - 2U^2V^2 - U^4) + (U^2 + V^2)^2] V\delta^6 \\ \quad + \mu \sum_{k \geq 4} (1-\mu)^{k-1} \bar{Q}_{2k-1}(U, V)\delta^{2k}, \end{array} \right. \quad (29)$$

258 which is an analytical system of ODEs in δ and $\bar{P}_{2k-1}(U, V)$ and $\bar{Q}_{2k-1}(U, V)$ are polynomials sum of
259 monomials of degree $2k - 1$.

260 Before proceeding it is important to make two observations:

261 1. We can introduce the parameter $\varepsilon = (1-\mu)^{1/3}\delta$. So we have, using that $\delta = \frac{1}{\sqrt{C-3\mu}}$:

$$\varepsilon^2 = (1-\mu)^{2/3}\delta^2 = \frac{(1-\mu)^{2/3}}{C-3\mu}. \quad (30)$$

262 2. We also know that $C \geq C_{L_1}(\mu)$ since otherwise the Hill region of motion allows transits between
263 both primaries and, in this sense, Hill's region is not regular anymore. As it is well known the
264 expansion of $C_{L_1}(\mu)$ is (see [28])

$$C_{L_1}(\mu) = 3 + 9 \left(\frac{1-\mu}{3} \right)^{2/3} - 7 \frac{1-\mu}{3} + \mathcal{O}((1-\mu)^{4/3}), \quad (31)$$

265 therefore, we would like to have a uniform parameter K in order to express the value of the
266 Jacobi Constant C with the same order in $(1-\mu)$ as $C_{L_1}(\mu)$. So, introducing the variable K as

$$C = 3\mu + K(1-\mu)^{2/3}, \quad (32)$$

267 we have that the previous expression (30) becomes:

$$\varepsilon^2 = \frac{1}{K}.$$

268 The change (25) using (32) becomes:

$$\left\{ \begin{array}{l} u = \frac{\sqrt{2}(1-\mu)^{1/6}}{\sqrt{K}} U, \\ v = \frac{\sqrt{2}(1-\mu)^{1/6}}{\sqrt{K}} V, \\ \tau = 2\sqrt{K}(1-\mu)^{1/3} s, \\ C = 3\mu + K(1-\mu)^{2/3}. \end{array} \right. \quad (33)$$

269 Note that the value K is related with the Hill constant by (15) when μ tends to 1.

270 So, in terms of $\varepsilon = 1/\sqrt{K}$ the system (29) has the following expression:

$$\left\{ \begin{array}{l} \ddot{U} = -U + 8(U^2 + V^2)\dot{V}\varepsilon^3 + 12 [2\mu(U^4 - 2U^2V^2 - V^4) + (U^2 + V^2)^2] U\varepsilon^6 \\ \quad + \mu \sum_{k \geq 4} (1 - \mu)^{\frac{k-3}{3}} \bar{P}_{2k-1}(U, V)\varepsilon^{2k}, \\ \ddot{V} = -V - 8(U^2 + V^2)\dot{U}\varepsilon^3 + 12 [2\mu(V^4 - 2U^2V^2 - U^4) + (U^2 + V^2)^2] V\varepsilon^6 \\ \quad + \mu \sum_{k \geq 4} (1 - \mu)^{\frac{k-3}{3}} \bar{Q}_{2k-1}(U, V)\varepsilon^{2k}. \end{array} \right. \quad (34)$$

271 Second let us prove the following characterization for an EC orbit, based upon the zero value of the
272 angular momentum at a minimum distance with the primary.

273 **Lemma 1.** *Assume C large enough. An ejection orbit is an EC orbit if and only if it satisfies that*
274 *at a minimum in the distance (with the primary) the angular momentum $M = U\dot{V} - V\dot{U} = 0$.*

275 *Proof.* The minimum distance condition is given by:

$$\begin{aligned} U\dot{U} + V\dot{V} &= 0, \\ U\ddot{U} + \dot{U}^2 + V\ddot{V} + \dot{V}^2 &> 0, \end{aligned} \quad (35)$$

276 and the angular momentum condition $M = U\dot{V} - V\dot{U} = 0$:

$$U\dot{V} = V\dot{U}. \quad (36)$$

277 We will distinguish between two cases:

278 1. $\dot{V} \neq 0$. Then, from (36):

$$U = \frac{V\dot{U}}{\dot{V}} \quad \text{and by (35)} \implies \frac{V\dot{U}}{\dot{V}}\dot{U} + V\dot{V} = 0 \implies V\dot{U}^2 + V\dot{V}^2 = V(\dot{U}^2 + \dot{V}^2) = 0 \implies V = 0,$$

279 and, by (36) also $U = 0$.

280 2. $\dot{V} = 0$, we will have two subcases:

281 (a) if $\dot{U} \neq 0$, then by (35) and (36) we get $U = V = 0$.

282 (b) $\dot{U} = 0$ then, using equations (34):

$$U\ddot{U} + V\ddot{V} = -(U^2 + V^2) [1 + \mathcal{O}(\varepsilon^6(|U|^4 + |V|^4))],$$

283 but this quantity is negative for ε small enough, if $U^2 + V^2 > 0$, which contradicts the
284 second item of (35). We conclude that $U = V = 0$.

285 On the other hand, it is clear that if a collision takes place, i. e. $U = V = 0$ and $\dot{U}^2 + \dot{V}^2 = \sqrt{8(1 - \mu)}$,
286 then conditions (35) and (36) are trivially satisfied. \square

287 **Remark.** The condition ε small enough comes from the perturbative approach chosen to prove the
288 lemma. Note that if we impose that $\dot{U}^2 + \dot{V}^2 > 0$ we can remove this condition. This will be very
289 useful when we study these orbits numerically. More precisely, we will check that an ejection orbit is
290 an n -EC orbit if the angular momentum at the n -th minimum is zero and $\dot{U}^2 + \dot{V}^2 > 0$.

291 Now let us proceed. Using the vectorial notation $\mathbf{U} = (U, V, \dot{U}, \dot{V})^T$, the second order system of ODEs
 292 (34) can be written as

$$\dot{\mathbf{U}} = \mathbf{G}(\mathbf{U}) = \mathbf{G}_0(\mathbf{U}) + \varepsilon^3 \mathbf{G}_3(\mathbf{U}) + \varepsilon^6 \mathbf{G}_6(U, V) + \sum_{k \geq 4} \varepsilon^{2k} \mathbf{G}_{2k}(U, V), \quad (37)$$

293 where

$$\begin{aligned} \mathbf{G}_0(\mathbf{U}) &= \begin{pmatrix} \dot{U} \\ \dot{V} \\ -U \\ -V \end{pmatrix}, & \mathbf{G}_3(\mathbf{U}) &= 8 \begin{pmatrix} 0 \\ 0 \\ (U^2 + V^2)\dot{V} \\ -(U^2 + V^2)\dot{U} \end{pmatrix}, \\ \mathbf{G}_6(U, V) &= 12 \begin{pmatrix} 0 \\ 0 \\ [2\mu(U^4 - 2U^2V^2 - V^4) + (U^2 + V^2)^2]U \\ [2\mu(V^4 - 2U^2V^2 - U^4) + (U^2 + V^2)^2]V \end{pmatrix}, & (38) \\ \mathbf{G}_{2k}(U, V) &= \mu(1 - \mu)^{\frac{k-3}{3}} \begin{pmatrix} 0 \\ 0 \\ \bar{P}_{2k-1}(U, V) \\ \bar{Q}_{2k-1}(U, V) \end{pmatrix}, \text{ for } k \geq 4. \end{aligned}$$

294 We remark that \mathbf{G}_0 and \mathbf{G}_3 are the only functions that depend on \dot{U} and \dot{V} , the remaining ones
 295 depending only on U and V . Moreover we observe that the expressions appearing in the expansions
 296 are polynomials. Both properties allow to significantly simplify the computations.

297 The next natural step consists in obtaining a solution $\mathbf{U} = \mathbf{U}(\tau)$ as a series expansion in ε :

$$\mathbf{U} = \sum_{j \geq 0} \mathbf{U}_j \varepsilon^j. \quad (39)$$

298 As a usual procedure to obtain the functions \mathbf{U}_j , we plug \mathbf{U} in system (37), and comparing the powers
 299 in ε , we obtain a system of ODEs for \mathbf{U}_j .

300 Computation of the functions \mathbf{U}_j

301 Now we proceed to compute the explicit expressions for $\mathbf{U}_j(\tau) = (U_j(\tau), V_j(\tau), \dot{U}_j(\tau), \dot{V}_j(\tau))$, for any j .
 302 Actually we will show that, in order to prove Theorem 2, we only need to find explicitly the functions
 303 \mathbf{U}_j up to order $j = 6$.

304 From Definition 4.a and the scaling (33), any ejection orbit $\mathbf{U}(\tau) = \mathbf{U}(\tau, \theta_0)$, has the initial condition

$$\mathbf{U}(0) = (0, 0, \cos \theta_0, \sin \theta_0), \quad \theta_0 \in [0, 2\pi), \quad (40)$$

305 so we have

$$\mathbf{U}_0(0) = (0, 0, \cos \theta_0, \sin \theta_0), \quad \mathbf{U}_j(0) = \mathbf{0}, \quad j \geq 1. \quad (41)$$

306 Solution for $\varepsilon = 0$:

307 We must solve the linear system:

$$\begin{cases} \ddot{U}_0 = -U_0, \\ \ddot{V}_0 = -V_0, \end{cases} \quad (42)$$

308 which is a harmonic oscillator, with initial condition (40). Then the ejection orbit \mathbf{U}_0 is given by
 309 $\mathbf{U}_0 = (U_0, V_0, \dot{U}_0, \dot{V}_0)$, with:

$$\begin{aligned} U_0(\tau) &= \cos \theta_0 \sin \tau, \\ V_0(\tau) &= \sin \theta_0 \sin \tau, \\ \dot{U}_0(\tau) &= \cos \theta_0 \cos \tau, \\ \dot{V}_0(\tau) &= \sin \theta_0 \cos \tau. \end{aligned} \tag{43}$$

310 **Solution for $\varepsilon \neq 0$:**

311 In order to find the functions \mathbf{U}_j , we must solve the successive resulting ODEs when substituting \mathbf{U}
 312 by the series expansion in (34) up to the desired order.

313 We observe that, for $j \geq 1$, the linear non homogeneous system of ODEs to be solved is

$$\frac{d\mathbf{U}_j}{d\tau} = D\mathbf{G}_0(\mathbf{U}_0)\mathbf{U}_j + \mathbf{F}_j(\mathbf{U}_0, \mathbf{U}_1, \dots, \mathbf{U}_{j-3}) = \mathbf{G}_0(\mathbf{U}_j) + \mathbf{F}_j(\mathbf{U}_0, \mathbf{U}_1, \dots, \mathbf{U}_{j-3}),$$

314 where the homogeneous system is always the same but the independent term changes and increases
 315 in complexity with j .

316 Since a fundamental matrix for the homogeneous system (the first order variational equations) is given
 317 by

$$X(\tau) = \begin{pmatrix} \cos \tau & 0 & \sin \tau & 0 \\ 0 & \cos \tau & 0 & \sin \tau \\ -\sin \tau & 0 & \cos \tau & 0 \\ 0 & -\sin \tau & 0 & \cos \tau \end{pmatrix}, \tag{44}$$

318 and the initial conditions are $\mathbf{U}_j(0) = \mathbf{0}$ for $j \geq 1$, we obtain the following well known formula

$$\mathbf{U}_j(\tau) = X(\tau) \int_0^\tau X^{-1}(s) \mathbf{F}_j(\mathbf{U}_0(s), \dots, \mathbf{U}_{j-3}(s)) ds. \tag{45}$$

319 Remark that from (45) and the expression of (37), $\mathbf{G}_1(\mathbf{U}) = \mathbf{G}_2(\mathbf{U}) = \mathbf{G}_4(\mathbf{U}) = \mathbf{G}_5(\mathbf{U}) = \mathbf{0}$, we
 320 know a priori that $\mathbf{U}_j(\tau) = \mathbf{0}$, for $j = 1, 2, 4, 5$.

321 The corresponding explicit expressions are the following:

$$\begin{aligned} U_3(\tau) &= (\tau \sin \tau - \cos \tau \sin \tau) \sin \theta_0, \\ V_3(\tau) &= -(\tau \sin \tau - \cos \tau \sin \tau) \cos \theta_0, \\ U_6(\tau) &= -\frac{(\tau - \cos \tau \sin \tau)^2 \sin \tau - \mu(15\tau \cos \tau - (8 + 9 \cos^2 \tau - 2 \cos^4 \tau) \sin \tau)(1 - 2 \cos^4 \theta_0)}{2} \cos \theta_0, \\ V_6(\tau) &= -\frac{(\tau - \cos \tau \sin \tau)^2 \sin \tau - \mu(15\tau \cos \tau - (8 + 9 \cos^2 \tau - 2 \cos^4 \tau) \sin \tau)(1 - 2 \sin^4 \theta_0)}{2} \sin \theta_0, \end{aligned} \tag{46}$$

322 and $U_7(\tau) = V_7(\tau) = 0$. Once we have the ejection solution up to order $j = 6$, the next step consists
 323 of computing the n -th minimum in the distance to the primary (located at the origin) the particle
 324 ejected from as a function of the initial θ_0 . Equivalently we want to compute the n -th minimum
 325 of the function $(U^2 + V^2)(\tau)$. This requires to compute the precise time denoted by τ^* , needed

326 to reach the n -th minimum in distance. We apply the Implicit Function Theorem to the function
 327 $(U\dot{U} + V\dot{V})(\tau^*) = 0$ in order to obtain an expansion series in ε , i.e.:

$$\tau^* = \sum_{i=0}^6 \tau_i^* \varepsilon^i + \mathcal{O}(\varepsilon^7).$$

328 We can easily compute τ_0^* , since we have a harmonic oscillator:

$$\tau_0^* = n\pi.$$

329 Writing the function $(U\dot{U} + V\dot{V})(\tau)$ as an expansion series in ε and collecting terms of the same order,
 330 we can successively find the terms τ_i^* (up to order 6, higher order terms in Appendix A):

$$\tau_6^*(n) = \frac{15\mu n\pi(1 + 3\cos(4\theta_0))}{8}, \quad (47)$$

331 with $\tau_i(n, \theta_0) = 0$ for $i = 1, 2, 3, 4, 5, 7$.

332 Now we are ready to compute the angular momentum $M(n, \theta_0) = (U\dot{V} - V\dot{U})(\tau^*)$ whose expansion
 333 is:

$$M(n, \theta_0) = \mu\varepsilon^6 \left(-\frac{15n\pi \sin(4\theta_0)}{4} + \mathcal{O}(\varepsilon^2) \right), \quad (48)$$

334 or in short, since we look for the zeros of $M(n, \theta_0) = 0$, we write, dividing the previous equation by
 335 $\mu\varepsilon^6$,

$$\hat{M}(n, \theta_0) = -\frac{15n\pi \sin(4\theta_0)}{4} + \mathcal{O}(\varepsilon^2). \quad (49)$$

336 Now we apply the Implicit Function Theorem and for $\varepsilon > 0$ small enough we obtain that the equation
 337 (49) has four and only four roots in $[0, \pi)$ given by

$$\theta_0 = \frac{\pi m}{4} + \mathcal{O}(\varepsilon^2), \quad m = 0, 1, 2, 3. \quad (50)$$

338 regardless of the value of the parameter μ . It is clear from (49) that the roots θ_0 are simple.

339 So we have proved that there exist four n -EC orbits. Moreover, applying the symmetries of the
 340 system we can conclude that those EC orbits with an intersection angle with $m = 0, 2$ correspond
 341 to symmetric n -EC orbits (in the sense that the (x, y) projection is symmetric with respect to the x
 342 axis). Those EC orbits with an intersection angle with $m = 1, 3$ correspond to symmetric n -EC orbits
 343 (in the sense that the (x, y) projection is symmetric one with respect to the other one).

344 This finishes the proof of Theorem 2.

345 In order to illustrate the results of Theorem 2, in Figure 4 top we plot the function $M(n, \theta_0)$ for
 346 $\mu = 0.1$, $C = 6$ and the values of $n = 2$ (continuous line) and $n = 4$ (discontinuous line). We remark
 347 its sinusoidal behaviour in accordance with equation (49). Consistently with Theorem 2, the curve
 348 $M(n, \theta_0)$ intersects four times $M(n, \theta_0) = 0$.

349 The four specific values of θ_0 give rise to four n -EC orbits. When varying ε (or, equivalently, K and
 350 therefore C in (32)), we obtain four families denoted by α_n , β_n , γ_n and δ_n . In particular, γ_n and
 351 α_n correspond to the families of orbits that are themselves symmetric with respect to the x axis that
 352 when $C \rightarrow +\infty$ have initial angles 0 and $\pi/2$ respectively and δ_n and β_n correspond to the families of
 353 orbits that are one symmetric to the other with respect to the x axis that when $C \rightarrow +\infty$ have initial
 354 angles $\pi/4$ and $3\pi/4$ respectively. The corresponding EC orbits are shown in the bottom figure in
 355 usual synodical coordinates (x, y) .

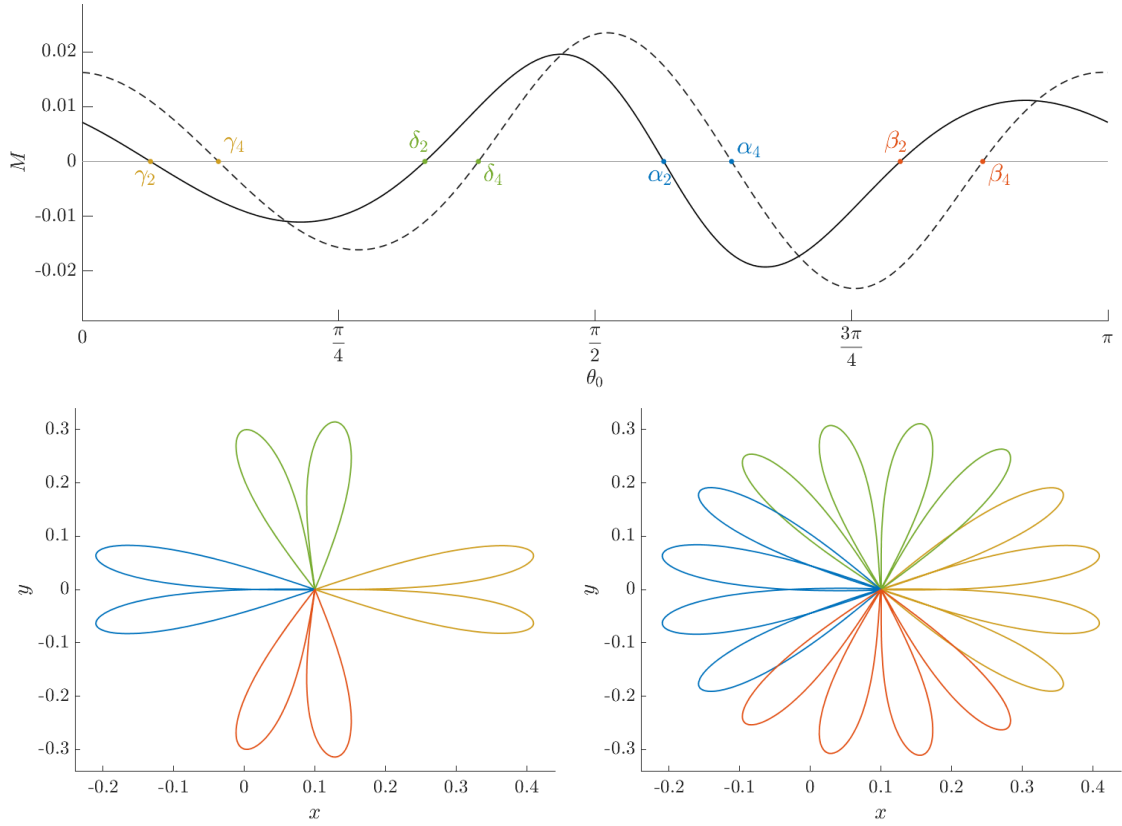


Figure 4: $\mu = 0.1$, $C = 6$. Top. Angular momentum $M(n, \theta_0)$ for $n = 2$ (continuous line) and $n = 4$ (discontinuous line). Bottom. The corresponding four n -EC orbits in the plane (x, y) (left for $n = 2$ and right for $n = 4$).

6 Analysis of Bifurcations

So far we have applied the Implicit Function Theorem to infer the existence of four and only four n -EC orbits, for any value of μ and $C = 3\mu + K(1 - \mu)^{1/3}$ (see (32)) with K big enough, that is $\varepsilon = 1/\sqrt{K}$ small enough. In this procedure the minimum order required in the ε expansions for both the functions U_j and τ_j^* was order 6. Of course, when ε becomes bigger, the Implicit Function Theorem may not be applied anymore and bifurcations can appear. This section is focused on such bifurcations.

We will focus on two purposes: on the one hand, the illustration of the appearance and collapsing of bifurcating families of n -EC orbits when doing the continuation of families varying C as parameter; and on the other hand, the behavior of $\hat{K}(n)$ and its associated value $\hat{C}(\mu, n) = 3\mu + \hat{K}(n)(1 - \mu)^{1/3}$ provided by Theorem 2, for any value of $\mu \in (0, 1)$ and varying n .

6.1 Bifurcating families

The first task is to compute the angular momentum $M(n, \theta_0)$ to higher order. To do so we need higher order terms for both the functions U_j and τ_j^* . We have proceeded as in the previous Section; however, there, expressions up to order 6 were enough. To analyze the bifurcations, we provide their expressions for j up to order 10 in the Appendix. Now we are ready to compute the explicit expression for the angular momentum $M(n, \theta_0) = (U\dot{V} - V\dot{U})(\tau^*)$ up to order 10 which is the following:

$$\begin{aligned}
M(n, \theta_0) = & -\frac{15\mu n\pi \sin(4\theta_0)}{4}\varepsilon^6 + \frac{105\mu(1-\mu)^{1/3}n\pi(\sin(2\theta_0) + 5\sin(6\theta_0))}{64}\varepsilon^8 + \frac{15\mu n^2\pi^2 \cos(4\theta_0)}{2}\varepsilon^9 \\
& - \frac{315\mu(1-\mu)^{2/3}n\pi(2\sin(4\theta_0) + 7\sin(8\theta_0))}{128}\varepsilon^{10} + \mathcal{O}(\varepsilon^{11}).
\end{aligned}
\tag{51}$$

373 It is clear that if ε is small enough, the dominant term is ε^6 , and the zeros of $M(n, \theta_0)$ are related to
374 the term $\sin(4\theta_0)$. Therefore we obtain four n -EC orbits.

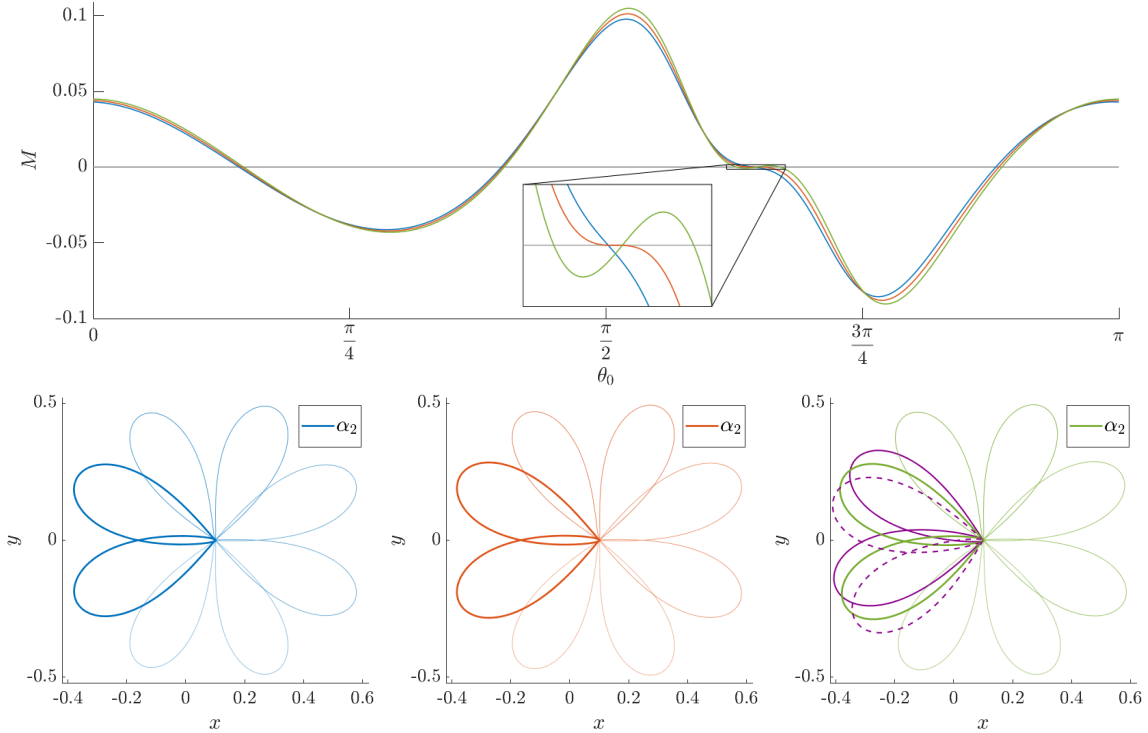


Figure 5: $\mu = 0.1$, Top. We plot the angular momentum $M(2, \theta_0)$. Notice the zoom area where the appearance of two new bifurcating orbits (in green), besides the family α_2 is observed when decreasing C . Bottom. Left, middle and right. Four 2-EC orbits (the colour code corresponds to the top figure) for $C = 3.76$ (in blue), $C_{bif} = 3.72442505$ (the bifurcating value, in red), $C = 3.69$ (in green). Darker colour: those 2-EC orbits belonging to family α_2 . In the right plot, also the two new bifurcated 2-EC orbits are plotted in continuous and discontinuous purple color.

375 However let us discuss what happens for bigger values of ε , or equivalently for smaller values of C .
376 We will illustrate two different kind of bifurcations that take place when doing the continuation of
377 families of n -EC orbits and that can be explained precisely from the analytical expression of $M(n, \theta_0)$
378 to higher order just obtained.

379 The first kind of bifurcation can be inferred just taking into account the terms of $M(n, \theta_0)$ up to
380 order 8 in (51). The bifurcation is associated with the term $\sin(6\theta_0)$. See Figure 5 top for $\mu = 0.1$
381 and $n = 2$. We can clearly see how increasing ε (decreasing C), the bifurcation takes place. Let us
382 describe the bifurcation close to the 2-EC orbit belonging to family α_2 . See the zoom area in Figure 5
383 top. Locally, at a neighbourhood of the value of θ_0 of such EC orbit, for some value of C the angular
384 momentum has a unique transversal intersection with the x -axis (that is $M(2, \theta_0) = 0$, $M'(2, \theta_0) \neq 0$).
385 For $C = 3.76$ this intersection corresponds to the 2-EC orbit belonging to the family α_2 (see the blue
386 curve). For the bifurcating value $C_{bif} = 3.72442505$, $M(2, \theta_0)$ crosses tangentially the x axis (see the
387 red curve). For smaller values of C , $M(2, \theta_0)$ crosses the x axis three times, giving rise to two new

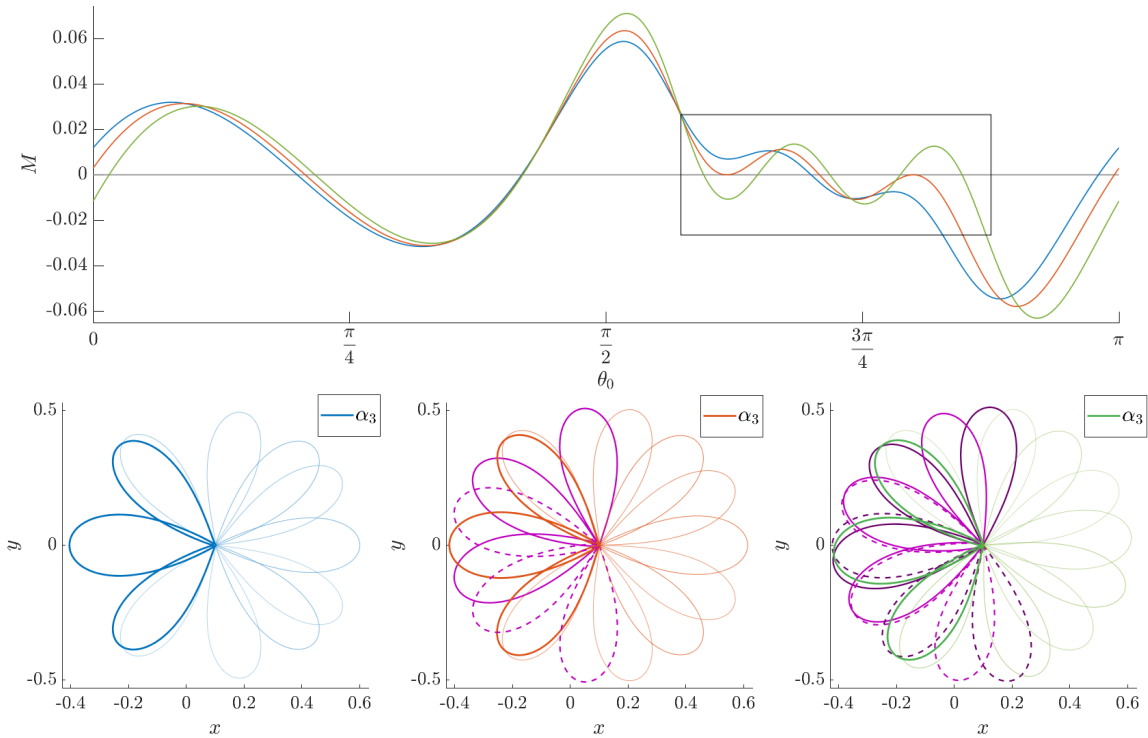


Figure 6: $\mu = 0.1$, $n = 3$. Top. We plot the angular momentum $M(n, \theta_0)$. Notice the zoom area where the appearance of four new bifurcating orbits (in green), besides the family α_3 is observed when decreasing C . Bottom. Left, middle and right. Four 3-EC orbits (the colour code corresponds to the top figure) for $C = 3.9$ (in blue), $C_{bif} = 3.80644009$ (the bifurcating value, in red), $C = 3.7$ (in green). Darker colour: those 3-EC orbits belonging to family α_3 . In the middle plot, also the two tangent new bifurcated 3-EC orbits are plotted. In the right plot, also the four new bifurcated 3-EC orbits are plotted. The bifurcated orbits are plotted in continuous and discontinuous purple color.

388 bifurcating families of 2-EC orbits (see the green curve) besides family α_2 which persists. The new
389 2-EC orbits are (obviously due to symmetry (4)) one symmetric with respect to the other. From a
390 global point of view, for a range $C < C_{bif}$, varying $\theta_0 \in [0, \pi)$, $M(2, \theta_0)$ crosses six times, that is, we
391 obtain six 2-EC orbits, and this is related to the term $\sin(6\theta_0)$, which becomes the dominant term
392 in $M(2, \theta_0)$. We show these 2-EC orbits in Figure 5 bottom. More precisely, on the three plots, the
393 four 2-EC orbits are shown (in the plane (x, y)) and those 2-EC orbits of family α_2 are plotted in a
394 darker colour. Since the family α_2 persists after the bifurcation, the 2-EC orbits are plotted in the
395 left, middle and right plots. The two new bifurcating 2-EC orbits after the bifurcation are also shown
396 on the right plot in continuous and discontinuous purple color.

397 The second kind of bifurcation can be inferred from the expression of $M(n, \theta_0)$ up to order 10 given
398 in (51). The bifurcation is associated with the term $\sin(8\theta_0)$. See Figure 6 top for $\mu = 0.1$ and $n = 3$.
399 We can clearly see how increasing ε (decreasing C), the angular momentum $M(3, \theta_0)$ typically crosses
400 four times the x -axis (for $\theta_0 \in [0, \pi)$), as expected (see the blue curve in the top figure). However at
401 some bifurcating value C_{bif} there appear two tangencies (say from nowhere, see the red curve in the
402 zoom area in Figure 6 top); each tangency gives rise to two families when doing the continuation of
403 families decreasing C . See the green curve in the zoom area in Figure 6 top. So from a global point
404 of view, for a range of $C < C_{bif}$ and $\theta_0 \in [0, \pi)$, the angular momentum $M(3, \theta_0) = 0$ crosses eight
405 times the x -axis, giving rise to eight 3-EC orbits related to the term $\sin(8\theta_0)$. We show these 3-EC
406 orbits in Figure 6 bottom. More specifically, on the three plots, the four 3-EC orbits are shown (in the
407 plane (x, y)) and those 3-EC orbits of family α_3 are plotted in a darker colour. The two 3-EC
408 orbits that appear due to the tangency of $M(3, \theta_0)$ with the x -axis are also plotted on the middle plot, in

409 purple color. Moreover, the four new bifurcating 3-EC orbits after the bifurcation are also shown on
410 the right plot, in purple color. A continuous and discontinuous line with the same colour correspond
411 to EC orbits that are symmetric one with respect to the other one. In fact, due to the symmetry of
412 the problem, we might only consider the two intersection points (those on the left hand side or on
413 the right one of the value of θ_0 in α_3), and the other two intersection points would be obtained by
414 symmetry.

μ	$n = 2$	$n = 3$	$n = 4$	$n = 5$	$n = 6$	$n = 7$	$n = 8$
0.1	3.72442505	3.80644009	4.46458918	4.98305580	5.54170719	6.06561273	6.56667290
0.8				4.10028567	4.29693486	4.48498073	4.66568948

Table 1: Values of $\hat{C}(\mu, n)$ computed for $\mu = 0.1$, $\mu = 0.8$ and $n = 2, \dots, 8$.

415 So far we have described two specific kinds of bifurcations that take place for $n = 2$ and $n = 3$,
416 for $\mu = 0.1$. But from the expression of the angular momentum (51) and the previous discussion,
417 we can foresee a great and rich variety of bifurcations. To have a global and exhaustive insight, we
418 have done massive numerical simulations in the following sense: we have fixed a value of μ , and, for
419 a range of values of $C \geq C_{L_1}$ (for example $C \in [C_{L_1}, 8]$), we have taken a mesh of 2000×2000
420 points in the plane $(\theta, C) \in [0, \pi] \times [C_{L_1}, 8]$, and for each point we have computed the function
421 $M_{LC}(n, \theta_0) = \frac{4(1-\mu)}{\sqrt{C-3\mu}} M(n, \theta_0)$, i.e. the angular momentum in the original Levi-Civita variables, for
422 $n = 1, \dots, 8$. In Figures 7 and 8 we plot the obtained results for $\mu = 0.1$ and $\mu = 0.8$, what we
423 call *bifurcation diagrams*. For n fixed, we plot the diagram (θ_0, C) and the colour standing for the
424 value of $M_{LC}(n, \theta_0)$. The drastic change of colour (from yellow to green) describes the change of sign
425 of $M_{LC}(n, \theta_0)$ and therefore the existence of an n -EC orbit. So for any C fixed, we clearly see the
426 number of n -EC orbits. Some comments about Figure 7 must be made: (i) for big values of C , the
427 bifurcation diagrams show clearly four n -EC orbits for any value of n , in accordance with Theorem 2.
428 See any plot in the figure. (ii) In the first row, right plot, and C close to 3.7, we see the first kind of
429 bifurcation described above for $n = 2$. In the second row, left plot, and C close to 3.9, we recognise the
430 second kind of bifurcation described above for $n = 3$. (iii) It is clear from such diagrams that, when
431 we decrease C and increase the value of n , several phenomena of collapse of families and bifurcation of
432 new families are more visible. See for example the third row plots, when decreasing C , for $\theta_0 < \pi/2$,
433 the collapse of two families, and the appearance of two new ones for $\theta_0 > \pi/2$. Even richer are the
434 diagrams on the last row of the figure. (iv) We have also plotted on each bifurcation diagram the value
435 of the first bifurcation value of C (decreasing C), which is precisely the value $\hat{C}(\mu, n)$, for $\mu = 0.1$
436 mentioned in Theorem 2. We notice in the plot how this value $\hat{C}(\mu, n)$ increases when n increases (see
437 Table 1).

438 When we take a bigger value of μ , for example, $\mu = 0.8$, we obtain Figure 8. Comparing the plots
439 obtained with those of Figure 7, we observe two effects: the value of $\hat{C}(\mu, n)$ is smaller, for the same
440 value of n , and moreover, for $n = 2, 3, 4$, a value of $\hat{C}(\mu, n)$ really smaller than C_{L_1} is required (compare
441 the four first plots in Figures 7 and 8 and see also Table 1). For bigger values of μ and for the same
442 value of $C \geq C_{L_1}$, the Hill region gets really smaller, when increasing μ , so quite naturally, the
443 probability of bifurcations decreases. On the other hand, taking $C < C_{L_1}$ represents an enlarging of
444 the Hill's region and therefore a more powerful influence of the big primary, so an easier scenario to
445 have bifurcations.

446 **Remark.** We notice that Lemma 1 provides a characterization of an EC orbit if C is large enough.
447 Along the numerical simulations done, where the values of C are not so large, we have also used the
448 same characterization, but additionally checking that when $M = 0$ at a minimum distance $\dot{U}^2 + \dot{V}^2 > 0$
449 so $U = V = 0$.

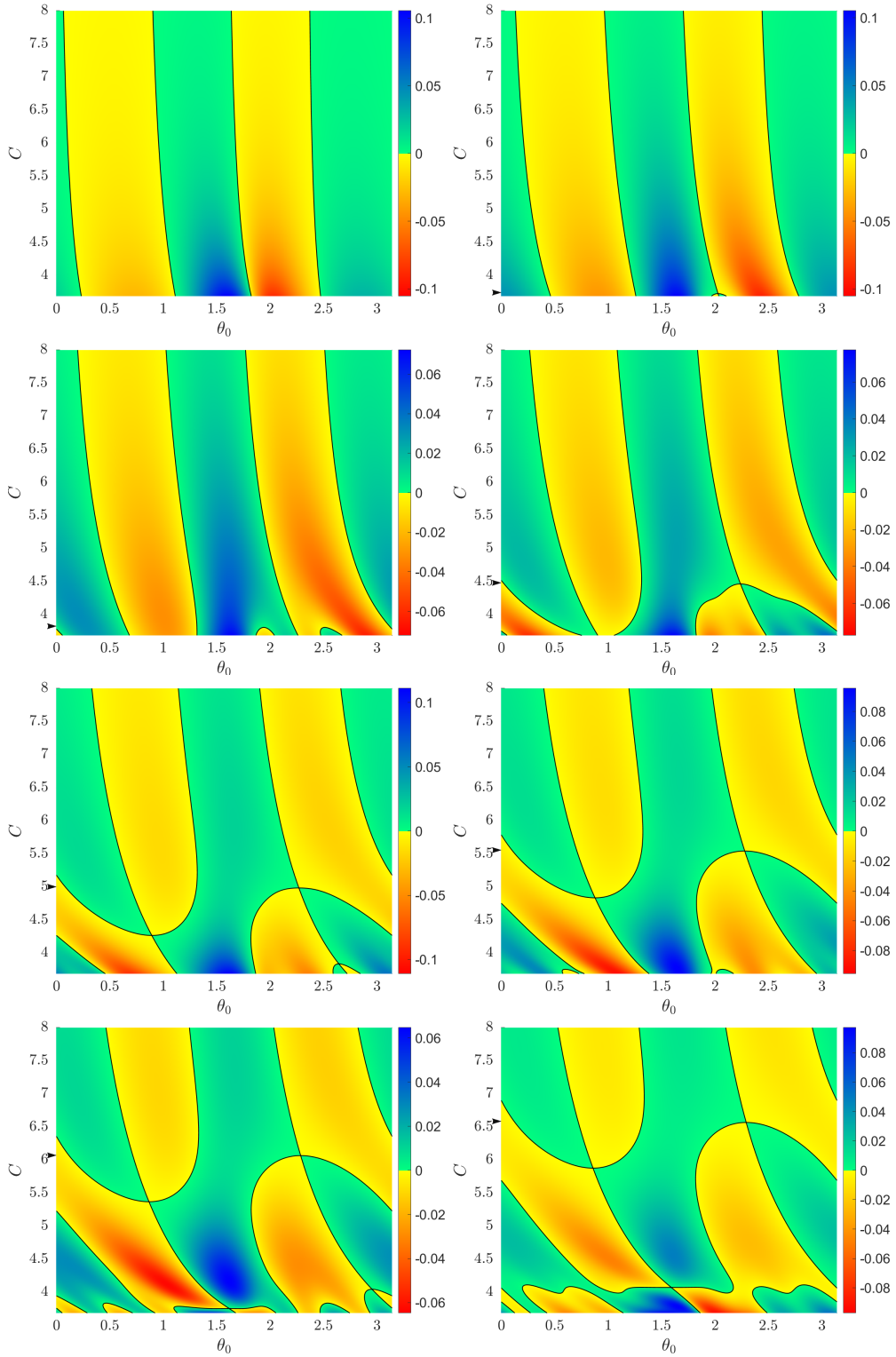


Figure 7: Bifurcation diagrams for $\mu = 0.1$, $n = 1, \dots, 8$ and C in $[C_{L_1}, 8]$. The color indicates the value of $M_{LC}(n, \theta_0)$ and the black curves correspond to the values $M_{LC}(n, \theta_0) = 0$. The value of $\hat{C}(\mu, n)$, for $\mu = 0.1$ is indicated in each plot with an arrow in the vertical axis (see also Table 1).

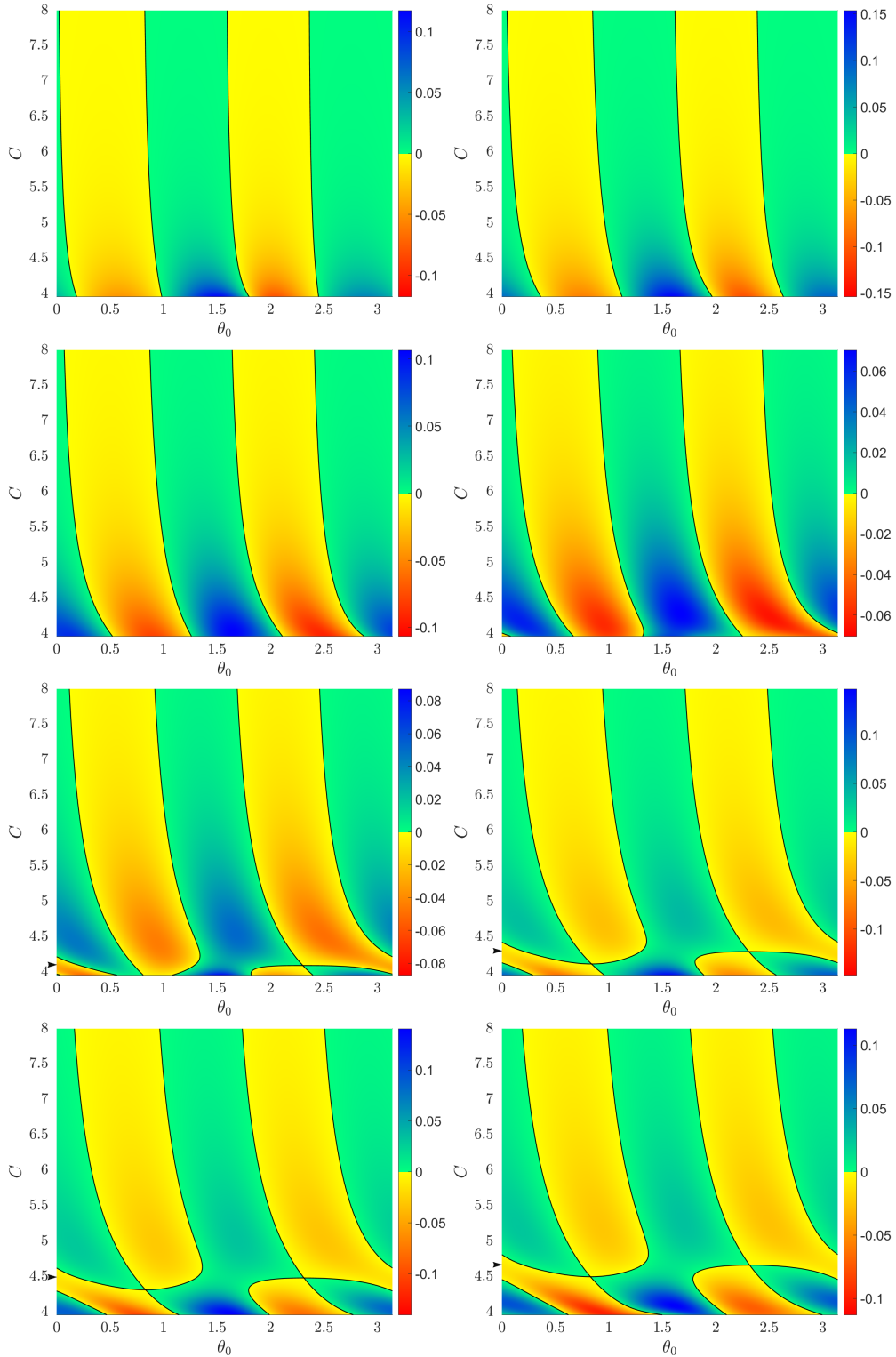


Figure 8: Bifurcation diagrams for $\mu = 0.8$, $n = 1, \dots, 8$ and C in $[C_{L_1}, 8]$. The color indicates the value of $M_{LC}(n, \theta_0)$ and the black curves correspond to the values $M_{LC}(n, \theta_0) = 0$. The value of $\hat{C}(\mu, n)$, for $\mu = 0.1$ is indicated in each plot with an arrow in the vertical axis (see also Table 1).

450 6.2 Behaviour of $\hat{C}(\mu, n)$

451 As a final goal, we want to describe (numerically) the behaviour of $\hat{C}(\mu, n) = 3\mu + \hat{K}(1 - \mu)^{2/3}$ for
 452 any value of $\mu \in (0, 1)$ and n . More precisely, for each value of μ and n , and C big enough, Theorem

453 1 claims that there exist exactly four families of n -EC orbits. As discussed in the previous subsection,
 454 when decreasing C bifurcations appear in a natural way. So for fixed μ and n , the first value of
 455 C (decreasing C) such that there appear more than four n -EC orbits is precisely the value $\hat{C}(\mu, n)$
 456 formulated in Theorem 1.

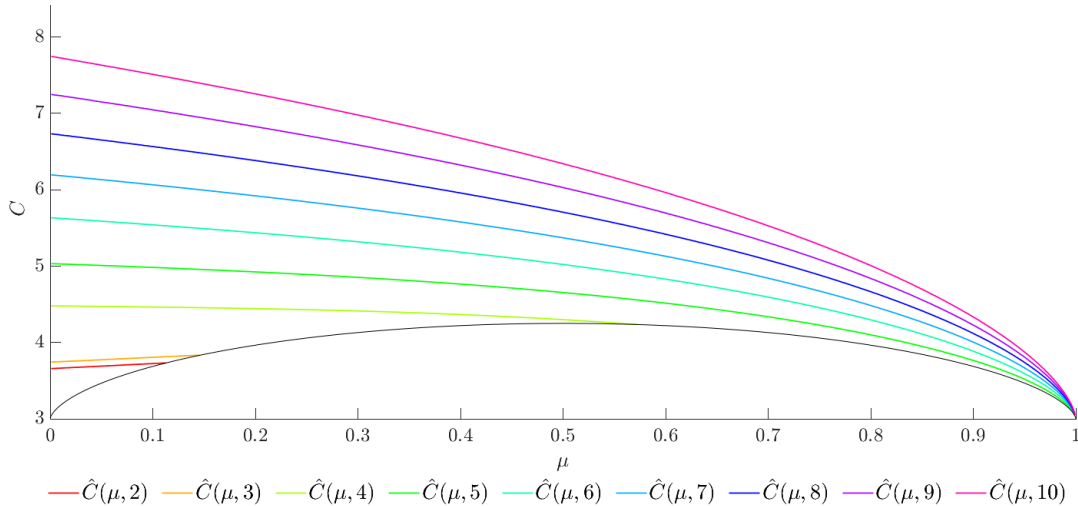


Figure 9: $\hat{C}(\mu, n)$

457 In the previous subsection, we have computed the value $\hat{C}(\mu, n)$, just for $\mu = 0.1$ and $n = 1, \dots, 8$.
 458 Our purpose now is to compute $\hat{C}(\mu, n)$ for any $\mu \in (0, 1)$ and n . We will always assume that any value
 459 of C considered satisfies $C \geq C_{L_1}$ (recall the Hill regions in Figure 1, there is no possible connection
 460 between P_1 and P_2 , and therefore the dynamics around each primary is the simplest possible).

461 The strategy to compute numerically \hat{C} , for a fixed $\mu \in (0, 1)$ and given n , is the following: we take
 462 the interval $I = [C_{L_1}, C_b]$ of values of C , and for each $C \in I$, (starting at C_b) we vary $\theta_0 \in [0, \pi)$
 463 (that defines the initial conditions of an ejection orbit in synodical Levi-Civita variables) and find the
 464 four specific values of θ_0 (such that $M(n, \theta_0) = 0$) corresponding to the expected four n -EC orbits.
 465 So we have four n -EC orbits for that value of C and decreasing C we obtain four families of n -EC
 466 orbits. However as we decrease C , we find a value of $C \in I$ such that more than four n -EC orbits are
 467 found. This means that new families have bifurcated. Next we refine the value of C such that it is
 468 the frontier before appearing new families of n -EC orbits. That is precisely the specific value of \hat{C} .

469 In Figure 9 we show the results obtained for $\mu \in (0, 1)$ and $n = 2, \dots, 10$. Also the curve (μ, C_{L_1}) has
 470 been plotted (in black). Recall that, as mentioned above, we are focussed on values of $C \geq C_{L_1}$. We
 471 remark that for $n = 1$, the value $\hat{C}(\mu, 1)$ is less than C_{L_1} and therefore is not considered. Moreover
 472 for the specific values of $\mu = 0.1$ and $\mu = 0.8$ we recover the indicated values in Figures 7 and
 473 8 respectively. From Figure 9 it is clear that the value of $\hat{C}(\mu, n)$ increases when n increases. This
 474 means that for higher values of n , that is longer time spans integrations, the effect of the other primary
 475 is more visible.

476 We remark that the shape of the curves in Figure 9 provide a hint about the dependence of $K(n)$ in
 477 the expression $\hat{C}(\mu, n) = 3\mu + \hat{K}(n)(1 - \mu)^{2/3}$ obtained in Theorem 2, more specifically $\hat{K}(n) = \hat{L}n^{2/3}$.
 478 We will prove rigorously this dependence in Theorem 1 in the next Section.

7 Proof of Theorem 1

The proof of Theorem 1 is also based on a perturbative approach. Let us introduce a new parameter L defined as $K = Ln^{2/3}$ in (32). In this way, we perform the change (33) and a new time $\hat{\mathcal{T}} = \tau/n$:

$$\begin{cases} u = \frac{\sqrt{2}(1-\mu)^{1/6}}{\sqrt{L}n^{1/3}}\mathcal{U}, \\ v = \frac{\sqrt{2}(1-\mu)^{1/6}}{\sqrt{L}n^{1/3}}\mathcal{V}, \\ \hat{\mathcal{T}} = \frac{2\sqrt{L}(1-\mu)^{1/3}}{n^{2/3}}s = \frac{\tau}{n}, \\ C = 3\mu + Ln^{2/3}(1-\mu)^{2/3}, \end{cases} \quad (52)$$

where we introduce the functions in the new time:

$$\mathcal{U}(\hat{\mathcal{T}}) = U(\tau), \quad \mathcal{V}(\hat{\mathcal{T}}) = V(\tau)$$

The system (6) becomes, denoting $\dot{} = \frac{d}{d\tau}$

$$\begin{cases} \ddot{\mathcal{U}} = -n^2\mathcal{U} + \frac{8(\mathcal{U}^2 + \mathcal{V}^2)\dot{\mathcal{V}}}{L^{3/2}} + \frac{12(\mathcal{U}^2 + \mathcal{V}^2)^2\mathcal{U}}{L^3} \\ \quad + 2\mu \left[\frac{n^{4/3}}{L(1-\mu)^{2/3}} \left(\frac{1}{r_2} - 1 \right) - \frac{4(\mathcal{U}^2 + \mathcal{V}^2)^2}{L^3 r_2^3} - \frac{2n^{2/3}(\mathcal{U}^2 + \mathcal{V}^2)}{L^2(1-\mu)^{1/3}r_2^3} + \frac{4n^{2/3}\mathcal{U}^2}{L^2(1-\mu)^{1/3}} \right] \mathcal{U}, \\ \ddot{\mathcal{V}} = -n^2\mathcal{V} - \frac{8(\mathcal{U}^2 + \mathcal{V}^2)\dot{\mathcal{U}}}{L^{3/2}} + \frac{12(\mathcal{U}^2 + \mathcal{V}^2)^2\mathcal{V}}{L^3} \\ \quad + 2\mu \left[\frac{n^{4/3}}{L(1-\mu)^{2/3}} \left(\frac{1}{r_2} - 1 \right) - \frac{4(\mathcal{U}^2 + \mathcal{V}^2)^2}{L^3 r_2^3} + \frac{2n^{2/3}(\mathcal{U}^2 + \mathcal{V}^2)}{L^2(1-\mu)^{1/3}r_2^3} - \frac{4n^{2/3}\mathcal{V}^2}{L^2(1-\mu)^{1/3}} \right] \mathcal{V}, \end{cases} \quad (53)$$

with $r_2 = \sqrt{1 + \frac{4(1-\mu)^{1/3}(\mathcal{U}^2 - \mathcal{V}^2)}{Ln^{2/3}} + \frac{4(1-\mu)^{2/3}(\mathcal{U}^2 + \mathcal{V}^2)^2}{L^2n^{4/3}}}$. Let us introduce the parameter $\xi = 1/\sqrt{L}$, in this way the system (53) becomes

$$\begin{cases} \ddot{\mathcal{U}} = -n^2\mathcal{U} + 8(\mathcal{U}^2 + \mathcal{V}^2)\dot{\mathcal{V}}\xi^3 + 12(\mathcal{U}^2 + \mathcal{V}^2)^2\mathcal{U}\xi^6 \\ \quad + 2\mu \left[\frac{n^{4/3}}{(1-\mu)^{2/3}} \left(\frac{1}{r_2} - 1 \right) \xi^2 - \frac{4(\mathcal{U}^2 + \mathcal{V}^2)^2}{r_2^3} \xi^6 - \frac{2n^{2/3}(\mathcal{U}^2 + \mathcal{V}^2)}{(1-\mu)^{1/3}r_2^3} \xi^4 + \frac{4n^{2/3}\mathcal{U}^2}{(1-\mu)^{1/3}} \xi^4 \right] \mathcal{U}, \\ \ddot{\mathcal{V}} = -n^2\mathcal{V} - 8(\mathcal{U}^2 + \mathcal{V}^2)\dot{\mathcal{U}}\xi^3 + 12(\mathcal{U}^2 + \mathcal{V}^2)^2\mathcal{V}\xi^6 \\ \quad + 2\mu \left[\frac{n^{4/3}}{(1-\mu)^{2/3}} \left(\frac{1}{r_2} - 1 \right) \xi^2 - \frac{4(\mathcal{U}^2 + \mathcal{V}^2)^2}{r_2^3} \xi^6 + \frac{2n^{2/3}(\mathcal{U}^2 + \mathcal{V}^2)}{(1-\mu)^{1/3}r_2^3} \xi^4 - \frac{4n^{2/3}\mathcal{V}^2}{(1-\mu)^{1/3}} \xi^4 \right] \mathcal{V}, \end{cases} \quad (54)$$

with

$$r_2 = \sqrt{1 + \frac{4(1-\mu)^{1/3}(\mathcal{U}^2 - \mathcal{V}^2)}{n^{2/3}} \xi^2 + \frac{4(1-\mu)^{2/3}(\mathcal{U}^2 + \mathcal{V}^2)^2}{n^{4/3}} \xi^4}. \quad (55)$$

Let us introduce the vectorial notation $\mathbf{U} = (\mathcal{U}, \mathcal{V}, \dot{\mathcal{U}}, \dot{\mathcal{V}})$. The system (54) can be written as

$$\dot{\mathbf{U}} = \mathcal{F}_0(\mathbf{U}) + \mu\mathcal{F}_1(\mathbf{U}), \quad (56)$$

488 where

$$\begin{aligned}
\mathcal{F}_0(\mathbf{U}) &= \begin{pmatrix} \dot{U} \\ \dot{V} \\ -n^2U + 8(U^2 + V^2)\dot{V}\xi^3 + 12(U^2 + V^2)^2U\xi^6 \\ -n^2V - 8(U^2 + V^2)\dot{U}\xi^3 + 12(U^2 + V^2)^2V\xi^6 \end{pmatrix}, \\
\mathcal{F}_1(\mathbf{U}) &= \begin{pmatrix} 0 \\ 0 \\ 2 \left[\frac{n^{4/3}}{(1-\mu)^{2/3}} \left(\frac{1}{r_2} - 1 \right) \xi^2 - \frac{4(U^2+V^2)^2}{r_2^3} \xi^6 - \frac{2n^{2/3}(U^2+V^2)}{(1-\mu)^{1/3}r_2^3} \xi^4 + \frac{4n^{2/3}U^2}{(1-\mu)^{1/3}} \xi^4 \right] U \\ 2 \left[\frac{n^{4/3}}{(1-\mu)^{2/3}} \left(\frac{1}{r_2} - 1 \right) \xi^2 - \frac{4(U^2+V^2)^2}{r_2^3} \xi^6 + \frac{2n^{2/3}(U^2+V^2)}{(1-\mu)^{1/3}r_2^3} \xi^4 - \frac{4n^{2/3}V^2}{(1-\mu)^{1/3}} \xi^4 \right] V \end{pmatrix}.
\end{aligned} \tag{57}$$

489 **Remark.** Note that $\mathcal{F}_1(\mathbf{U})$ only depends on the position variables, $\mathcal{F}_1(\mathbf{U}) = \mathcal{F}_1(U, V)$.

490 At this point, our next goal is to find the solution as $\mathbf{U} = \mathbf{U}_0 + \mathbf{U}_1$ where

$$491 \quad \dot{\mathbf{U}}_0 = \mathcal{F}_0(\mathbf{U}_0), \tag{58a}$$

$$491 \quad \dot{\mathbf{U}}_1 = \mu \mathcal{F}_1(\mathbf{U}_0 + \mathbf{U}_1) + \mathcal{F}_0(\mathbf{U}_0 + \mathbf{U}_1) - \mathcal{F}_0(\mathbf{U}_0). \tag{58b}$$

492 Notice that \mathbf{U}_0 is the solution of the 2-body problem ($\mu = 0$) in synodical (rotating) Levi-Civita
493 coordinates. That is, we consider system (56) as a perturbation of the 2-body problem (58a) where
494 the perturbation parameter is ξ which will be small enough and for any value of $\mu \in (0, 1)$. Roughly
495 speaking, for big values of the Jacobi constant the problem is close the two body problem of the
496 mass-less body and the collision primary, regardless the value of the mass parameter μ .

497 Note that we are interested only in the ejection orbits $\mathbf{U}^e = \mathbf{U}_0^e + \mathbf{U}_1^e$ and the initial conditions of
498 these orbits are given by

$$498 \quad \mathbf{U}_0^e(0) = (0, 0, n \cos \theta_0, n \sin \theta_0) \quad \text{and} \quad \mathbf{U}_1^e(0) = \mathbf{0}. \tag{59}$$

499 To prove the theorem we will use the same strategy of computing the angular momentum $\mathcal{M}(n, \theta_0)$
500 at the n -th minimum of the distance to the origin and find the values of θ_0 such that $\mathcal{M}(n, \theta_0) = 0$.

501 Thus, we will compute \mathbf{U}^e and the time needed to reach n -th minimum solving $\left[U^e \dot{U}^e + V^e \dot{V}^e \right] (\theta_0, \hat{T}^*) =$
502 0 . The last step will be to calculate $\mathcal{M}(n, \theta_0)$.

503 The unperturbed system

504 As a first step we must solve system (58a)

$$\begin{cases} \ddot{U}_0 = -n^2U_0 + 8(U_0^2 + V_0^2)\dot{V}_0\xi^3 + 12(U_0^2 + V_0^2)^2U_0\xi^6, \\ \ddot{V}_0 = -n^2V_0 - 8(U_0^2 + V_0^2)\dot{U}_0\xi^3 + 12(U_0^2 + V_0^2)^2V_0\xi^6, \end{cases} \tag{60}$$

505 with initial conditions $\mathbf{U}_0(0) = (0, 0, n \cos \theta_0, n \sin \theta_0)$.

506 In order to obtain the solution of this system, we first consider the 2-body problem in sidereal coordi-
507 nates:

$$\begin{cases} \ddot{\bar{U}}_0 = - \left[n^2 - 4(\bar{U}_0 \dot{\bar{V}}_0 - \bar{V}_0 \dot{\bar{U}}_0) \xi^3 \right] \bar{U}_0, \\ \ddot{\bar{V}}_0 = - \left[n^2 - 4(\bar{U}_0 \dot{\bar{V}}_0 - \bar{V}_0 \dot{\bar{U}}_0) \xi^3 \right] \bar{V}_0, \end{cases} \tag{61}$$

508 and the change of time

$$\frac{dt}{d\hat{\mathcal{T}}} = 4(\bar{\mathcal{U}}_0^2 + \bar{\mathcal{V}}_0^2)\xi^3. \quad (62)$$

509 being $(\bar{\mathcal{U}}_0(\hat{\mathcal{T}}), \bar{\mathcal{V}}_0(\hat{\mathcal{T}}))$ the associated solutions.

510 We recall that for the two body problem the angular momentum is constant, consequently

$$\left[\bar{\mathcal{U}}_0 \dot{\bar{\mathcal{V}}}_0 - \bar{\mathcal{V}}_0 \dot{\bar{\mathcal{U}}}_0 \right] (\hat{\mathcal{T}}) = \left(\bar{\mathcal{U}}_0 \dot{\bar{\mathcal{V}}}_0 - \bar{\mathcal{V}}_0 \dot{\bar{\mathcal{U}}}_0 \right) (0), \quad (63)$$

511 and therefore the solution of (61) is given by

$$\begin{cases} \bar{\mathcal{U}}_0(\hat{\mathcal{T}}) = \bar{\mathcal{U}}_0(0) \cos(\omega \hat{\mathcal{T}}) + \frac{\dot{\bar{\mathcal{U}}}_0(0)}{\omega} \sin(\omega \hat{\mathcal{T}}), \\ \bar{\mathcal{V}}_0(\hat{\mathcal{T}}) = \bar{\mathcal{V}}_0(0) \cos(\omega \hat{\mathcal{T}}) + \frac{\dot{\bar{\mathcal{V}}}_0(0)}{\omega} \sin(\omega \hat{\mathcal{T}}), \end{cases} \quad (64)$$

512 where $\omega = \sqrt{n^2 - 4(\bar{\mathcal{U}}_0 \dot{\bar{\mathcal{V}}}_0 - \bar{\mathcal{V}}_0 \dot{\bar{\mathcal{U}}}_0)(0)\xi^3}$. Moreover the value $t(\hat{\mathcal{T}})$ is simply obtained from (62) and
513 (64):

$$\begin{aligned} t(\hat{\mathcal{T}}) = 2 \left[(\bar{\mathcal{U}}_0^2 + \bar{\mathcal{V}}_0^2)(0) \left(\hat{\mathcal{T}} + \frac{\cos(\omega \hat{\mathcal{T}}) \sin(\omega \hat{\mathcal{T}})}{\omega} \right) + \frac{2(\bar{\mathcal{U}}_0 \dot{\bar{\mathcal{U}}}_0 + \bar{\mathcal{V}}_0 \dot{\bar{\mathcal{V}}}_0)(0)}{\omega^2} \sin^2(\omega \hat{\mathcal{T}}) \right. \\ \left. + \frac{(\dot{\bar{\mathcal{U}}}_0^2 + \dot{\bar{\mathcal{V}}}_0^2)(0)}{\omega^2} \left(\hat{\mathcal{T}} - \frac{\cos(\omega \hat{\mathcal{T}}) \sin(\omega \hat{\mathcal{T}})}{\omega} \right) \right] \xi^3, \end{aligned} \quad (65)$$

514 Now we apply the rotation transformation to (64) to obtain the solution of system in synodical
515 coordinates (60),

$$\begin{cases} \mathcal{U}_0(\hat{\mathcal{T}}) = \bar{\mathcal{U}}_0(\hat{\mathcal{T}}) \cos(-t/2) - \bar{\mathcal{V}}_0(\hat{\mathcal{T}}) \sin(-t/2), \\ \mathcal{V}_0(\hat{\mathcal{T}}) = \bar{\mathcal{U}}_0(\hat{\mathcal{T}}) \sin(-t/2) + \bar{\mathcal{V}}_0(\hat{\mathcal{T}}) \cos(-t/2), \\ \dot{\mathcal{U}}_0(\hat{\mathcal{T}}) = \left[\dot{\bar{\mathcal{U}}}_0 + 2(\bar{\mathcal{U}}_0^2 + \bar{\mathcal{V}}_0^2)\bar{\mathcal{V}}_0\xi^3 \right] \cos(-t/2) - \left[\dot{\bar{\mathcal{V}}}_0 - 2(\bar{\mathcal{U}}_0^2 + \bar{\mathcal{V}}_0^2)\bar{\mathcal{U}}_0\xi^3 \right] \sin(-t/2), \\ \dot{\mathcal{V}}_0(\hat{\mathcal{T}}) = \left[\dot{\bar{\mathcal{U}}}_0 + 2(\bar{\mathcal{U}}_0^2 + \bar{\mathcal{V}}_0^2)\bar{\mathcal{V}}_0\xi^3 \right] \sin(-t/2) + \left[\dot{\bar{\mathcal{V}}}_0 - 2(\bar{\mathcal{U}}_0^2 + \bar{\mathcal{V}}_0^2)\bar{\mathcal{U}}_0\xi^3 \right] \cos(-t/2), \end{cases} \quad (66)$$

516 Notice that the relation between the sidereal initial conditions and the synodical ones $(\mathcal{U}_0 \mathcal{V}_0, \dot{\mathcal{U}}_0 \dot{\mathcal{V}}_0)(0)$,
517 are obtained simply from (66) putting $\hat{\mathcal{T}} = 0$

$$\begin{cases} \mathcal{U}_0(0) = \bar{\mathcal{U}}_0(0), \\ \mathcal{V}_0(0) = \bar{\mathcal{V}}_0(0), \\ \dot{\mathcal{U}}_0(0) = \dot{\bar{\mathcal{U}}}_0(0) + 2(\bar{\mathcal{U}}_0^2 + \bar{\mathcal{V}}_0^2)(0)\bar{\mathcal{V}}_0(0)\xi^3, \\ \dot{\mathcal{V}}_0(0) = \dot{\bar{\mathcal{V}}}_0(0) - 2(\bar{\mathcal{U}}_0^2 + \bar{\mathcal{V}}_0^2)(0)\bar{\mathcal{U}}_0(0)\xi^3, \end{cases} \quad \begin{cases} \bar{\mathcal{U}}_0(0) = \mathcal{U}_0(0), \\ \bar{\mathcal{V}}_0(0) = \mathcal{V}_0(0), \\ \dot{\bar{\mathcal{U}}}_0(0) = \dot{\mathcal{U}}_0(0) - 2(\mathcal{U}_0^2 + \mathcal{V}_0^2)(0)\mathcal{V}_0(0)\xi^3, \\ \dot{\bar{\mathcal{V}}}_0(0) = \dot{\mathcal{V}}_0(0) + 2(\mathcal{U}_0^2 + \mathcal{V}_0^2)(0)\mathcal{U}_0(0)\xi^3. \end{cases} \quad (67)$$

518 Since we are interested in the particular case of ejection orbits, which have as their initial condition

$$\bar{\mathcal{U}}_0(0) = (0, 0, n \cos \theta_0, n \sin \theta_0), \quad (68)$$

519 the corresponding ejection solution is given by $\mathcal{U}_0^e = (\mathcal{U}_0^e, \mathcal{V}_0^e, \dot{\mathcal{U}}_0^e, \dot{\mathcal{V}}_0^e)$, where:

$$\begin{cases} \mathcal{U}_0^e(\theta_0, \hat{\mathcal{T}}) = [\cos \theta_0 \cos(-t/2) - \sin \theta_0 \sin(-t/2)] \sin(n\hat{\mathcal{T}}) = \cos(\theta_0 - t/2) \sin(n\hat{\mathcal{T}}), \\ \mathcal{V}_0^e(\theta_0, \hat{\mathcal{T}}) = [\cos \theta_0 \sin(-t/2) + \sin \theta_0 \cos(-t/2)] \sin(n\hat{\mathcal{T}}) = \sin(\theta_0 - t/2) \sin(n\hat{\mathcal{T}}), \end{cases} \quad (69)$$

520 with

$$t = 2 \left[\hat{\mathcal{T}} - \frac{\cos(n\hat{\mathcal{T}}) \sin(n\hat{\mathcal{T}})}{n} \right] \xi^3. \quad (70)$$

521 If we denote by $\hat{\mathcal{T}}_0^*$ the time needed by $\mathbf{u}_0^e(\hat{\mathcal{T}})$ to reach the n -th minimum distance to the origin, it is
522 clear from (69) that

$$\hat{\mathcal{T}}_0^* = \pi. \quad (71)$$

523 The perturbed system

524 In order to solve the perturbed problem (i.e. $\mu \neq 0$) we rewrite system (58b) as

$$\dot{\mathbf{u}}_1 = D\mathcal{F}_0(\mathbf{u}_0)\mathbf{u}_1 + \mathcal{G}(\mathbf{u}_1), \quad (72)$$

525 where $\mathbf{u}_0 = \mathbf{u}_0^e$ is the ejection solution (69) of the two body problem and

$$\mathcal{G}(\mathbf{u}_1) = \mu \mathcal{F}_1(\mathbf{u}_0^e + \mathbf{u}_1) + \mathcal{F}_0(\mathbf{u}_0^e + \mathbf{u}_1) - \mathcal{F}_0(\mathbf{u}_0^e) - D\mathcal{F}_0(\mathbf{u}_0^e)\mathbf{u}_1. \quad (73)$$

526 Note that the ejection solution \mathbf{u}_1^e has zero initial condition and therefore is the solution of the implicit
527 equation

$$\mathbf{u}_1^e = \mathcal{H}\{\mathbf{u}_1^e\}, \quad (74)$$

528 where we define

$$\mathcal{H}\{\mathbf{u}\}(\hat{\mathcal{T}}) = X(\hat{\mathcal{T}}) \int_0^{\hat{\mathcal{T}}} X^{-1}(\hat{\mathcal{T}}) \mathcal{G}(\mathbf{u}(\hat{\mathcal{T}})) d\hat{\mathcal{T}}, \quad (75)$$

529 and $X(\hat{\mathcal{T}})$ is the fundamental matrix of the linear system:

$$\dot{\mathbf{u}}_1 = D\mathcal{F}_0(\mathbf{u}_0^e)\mathbf{u}_1. \quad (76)$$

530 We will apply a Fixed Point Theorem to prove the existence of the solution \mathbf{u}_1^e . Thus we consider the
531 space

$$\chi = \{\mathbf{u} : [0, T] \rightarrow \mathbb{R}^4, \quad \mathbf{u} \text{ continuous}\},$$

532 for a given T , for example $T = 2\pi$.

533 For a given function $\mathbf{u} = (\mathcal{U}, \mathcal{V}, \dot{\mathcal{U}}, \dot{\mathcal{V}}) \in \chi$ we consider the norm:

$$\|\mathbf{u}\| = \sup_{\hat{\mathcal{T}} \in [0, T]} (n|\mathcal{U}(\hat{\mathcal{T}})| + n|\mathcal{V}(\hat{\mathcal{T}})| + |\dot{\mathcal{U}}(\hat{\mathcal{T}})| + |\dot{\mathcal{V}}(\hat{\mathcal{T}})|). \quad (77)$$

534 With this norm χ is a Banach space.

535 As usual, given an $R > 0$, we define the ball $B_R(\mathbf{0}) \subset \chi$ as the functions $\mathbf{u} \in \chi$ such that $\|\mathbf{u}\| \leq R$.

536 Next lemmas show that the required hypotheses for the Fixed Point Theorem to be applied are
537 satisfied.

538 **Lemma 2.** *There exist $\xi_0 > 0$ and a constant $M_1 > 0$ such that, for $0 < \xi < \xi_0$, $0 < \mu < 1$ and
539 $n \in \mathbb{N}$,*

$$\|\mathcal{H}\{\mathbf{0}\}\| \leq M_1 \mu \xi^6.$$

540 *Proof.* See Appendix B.1. □

541 **Lemma 3.** *There exist $0 < \xi_1 \leq \xi_0$ and a constant $M_2 \geq M_1$ such that, for $0 < \xi < \xi_1$, $0 < \mu < 1$
542 and $n \in \mathbb{N}$, given $\mathbf{u}_\oplus, \mathbf{u}_\ominus \in B_R(\mathbf{0})$ with $R = 2M_1 \mu \xi^6$ then*

$$\|\mathcal{H}\{\mathbf{u}_\oplus\} - \mathcal{H}\{\mathbf{u}_\ominus\}\| \leq M_2 \mu \xi^6 \|\mathbf{u}_\oplus - \mathbf{u}_\ominus\|.$$

543 *Proof.* See Appendix B.2. □

544 At this point we select ξ_1 s.t. $M_2\mu\xi_1^6 < 1/2$, so we have the following result

545 **Lemma 4.** *Under the same hypotheses of Lemma 3 if we reduce ξ_1 such that $M_2\mu\xi_1^6 < 1/2$, one*
 546 *has that the operator $\mathcal{H} : B_R(\mathbf{0}) \rightarrow B_R(\mathbf{0})$ and it is a contraction and therefore there exists a unique*
 547 *$\mathcal{U}_1^e \in B_R(\mathbf{0})$ which is solution of the equation (74) in χ .*

548 *Proof.* If $\mathcal{U} \in B_R(\mathbf{0})$, then:

$$\|\mathcal{H}\{\mathcal{U}\}\| = \|\mathcal{H}\{\mathbf{0}\} + \mathcal{H}\{\mathcal{U}\} - \mathcal{H}\{\mathbf{0}\}\| \leq \|\mathcal{H}\{\mathbf{0}\}\| + \|\mathcal{H}\{\mathcal{U}\} - \mathcal{H}\{\mathbf{0}\}\| \leq \frac{R}{2} + \frac{R}{2} = R,$$

549 and we already know by Lemma 3 that \mathcal{H} is Lipschitz with Lipschitz constant $M_2\mu\xi^6 < 1/2$.

550 By the Fixed Point Theorem there exists a unique $\mathcal{U}_1^e \in B_R(\mathbf{0})$ which is solution of the equation
 551 (74). □

552 Observe that once we know the existence and bounds of the function \mathcal{U}_1^e , its smoothness is a conse-
 553 quence of being solution of a smooth differential equation.

554 The results of the previous lemmas give us the following properties:

- 555 • $\|\mathcal{U}_1^e\| \leq R = 2M_1\mu\xi^6$,
- 556 • $\|\mathcal{U}_1^e - \mathcal{H}\{\mathbf{0}\}\| = \|\mathcal{H}\{\mathcal{U}_1^e\} - \mathcal{H}\{\mathbf{0}\}\| \leq M_2\mu\xi^6\|\mathcal{U}_1^e\| \leq 2M_1M_2\mu^2\xi^{12}$.

557 Writing these inequalities in components, and using the definition of the norm (77), we have

558 • $\mathcal{U}_1^e = \mathcal{H}_1\{\mathbf{0}\} + \frac{\mu^2}{n}\mathcal{O}(\xi^{12})$,

559 • $\mathcal{V}_1^e = \mathcal{H}_2\{\mathbf{0}\} + \frac{\mu^2}{n}\mathcal{O}(\xi^{12})$,

560 • $\dot{\mathcal{U}}_1^e = \mathcal{H}_3\{\mathbf{0}\} + \mu^2\mathcal{O}(\xi^{12})$,

561 • $\dot{\mathcal{V}}_1^e = \mathcal{H}_4\{\mathbf{0}\} + \mu^2\mathcal{O}(\xi^{12})$,

562 where $\mathcal{H} = (\mathcal{H}_1, \mathcal{H}_2, \mathcal{H}_3, \mathcal{H}_4)$.

563 **Lemma 5.** *With the same hypotheses of Lemma 4, the value of $\mathcal{H}\{\mathbf{0}\}$ is given by*

$$\begin{aligned} \mathcal{H}_1\{\mathbf{0}\} &= \mathcal{U}_6^e(\hat{\mathcal{T}})\xi^6 + \frac{\mu}{n}\mathcal{O}(\xi^8), \\ \mathcal{H}_2\{\mathbf{0}\} &= \mathcal{V}_6^e(\hat{\mathcal{T}})\xi^6 + \frac{\mu}{n}\mathcal{O}(\xi^8), \\ \mathcal{H}_3\{\mathbf{0}\} &= \dot{\mathcal{U}}_6^e(\hat{\mathcal{T}})\xi^6 + \mu\mathcal{O}(\xi^8), \\ \mathcal{H}_4\{\mathbf{0}\} &= \dot{\mathcal{V}}_6^e(\hat{\mathcal{T}})\xi^6 + \mu\mathcal{O}(\xi^8). \end{aligned} \tag{78}$$

564 where $\mathbf{U}_6^e(\hat{\mathcal{T}}) = (\mathcal{U}_6^e, \mathcal{V}_6^e, \dot{\mathcal{U}}_6^e, \dot{\mathcal{V}}_6^e)(\hat{\mathcal{T}})$ are the coefficients of \mathbf{U}_1^e of order 6 in ξ . They are given by:

$$\begin{aligned}
\mathcal{U}_6^e(\hat{\mathcal{T}}) &= -\frac{\mu \cos \theta_0 (2 \cos^4 \theta_0 - 1) \left(60n\hat{\mathcal{T}} - 16 \sin(2n\hat{\mathcal{T}}) + \sin(4n\hat{\mathcal{T}}) \right) \cos(n\hat{\mathcal{T}})}{8n^2}, \\
\mathcal{V}_6^e(\hat{\mathcal{T}}) &= -\frac{\mu \sin \theta_0 (2 \sin^4 \theta_0 - 1) \left(60n\hat{\mathcal{T}} - 16 \sin(2n\hat{\mathcal{T}}) + \sin(4n\hat{\mathcal{T}}) \right) \cos(n\hat{\mathcal{T}})}{8n^2}, \\
\dot{\mathcal{U}}_6^e(\hat{\mathcal{T}}) &= -\frac{\mu \cos \theta_0 (2 \cos^4 \theta_0 - 1) \left[\left(33 - 35 \cos^2(n\hat{\mathcal{T}}) + 10 \cos^4(n\hat{\mathcal{T}}) \right) \cos(n\hat{\mathcal{T}}) - 15n\hat{\mathcal{T}} \sin(n\hat{\mathcal{T}}) \right]}{2n}, \\
\dot{\mathcal{V}}_6^e(\hat{\mathcal{T}}) &= -\frac{\mu \sin \theta_0 (2 \sin^4 \theta_0 - 1) \left[\left(33 - 35 \cos^2(n\hat{\mathcal{T}}) + 10 \cos^4(n\hat{\mathcal{T}}) \right) \cos(n\hat{\mathcal{T}}) - 15n\hat{\mathcal{T}} \sin(n\hat{\mathcal{T}}) \right]}{2n}.
\end{aligned} \tag{79}$$

565 *Proof.* See Appendix B.3. □

566 With this notation, we have

567 • $\mathcal{U}^e(\hat{\mathcal{T}}) = \mathcal{U}_0^e(\hat{\mathcal{T}}) + \mathcal{U}_6^e(\hat{\mathcal{T}})\xi^6 + \frac{\mu}{n}\mathcal{O}(\xi^8),$

568 • $\mathcal{V}^e(\hat{\mathcal{T}}) = \mathcal{V}_0^e(\hat{\mathcal{T}}) + \mathcal{V}_6^e(\hat{\mathcal{T}})\xi^6 + \frac{\mu}{n}\mathcal{O}(\xi^8),$

569 • $\dot{\mathcal{U}}^e(\hat{\mathcal{T}}) = \dot{\mathcal{U}}_0^e(\hat{\mathcal{T}}) + \dot{\mathcal{U}}_6^e(\hat{\mathcal{T}})\xi^6 + \mu\mathcal{O}(\xi^8),$

570 • $\dot{\mathcal{V}}^e(\hat{\mathcal{T}}) = \dot{\mathcal{V}}_0^e(\hat{\mathcal{T}}) + \dot{\mathcal{V}}_6^e(\hat{\mathcal{T}})\xi^6 + \mu\mathcal{O}(\xi^8).$

571 From Lemma 5 we have that:

$$\begin{aligned}
\mathcal{U}_6^e(\hat{\mathcal{T}}_0^*) &= -\frac{15(-1)^n \mu \pi \cos \theta_0 (2 \cos^4 \theta_0 - 1)}{2n}, \\
\mathcal{V}_6^e(\hat{\mathcal{T}}_0^*) &= -\frac{15(-1)^n \mu \pi \sin \theta_0 (2 \sin^4 \theta_0 - 1)}{2n}, \\
\dot{\mathcal{U}}_6^e(\hat{\mathcal{T}}_0^*) &= -\frac{4(-1)^n \mu \cos \theta_0 (2 \cos^4 \theta_0 - 1)}{n}, \\
\dot{\mathcal{V}}_6^e(\hat{\mathcal{T}}_0^*) &= -\frac{4(-1)^n \mu \sin \theta_0 (2 \sin^4 \theta_0 - 1)}{n}.
\end{aligned} \tag{80}$$

572 The time needed to reach the n minimum in the distance with the first primary can be obtained from
573 the following Lemma:

574 **Lemma 6.** *With the same hypotheses of Lemma 4, the time $\hat{\mathcal{T}}^*$ needed for the ejection solution \mathbf{U}^e to*
575 *reach the n minimum in the distance with the first primary is given by $\hat{\mathcal{T}}^* = \hat{\mathcal{T}}_0^* + \hat{\mathcal{T}}_1^*$, where $\hat{\mathcal{T}}_0^* = \pi$*
576 *and:*

$$\hat{\mathcal{T}}_1^* = \frac{15\mu\pi(3\cos(4\theta_0) + 1)}{8n^2}\xi^6 + \frac{\mu}{n^2}\mathcal{O}(\xi^8). \tag{81}$$

577 *Proof.* In order to compute the n minimum in the distance with the first primary we have to solve

$$\begin{aligned}
0 &= (\mathcal{U}^e \dot{\mathcal{U}}^e + \mathcal{V}^e \dot{\mathcal{V}}^e) (\hat{\mathcal{T}}^*) \\
&= ([\mathcal{U}_0^e + \mathcal{U}_1^e][\dot{\mathcal{U}}_0^e + \dot{\mathcal{U}}_1^e] + [\mathcal{V}_0^e + \mathcal{V}_1^e][\dot{\mathcal{V}}_0^e + \dot{\mathcal{V}}_1^e]) (\hat{\mathcal{T}}^*) \\
&= (\mathcal{U}_0^e \dot{\mathcal{U}}_0^e + \mathcal{V}_0^e \dot{\mathcal{V}}_0^e) (\hat{\mathcal{T}}^*) + \xi^6 (\mathcal{U}_0^e \dot{\mathcal{U}}_6^e + \mathcal{U}_6^e \dot{\mathcal{U}}_0^e + \mathcal{V}_0^e \dot{\mathcal{V}}_6^e + \mathcal{V}_6^e \dot{\mathcal{V}}_0^e) (\hat{\mathcal{T}}^*) + \mu \mathcal{O}(\xi^8) \\
&\quad + \xi^{12} (\mathcal{U}_6^e \dot{\mathcal{U}}_6^e + \mathcal{V}_6^e \dot{\mathcal{V}}_6^e) (\hat{\mathcal{T}}^*) + \frac{\mu^2}{n} \mathcal{O}(\xi^{14}) \\
&= (\mathcal{U}_0^e \dot{\mathcal{U}}_0^e + \mathcal{V}_0^e \dot{\mathcal{V}}_0^e) (\hat{\mathcal{T}}^*) + \xi^6 (\mathcal{U}_0^e \dot{\mathcal{U}}_6^e + \mathcal{U}_6^e \dot{\mathcal{U}}_0^e + \mathcal{V}_0^e \dot{\mathcal{V}}_6^e + \mathcal{V}_6^e \dot{\mathcal{V}}_0^e) (\hat{\mathcal{T}}^*) + \mu \mathcal{O}(\xi^8) \\
&= (\mathcal{U}_0^e \dot{\mathcal{U}}_0^e + \mathcal{V}_0^e \dot{\mathcal{V}}_0^e) (\hat{\mathcal{T}}_0^* + \hat{\mathcal{T}}_1^*) + \xi^6 (\mathcal{U}_0^e \dot{\mathcal{U}}_6^e + \mathcal{U}_6^e \dot{\mathcal{U}}_0^e + \mathcal{V}_0^e \dot{\mathcal{V}}_6^e + \mathcal{V}_6^e \dot{\mathcal{V}}_0^e) (\hat{\mathcal{T}}_0^* + \hat{\mathcal{T}}_1^*) \\
&\quad + \mu \mathcal{O}(\xi^8) \\
&= (\mathcal{U}_0^e \dot{\mathcal{U}}_0^e + \mathcal{V}_0^e \dot{\mathcal{V}}_0^e) (\hat{\mathcal{T}}_0^*) + \hat{\mathcal{T}}_1^* (\mathcal{U}_0^e \ddot{\mathcal{U}}_0^e + \dot{\mathcal{U}}_0^{e^2} + \mathcal{V}_0^e \ddot{\mathcal{V}}_0^e + \dot{\mathcal{V}}_0^{e^2}) (\hat{\mathcal{T}}_0^*) \\
&\quad + \xi^6 (\mathcal{U}_0^e \dot{\mathcal{U}}_6^e + \mathcal{U}_6^e \dot{\mathcal{U}}_0^e + \mathcal{V}_0^e \dot{\mathcal{V}}_6^e + \mathcal{V}_6^e \dot{\mathcal{V}}_0^e) (\hat{\mathcal{T}}_0^*) + \mu \mathcal{O}(\xi^8) \\
&= \hat{\mathcal{T}}_1^* n^2 + \xi^6 (\mathcal{U}_6^e \dot{\mathcal{U}}_0^e + \mathcal{V}_6^e \dot{\mathcal{V}}_0^e) (\hat{\mathcal{T}}_0^*) + \mu \mathcal{O}(\xi^8),
\end{aligned}$$

578 and therefore we have

$$\mathcal{T}_1^* = \frac{(\mathcal{U}_6^e \dot{\mathcal{U}}_0^e + \mathcal{V}_6^e \dot{\mathcal{V}}_0^e) (\hat{\mathcal{T}}_0^*)}{n^2} \xi^6 + \frac{\mu}{n^2} \mathcal{O}(\xi^8) = \frac{15\mu\pi(3\cos(4\theta_0) + 1)}{8n^2} \xi^6 + \frac{\mu}{n^2} \mathcal{O}(\xi^8). \quad (82)$$

579

□

580 Finally the angular momentum at $\hat{\mathcal{T}}^*$ is given by

581 **Lemma 7.** *With the same hypotheses of Lemma 4, the angular momentum of the ejection solution*
582 \mathcal{U}^e *at time $\hat{\mathcal{T}}^*$ is given by:*

$$\mathcal{M}(n, \theta_0) = -\frac{15\mu\pi \sin(4\theta_0)}{4} \xi^6 + \mu \mathcal{O}(\xi^8).$$

Proof.

$$\begin{aligned}
\mathcal{M}(n, \theta_0) &= (\mathcal{U}^e \dot{\mathcal{V}}^e - \mathcal{V}^e \dot{\mathcal{U}}^e) (\hat{\mathcal{T}}^*) \\
&= (\mathcal{U}_0^e \dot{\mathcal{V}}_0^e - \mathcal{V}_0^e \dot{\mathcal{U}}_0^e) (\hat{\mathcal{T}}^*) + \xi^6 (\mathcal{U}_0^e \dot{\mathcal{V}}_6^e + \mathcal{U}_6^e \dot{\mathcal{V}}_0^e - \mathcal{V}_0^e \dot{\mathcal{U}}_6^e - \mathcal{V}_6^e \dot{\mathcal{U}}_0^e) (\hat{\mathcal{T}}^*) + \mu \mathcal{O}(\xi^8) \\
&= (\mathcal{U}_0^e \dot{\mathcal{V}}_0^e - \mathcal{V}_0^e \dot{\mathcal{U}}_0^e) (\hat{\mathcal{T}}_0^*) + \hat{\mathcal{T}}_1^* (\mathcal{U}_0^e \dot{\mathcal{V}}_0^e - \mathcal{V}_0^e \dot{\mathcal{U}}_0^e) (\hat{\mathcal{T}}_0^*) + \frac{\mu^2}{n} \mathcal{O}(\xi^{12}) \\
&\quad + \xi^6 (\mathcal{U}_0^e \dot{\mathcal{V}}_6^e + \mathcal{U}_6^e \dot{\mathcal{V}}_0^e - \mathcal{V}_0^e \dot{\mathcal{U}}_6^e - \mathcal{V}_6^e \dot{\mathcal{U}}_0^e) (\hat{\mathcal{T}}_0^*) + \mu \mathcal{O}(\xi^8) \\
&= (\mathcal{U}_0^e \dot{\mathcal{V}}_0^e - \mathcal{V}_0^e \dot{\mathcal{U}}_0^e) (\hat{\mathcal{T}}_0^*) + \xi^6 \hat{\mathcal{T}}_6^* (\mathcal{U}_0^e \dot{\mathcal{V}}_0^e - \mathcal{V}_0^e \dot{\mathcal{U}}_0^e) (\hat{\mathcal{T}}_0^*) \\
&\quad + \xi^6 (\mathcal{U}_0^e \dot{\mathcal{V}}_6^e + \mathcal{U}_6^e \dot{\mathcal{V}}_0^e - \mathcal{V}_0^e \dot{\mathcal{U}}_6^e - \mathcal{V}_6^e \dot{\mathcal{U}}_0^e) (\hat{\mathcal{T}}_0^*) + \mu \mathcal{O}(\xi^8) \\
&= \xi^6 (\mathcal{U}_6^e \dot{\mathcal{V}}_0^e - \mathcal{V}_6^e \dot{\mathcal{U}}_0^e) (\hat{\mathcal{T}}_0^*) + \mu \mathcal{O}(\xi^8) \\
&= -\frac{15\mu\pi \sin(4\theta_0)}{4} \xi^6 + \mu \mathcal{O}(\xi^8).
\end{aligned}$$

583

□

584 In this way, applying the Implicit Function Theorem, we have that for $\xi \geq 0$ small enough we obtain
 585 that $\mathcal{M}(n, \theta_0)$ has four and only four roots in $[0, \pi)$ given by

$$\theta_0 = \frac{\pi m}{4} + \mathcal{O}(\xi^2), \quad m = 0, 1, 2, 3$$

586 regardless of the values of the mass parameter μ and n . We can characterize this n -EC orbits in the
 587 same way as in Theorem 2.

588 This concludes the proof of Theorem 1.

589 8 Results for the Hill problem

590 As we have seen in Section 3, Hill problem is a limit case of RTBP. In this way, the results obtained
 591 in the previous sections can easily be extrapolated to the case of Hill problem. In particular, if in (18)
 592 we introduce the new variables

$$\begin{cases} u_h = \sqrt{\frac{2}{K}} U_h, \\ v_h = \sqrt{\frac{2}{K}} V_h, \\ \tau = 2\sqrt{K} s, \end{cases} \quad (83)$$

593 we obtain the system

$$\begin{cases} \ddot{U} = -U + \frac{8(U^2 + V^2)\dot{V}}{K^{3/2}} + \frac{12[2(U^4 - 2U^2V^2 - V^4) + (U^2 + V^2)^2]U}{K^3}, \\ \ddot{V} = -V - \frac{8(U^2 + V^2)\dot{U}}{K^{3/2}} + \frac{12[2(V^4 - 2U^2V^2 - U^4) + (U^2 + V^2)^2]V}{K^3}, \end{cases} \quad (84)$$

594 which is the same system of equations that we have obtained in (34) imposing now $\mu = 1$ and recalling
 595 that $\varepsilon = 1/\sqrt{K}$. So we already know the solution of system (84) which is the one obtained for system
 596 (34) with $\mu = 1$.

597 In this way, using the extra symmetry (16b) of the Hill problem we obtain the following Corollary of
 598 Theorem 2:

599 **Corollary 8.1.** *In the Hill problem, for all $n \in \mathbb{N}$, there exists a $\hat{K}(n)$ such that for $K \geq \hat{K}(n)$ there*
 600 *exist exactly four n -EC orbits, which can be characterized by:*

- 601 • *Two n -EC orbits themselves symmetric with respect to the x axis and one symmetric to the other*
 602 *over the y axis. The corresponding families are γ_n and α_n and, when $C \rightarrow +\infty$, have initial*
 603 *angles 0 and $\pi/2$ respectively.*
- 604 • *Two n -EC orbits themselves symmetric with respect to the y axis and one symmetric to the other*
 605 *over the x axis. The corresponding families are δ_n and β_n and, when $C \rightarrow +\infty$, have initial*
 606 *angles $\pi/4$ and $3\pi/4$ respectively.*

607 It is important to note that the proof is exactly the same with the observation, as we have said before,
 608 that the families of orbits that were symmetric with respect to the x axis in the RTBP (α_n and γ_n) are
 609 now also symmetric one of the other with respect to the y axis, and the families that were symmetric
 610 one of the other in the restricted problem (β_n and δ_n) are now also symmetric themselves with respect
 611 to the y axis (see Figure 10).

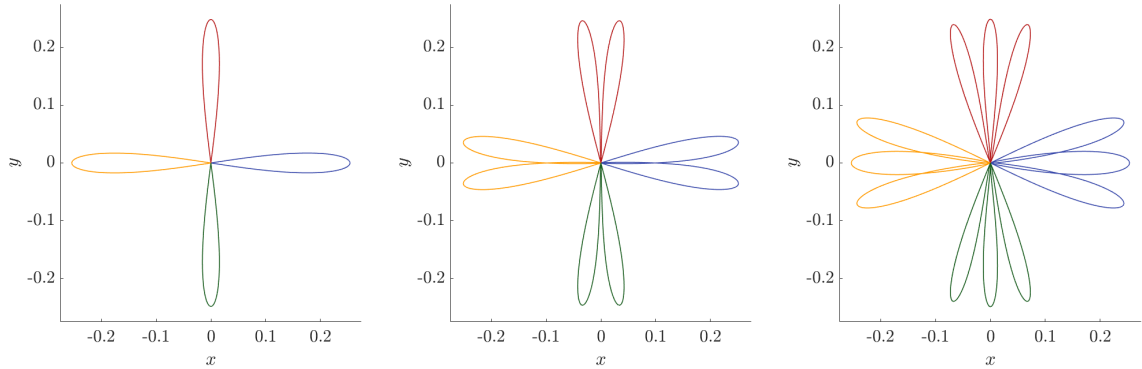


Figure 10: Trajectories of the four n -EC orbits α_n (yellow), β_n (green), γ_n (blue) and δ_n (red) for $n = 1, 2, 3$ (from left to right) and $K = 8$.

612 Furthermore, thanks to the fact that the polynomials \bar{P}_{2k} and \bar{Q}_{2k} disappear, it is not necessary
 613 to consider an expansion in terms of $\varepsilon = 1/\sqrt{K}$ and it can be considered directly an expansion on
 614 $\epsilon = 1/K^{3/2}$.

615 Similarly, if we introduce $K = Ln^{2/3}$, that is, we consider the change

$$\begin{cases} u_h = \frac{\sqrt{2}}{\sqrt{Ln^{1/3}}} \mathcal{U}_h, \\ v_h = \frac{\sqrt{2}}{\sqrt{Ln^{1/3}}} \mathcal{V}_h, \\ \hat{\mathcal{T}} = \frac{2\sqrt{L}}{n^{2/3}} s, \end{cases} \quad (85)$$

616 we obtain the same system of equations as (54) putting $\mu = 1$ and considering $\xi = 1/\sqrt{L}$. In this way
 617 we can obtain the following corollary of Theorem 1:

618 **Corollary 8.2.** *There exists an \hat{L} such that for $L \geq \hat{L}$ and for any value of $n \in \mathbb{N}$ and $K = Ln^{2/3}$,*
 619 *there exist exactly four n -EC orbits, which can be characterized in the same way as the previous*
 620 *corollary.*

621 In this way, if we do the numerical exploration to compute the n -EC orbits that exist for values of
 622 $K \geq K_L$ (see Figure 11) we see that, as expected by the Corollary 8.2, the value of \hat{K} grows with n .

623 Before going into more detail on the value of \hat{K} let us make a few comments about Figure 11. It is
 624 important to note that thanks to the extra symmetry we could only study the ejection orbits with
 625 $\theta_0 \in [0, \pi/2)$, but in order to visualize the evolution of the n -EC orbits we will consider the interval
 626 $\theta_0 \in [0, \pi)$ in Figure 11. In this figure we observe how at least the first new families of n -EC orbits
 627 that appear are born from two of the original families (α_n and γ_n , or β_n and δ_n) when the angle of
 628 ejection θ_0 is 0 and $\pi/2$ respectively (i.e. $\vartheta_0 = 0, \pi$) and collapse into the two other original families
 629 when the value of θ_0 is $\pi/4$ and $3\pi/4$ (i.e. $\vartheta_0 = \pi/2, 3\pi/2$) (see for example Figure 12).

630 These respective values are very particular, since when these bifurcations take place we have that the
 631 n -EC orbits are periodic or are part of a periodic EC orbit. In particular we have:

- 632 • If the θ_0 of β_n is 0 or $\pi/2$ (therefore θ_0 of δ_n is $\pi/2$ or 0) then we have periodic EC orbit formed
 633 by β_n and δ_n (see Figure 12 left). Analogously, if the θ_0 of α_n is $\pi/4$ or $3\pi/4$ (therefore θ_0 of
 634 γ_n is $3\pi/4$ or $\pi/4$) then we have periodic EC orbit formed by α_n and γ_n (see Figure 12 right).

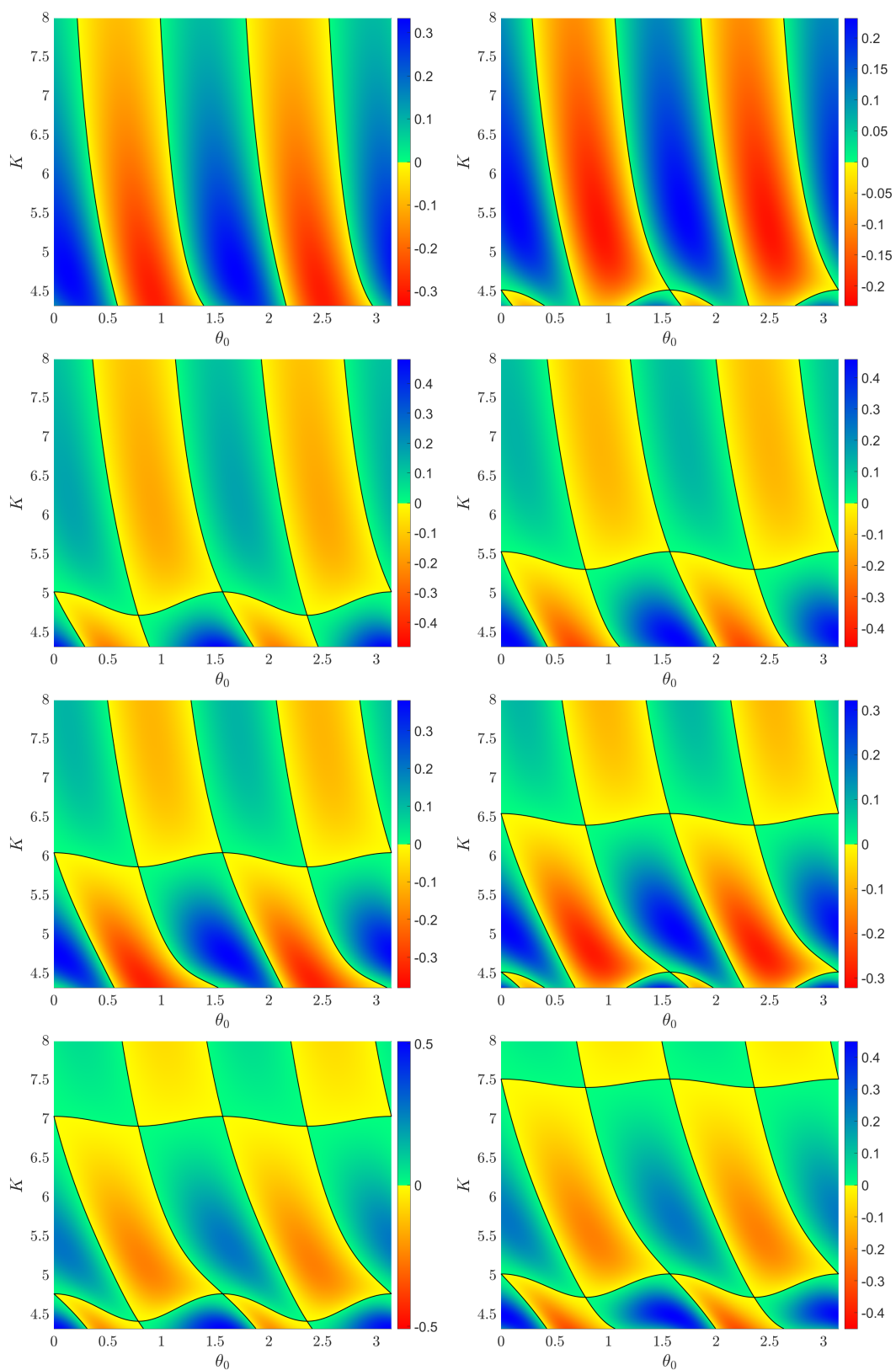


Figure 11: Value of the angular momentum of the ejection orbits at the n intersection with Σ_m for $K \in [K_{L_1}, 8]$ and $n = 3, \dots, 10$. In black the values corresponding to n -EC orbits.

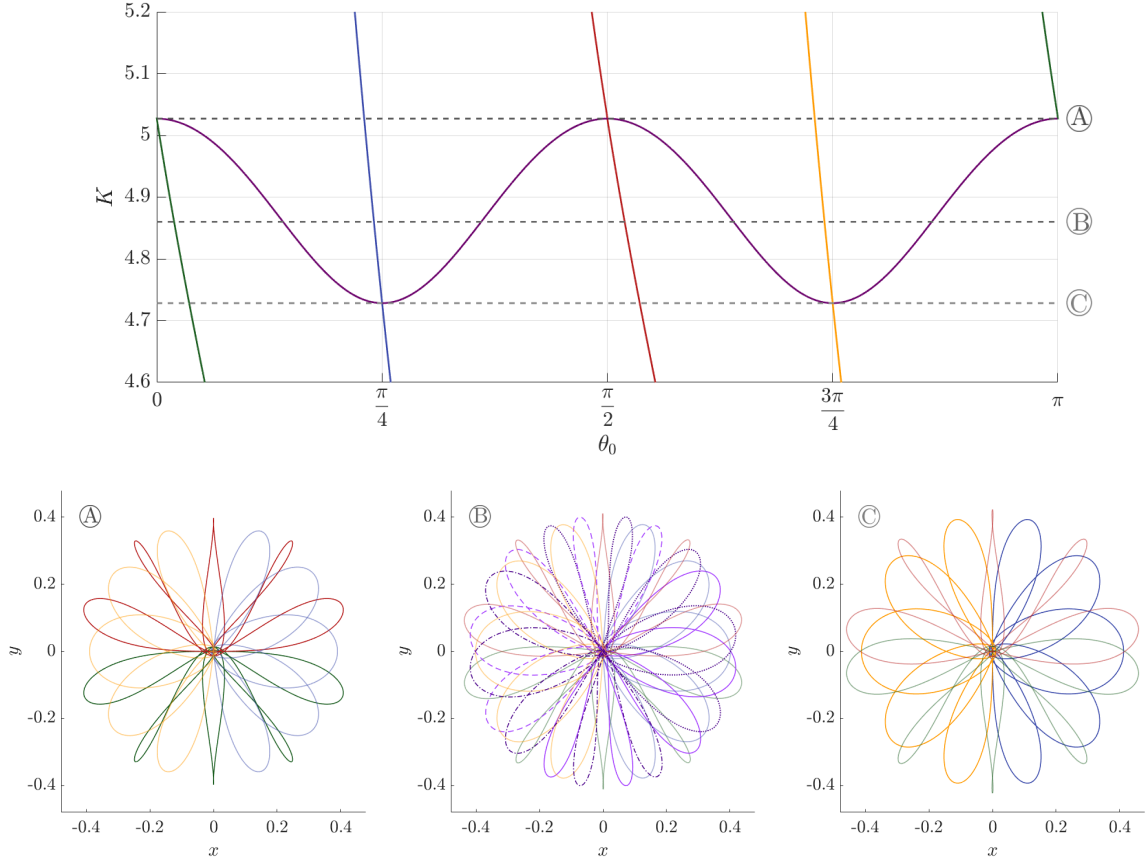


Figure 12: Top. Initial conditions for the 5-EC orbits corresponding to the families α_n (yellow), β_n (green), γ_n (blue), δ_n (red) and the new families of orbits (purple) as function of K . Bottom. The trajectories of the orbits (in correspondence with the previous color) that exist for the values of K denoted previously. The values of K correspond to the value of the bifurcation $K \approx 5.02714993$ (left), a value where we have eight 5-EC orbits $K = 4.86$ (middle) and the value of collapse $K \approx 4.72835275$.

- 635 • If the θ_0 of β_n is $\pi/4$ or $3\pi/4$ (therefore θ_0 of δ_n is $3\pi/4$ or $\pi/4$) then β_n and δ_n are periodic
636 EC orbits (see Figure 13 right). Analogously, if the θ_0 of α_n is 0 or $\pi/2$ (therefore θ_0 of γ_n is
637 $\pi/2$ or 0) then α_n and γ_n are periodic EC orbits (see Figure 13 left).

638 We have computed the value $\hat{K}(n)$ for $n = 1, \dots, 100$ (see Figure 14). It is important to remark that
639 the numerical value of $\hat{K}(n)$ obtained fits with the expression of the Corollary 8.2. In particular, if we
640 draw the curve $Ln^{2/3}$ with $L = 2^{2/3}$ we can see how it practically matches the value of the numerical
641 bound obtained for \hat{K} (see Figure 14).

642 To conclude, we have seen how not only does the value of $\hat{K}(n)$ follow the curve $Ln^{2/3}$ with $L = 2^{2/3}$,
643 but also the successive bifurcations (the values of K where appear new EC orbits) are closely related
644 to the curves $Ln^{2/3}$ with $L = (2/p)^{2/3}$ being p a natural number. In particular, in Figure 15 we can
645 see how the value of the successive bifurcations coincides with the curves $Ln^{2/3}$ with $L = (2/p)^{2/3}$
646 and $p = 1, \dots, 10$.

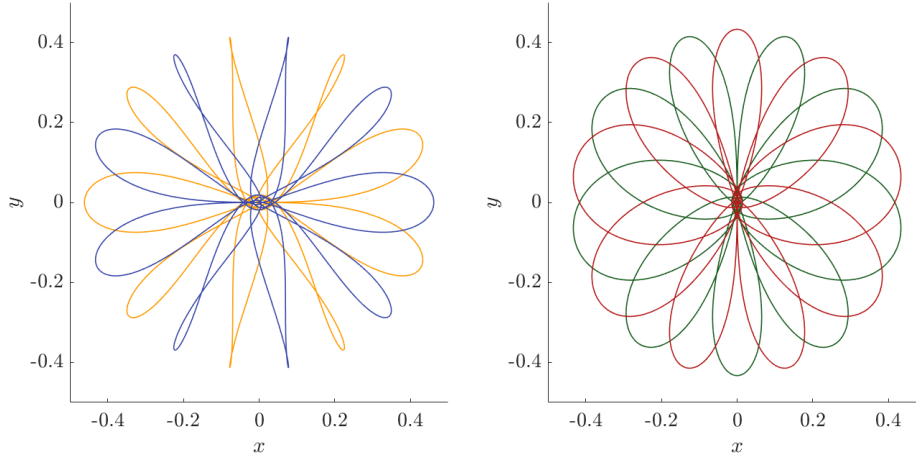


Figure 13: Trajectories of 9-EC periodic orbits associated with α_9 (yellow) and γ_9 (blue) for $K \approx 4.77318771$ (left) and β_9 (green) and δ_9 (red) for $K \approx 4.42215362$ (right).

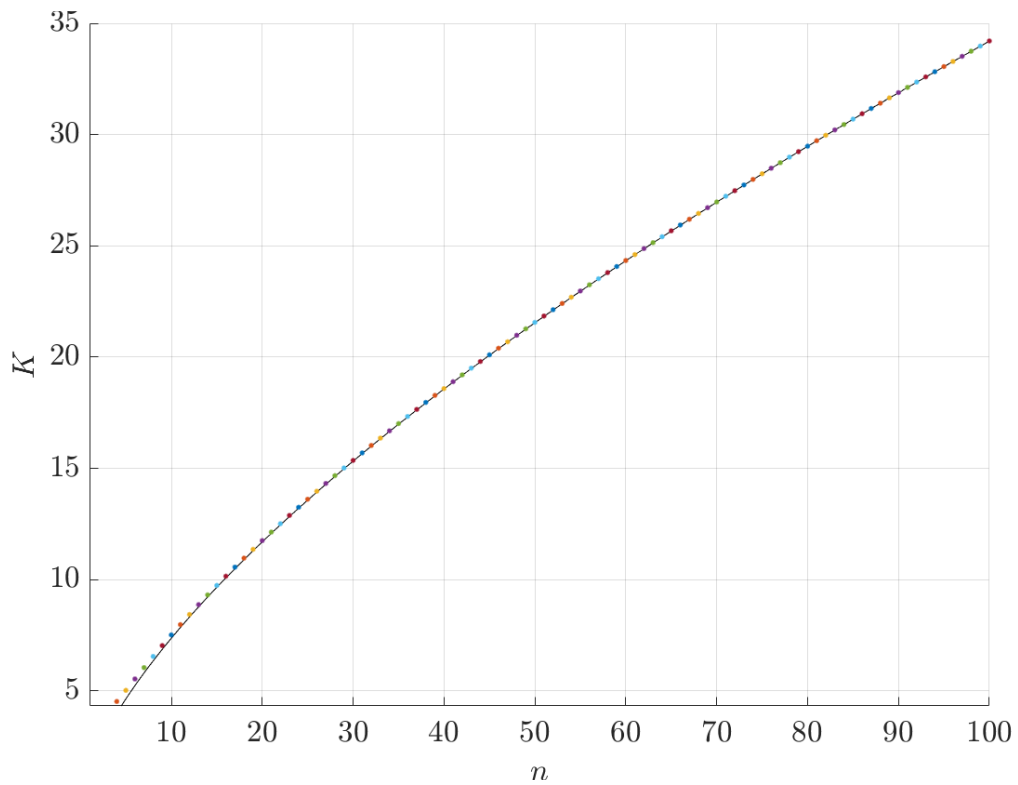


Figure 14: Dots: Values of $\hat{K}(n)$. Black line, curve $Ln^{2/3}$ with $L = 2^{2/3}$.

647 Data availability

648 The datasets generated during and/or analysed during the current study are available from the cor-
 649 responding author on reasonable request.

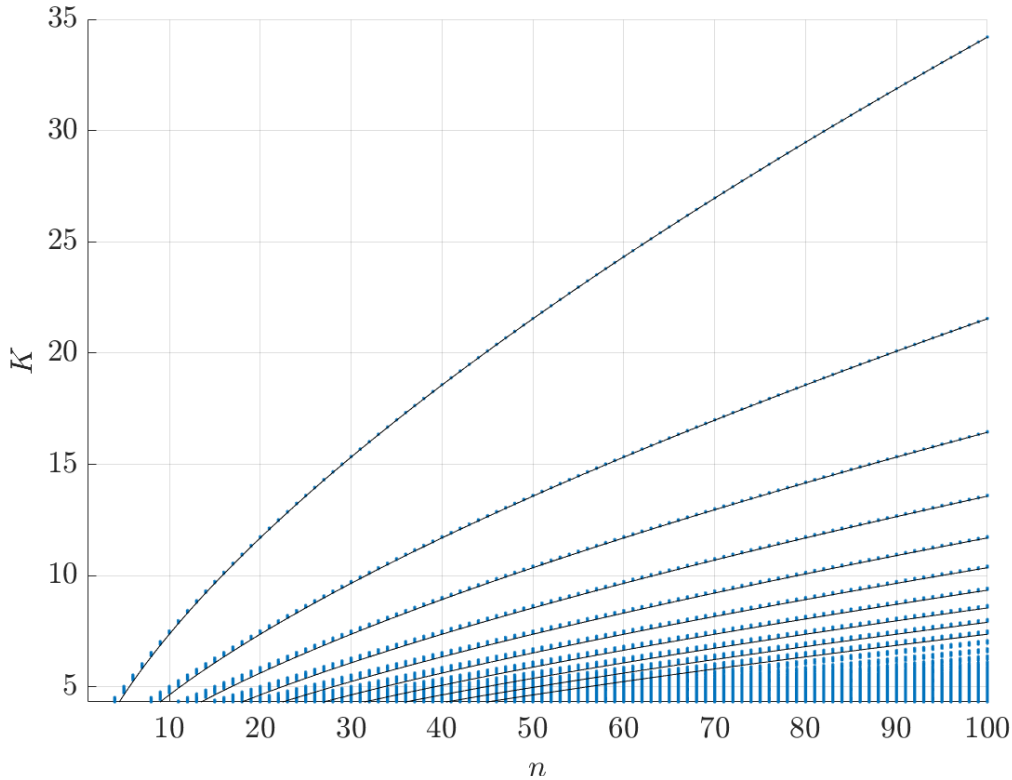


Figure 15: In color values of K where exists more than 4 n -EC orbits for $n = 1, \dots, 100$. The black lines correspond to the curves $Ln^{2/3}$ with $L = (2/p)^{2/3}$ and $p = 1, \dots, 10$.

9 Acknowledgements

This work is supported by the Spanish State Research Agency, through the Severo Ochoa and María de Maeztu Program for Centers and Units of Excellence in R&D (CEX2020-001084-M). T. M-Seara is supported by the Catalan Institution for Research and Advanced Studies via an ICREA Academia Prize 2019 and by the Spanish grants PGC2018-098676-B-100 and PID-2021-122954NB-100 funded by MCIN/AEI/10.13039/501100011033 and “ERDF A way of making Europe”. M. Ollé and Ó. Rodríguez were supported by the Spanish MINECO/FEDER grants PGC2018-100928-B-I00 and PID2021-123968NB-I00 (AEI/FEDER/UE).

References

- [1] S.A. Astakhov, A.D. Burbanks, S. Wiggins, and D. Farrelly. “Chaos-assisted capture of irregular moons”. In: *Nature* 423/6937 (2003), pp. 264–267. DOI: 10.1038/nature01622.
- [2] G. Bozis. “Sets of collision periodic orbits in the Restricted problem”. In: *Periodic orbits, stability and resonances*, G.E.O. Giacaglia (eds). Holland: D. Reidel Pub. Co. (1970), pp. 176–191.
- [3] A.F. Brunello, T. Uzer, and D. Farrelly. “Hydrogen atom in circularly polarized microwaves: Chaotic ionization via core scattering”. In: *Physical Review A* 55/5 (1997), pp. 3730–3745. DOI: 10.1103/PhysRevA.55.3730.
- [4] M. Capiński, S. Kepley, and J. D. Mireles. “Computer assisted proofs for transverse collision and near collision orbits in the restricted three body problem.”

- 668 [5] A. Chenciner and J. Llibre. “A note on the existence of invariant punctured tori in the planar
669 circular restricted three-body problem”. In: *Ergodic Theory and Dynamical Systems* 8/8* (1988),
670 pp. 63–72. DOI: 10.1017/s0143385700009330.
- 671 [6] R. L. Devaney. “Singularities in Classical Celestial Mechanics”. In: *Ergodic Theory and Dynamical
672 Systems I, Proceedings Special year, Maryland*. 1981, pp. 211–333. DOI: 10.1007/978-1-
673 4899-6696-4_7.
- 674 [7] J.R. Dormand and J.P. Prince. “A family of embedded Runge-Kutta formulae”. In: *J. Computat.
675 App. Math.* 6/1 (1980), pp. 19–26. DOI: 10.1016/0771-050X(80)90013-3.
- 676 [8] B. Érdi. “Global Regularization of the Restricted Problem of Three Bodies”. In: *Celestial Me-
677 chanics and Dynamical Astronomy* 90 (2004), pp. 35–42. DOI: 10.1007/s10569-004-8105-z.
- 678 [9] M. Hénon. “Exploration numérique du problème restreint I. Masses égales”. In: *Ann. d’Astrophys.*
679 28 (1965), pp. 499–511.
- 680 [10] M. Hénon. “Numerical exploration of the Restricted Problem V. Hill’s case: Periodic orbits and
681 Their Stability”. In: *Astron. Astrophys.* 1 (1969), pp. 223–238.
- 682 [11] J.R. Hurley, C.A. Tout, and O.R. Pols. “Evolution of binary stars and the effect of tides on
683 binary populations”. In: *Mont. Not. of the Roy. Astr. Soc.* 329/4 (2002), pp. 897–928. DOI:
684 10.1046/j.1365-8711.2002.05038.x.
- 685 [12] A. Jorba and M. Zou. “A software package for the numerical integration of ODE’s by means of
686 high-order taylor methods”. In: *Exp. Maths.* 14 (2005), pp. 99–117. DOI: 10.1080/10586458.
687 2005.10128904.
- 688 [13] E. A. Lacombe and J. Llibre. “Transversal ejection-collision orbits for the restricted problem
689 and the Hill’s problem with applications”. In: *Journal of Differential Equations* 74/1 (1988),
690 pp. 69–85. DOI: 10.1016/0022-0396(88)90019-8.
- 691 [14] T. Levi-Civita. “Sur la résolution qualitative du problème restreint des trois corps”. In: *Acta
692 Mathematica* 30 (1906), pp. 305–327. DOI: 10.1007/BF02418577.
- 693 [15] J. Llibre. “On the restricted three-body problem when the mass parameter is small”. In: *Celestial
694 Mechanics* 28 (1982), pp. 83–105. DOI: 10.1007/bf01230662.
- 695 [16] R. McGehee. “Triple Collision in the Collinear Three-Body Problem”. In: *Inventiones mathe-
696 maticae* 27 (1974), pp. 191–227. DOI: 10.1007/BF01390175.
- 697 [17] J.L. Modisette and Y. Kondo. “Mass Transfer between Binary Stars”. In: *Symposium - Interna-
698 tional Astronomical Union* 88 (1980), pp. 123–126. DOI: 10.1017/s0074180900064706.
- 699 [18] Jan Nagler. “Crash test for the Copenhagen problem”. In: *Physical Review E* 69/6 (2004),
700 p. 066218. DOI: 10.1103/physreve.69.066218.
- 701 [19] Jan Nagler. “Crash test for the restricted three-body problem”. In: *Physical Review E* 71/2
702 (2005), p. 026227. DOI: 10.1103/PhysRevE.71.026227.
- 703 [20] M. Ollé. “To and fro motion for the hydrogen atom in a circularly polarized microwave field”. In:
704 *Communications in Nonlinear Science and Numerical Simulation* 54 (2018), pp. 286–301. DOI:
705 10.1016/j.cnsns.2017.05.026.
- 706 [21] M. Ollé, Ó. Rodríguez, and J. Soler. “Analytical and numerical results on families of n-ejection-
707 collision orbits in the RTBP”. In: *Communications in Nonlinear Science and Numerical Simu-
708 lation* 90 (2020), p. 105294. DOI: 10.1016/j.cnsns.2020.105294.
- 709 [22] M. Ollé, Ó. Rodríguez, and J. Soler. “Ejection-collision orbits in the RTBP”. In: *Communications
710 in Nonlinear Science and Numerical Simulation* 55 (2018), pp. 298–315. DOI: 10.1016/j.cnsns.
711 2017.07.013.
- 712 [23] M. Ollé, Ó. Rodríguez, and J. Soler. “Regularisation in Ejection-Collision Orbits of the RTBP”.
713 In: *Recent Advances in Pure and Applied Mathematics* (2020), pp. 35–47. DOI: 10.1007/978-
714 3-030-41321-7_3.

- 715 [24] M. Ollé, Ó. Rodríguez, and J. Soler. “Transit regions and ejection/collision orbits in the RTBP.”
716 In: *Communications in Nonlinear Science and Numerical Simulation* 94 (2021), p. 105550. DOI:
717 10.1016/j.cnsns.2020.105550.
- 718 [25] R. Paez and M. Guzzo. “A study of temporary captures and collisions in the Circular Restricted
719 Three-Body Problem with normalizations of the Levi-Civita Hamiltonian”. In: *International*
720 *Journal of Non-Linear Mechanics* 120 (2020). DOI: 10.1016/j.ijnonlinmec.2020.103417.
- 721 [26] J.E. Pringle and R.A. Wade. *Interacting Binary Stars*. Cambridge Univ. Press, 1985.
- 722 [27] E. L. Stiefel and G. Scheifele. *Linear and Regular Celestial Mechanics*. Springer-Verlag, 1971.
- 723 [28] V.G. Szebehely. *Theory of Orbits - The Restricted Problem of Three Bodies*. Academic Press,
724 1967.
- 725 [29] R.A. Witjers, M.B. Davies, and C. Tout. “Evolutionary processes in binary stars”. In: *Proceedings*
726 *of the NATO ASI on evolutionary processes in binary stars* (1995).

727 A Values of the solutions

$$U_7(\tau, \theta_0) = 0,$$

$$V_7(\tau, \theta_0) = 0,$$

$$U_8(\tau, \theta_0) = \frac{\mu(1-\mu)^{1/3}}{6} [105\tau \cos \tau - (48 + 87 \cos^2 \tau - 38 \cos^4 \tau + 8 \cos^6 \tau) \sin \tau] \\ * (5 \cos^6 \theta_0 - 6 \cos^2 \theta_0 + 2) \cos \theta_0,$$

$$V_8(\tau, \theta_0) = -\frac{\mu(1-\mu)^{1/3}}{6} [105\tau \cos \tau - (48 + 87 \cos^2 \tau - 38 \cos^4 \tau + 8 \cos^6 \tau) \sin \tau] \\ * (5 \sin^6 \theta_0 - 6 \sin^2 \theta_0 + 2) \sin \theta_0,$$

$$U_9(\tau, \theta_0) = -\frac{1}{24} \left[4(\tau - \cos \tau \sin \tau)^3 \sin \tau - \mu \left(3\tau(23 + 144 \cos^2 \tau + 8 \cos^4 \tau) \sin \tau \right. \right. \\ \left. \left. - (379 - 217 \cos^2 \tau - 178 \cos^4 \tau + 16 \cos^6 \tau) \cos \tau - 480\tau(1 + 6 \cos^2 \tau) \sin \tau \cos^2 \theta_0 \right. \right. \\ \left. \left. + 32(81 - 53 \cos^2 \tau - 32 \cos^4 \tau + 4 \cos^6 \tau) \cos \tau \cos^2 \theta_0 - 360\tau^2 \cos \tau \cos^4 \theta_0 \right. \right. \\ \left. \left. + 240\tau(3 + 15 \cos^2 \tau - \cos^4 \tau) \sin \tau \cos^4 \theta_0 \right. \right. \\ \left. \left. - 8(374 - 257 \cos^2 \tau - 143 \cos^4 \tau + 26 \cos^6 \tau) \cos \tau \cos^4 \theta_0 \right) \right] \sin \theta_0,$$

$$V_9(\tau, \theta_0) = \frac{1}{24} \left[4(\tau - \cos \tau \sin \tau)^3 \sin \tau - \mu \left(3\tau(23 + 144 \cos^2 \tau + 8 \cos^4 \tau) \sin \tau \right. \right. \\ \left. \left. - (379 - 217 \cos^2 \tau - 178 \cos^4 \tau + 16 \cos^6 \tau) \cos \tau - 480\tau(1 + 6 \cos^2 \tau) \sin \tau \sin^2 \theta_0 \right. \right. \\ \left. \left. + 32(81 - 53 \cos^2 \tau - 32 \cos^4 \tau + 4 \cos^6 \tau) \cos \tau \sin^2 \theta_0 - 360\tau^2 \cos \tau \sin^4 \theta_0 \right. \right. \\ \left. \left. + 240\tau(3 + 15 \cos^2 \tau - \cos^4 \tau) \sin \tau \sin^4 \theta_0 \right. \right. \\ \left. \left. - 8(374 - 257 \cos^2 \tau - 143 \cos^4 \tau + 26 \cos^6 \tau) \cos \tau \sin^4 \theta_0 \right) \right] \cos \theta_0,$$

$$U_{10}(\tau, \theta_0) = \frac{\mu(1-\mu)^{2/3}}{8} \left[315\tau \cos \tau - (128 + 325 \cos^2 \tau - 210 \cos^4 \tau + 88 \cos^6 \tau \right. \\ \left. - 16 \cos^8 \tau) \sin \tau \right] (3 - 20 \cos^2 \theta_0 + 30 \cos^4 \theta_0 - 14 \cos^8 \theta_0) \cos \theta_0,$$

$$V_{10}(\tau, \theta_0) = \frac{\mu(1-\mu)^{2/3}}{8} \left[315\tau \cos \tau - (128 + 325 \cos^2 \tau - 210 \cos^4 \tau + 88 \cos^6 \tau - 16 \cos^8 \tau) \sin \tau \right] (3 - 20 \sin^2 \theta_0 + 30 \sin^4 \theta_0 - 14 \sin^8 \theta_0) \sin \theta_0.$$

Then, writing the function $U\dot{U} + V\dot{V}$ as an expansion series in ε and collecting terms of the same order, we can successively find the terms τ_i^* of order $i = 7, \dots, 10$ from $(U\dot{U} + V\dot{V})(\tau^*) = 0$:

$$\begin{aligned} \tau_7^*(n, \theta_0) &= 0, \\ \tau_8^*(n, \theta_0) &= -\frac{35\mu(1-\mu)^{1/3}n\pi \cos(2\theta_0)(5 \cos^2(2\theta_0) - 3)}{4}, \\ \tau_9^*(n, \theta_0) &= \frac{15\mu n^2 \pi^2 \sin(4\theta_0)}{2}, \\ \tau_{10}^*(n, \theta_0) &= \frac{315\mu(1-\mu)^{2/3}n\pi(13 - 10 \cos(4\theta_0) - 35 \cos^2(4\theta_0))}{256}. \end{aligned}$$

728 Now we are ready to compute the explicit expression for the angular momentum $M(n, \theta_0) = (U\dot{V} -$
729 $V\dot{U})(\tau^*)$ up to order 10 which is the following:

$$\begin{aligned} M(n, \theta_0) &= -\frac{15\mu n \pi \sin(4\theta_0)}{4} \varepsilon^6 + \frac{105\mu(1-\mu)^{1/3}n\pi(\sin(2\theta_0) + 5 \sin(6\theta_0))}{64} \varepsilon^8 + \frac{15\mu n^2 \pi^2 \cos(4\theta_0)}{2} \varepsilon^9 \\ &\quad - \frac{315\mu(1-\mu)^{2/3}n\pi(2 \sin(4\theta_0) + 7 \sin(8\theta_0))}{128} \varepsilon^{10} + \mathcal{O}(\varepsilon^{11}). \end{aligned}$$

730 which is precisely (51).

731 B Proof of the auxiliary lemmas

732 We must prove Lemmas 2, 3 and 5. First, let us fix some notation. Given a matrix $A = (a_{ij})_{i,j=1,\dots,4}$,
733 we denote the new matrix

$$|A| = (|a_{ij}|)_{i,j=1,\dots,4}.$$

734 Analogously for vectors $\mathbf{v} = (v_1, \dots, v_4)$:

$$|\mathbf{v}| = (|v_1|, \dots, |v_4|),$$

735 and given two vectors $\mathbf{v} = (v_1, \dots, v_4)$, $\mathbf{w} = (w_1, \dots, w_4)$, we will say that

$$\mathbf{v} \leq \mathbf{w} \quad \text{if} \quad v_i \leq w_i \quad \forall i = 1, \dots, 4.$$

736 Similarly with matrices $A \leq B$.

737 With this notation we have:

$$|A\mathbf{v}| \leq |A||\mathbf{v}|.$$

738 During this section we will use M to denote any constant which appears in the bounds and is inde-
739 pendent of ξ , μ and $n \in \mathbb{N}$.

740 **Lemma 8.** *The fundamental matrix X for system (76) can be expressed as*

$$X(\hat{\mathcal{T}}) = \begin{pmatrix} \cos(n\hat{\mathcal{T}}) + \mathcal{O}(\xi^3) & \mathcal{O}(\xi^3) & \frac{\sin(n\hat{\mathcal{T}}) + \mathcal{O}(\xi^3)}{n} & \frac{1}{n}\mathcal{O}(\xi^3) \\ \mathcal{O}(\xi^3) & \cos(n\hat{\mathcal{T}}) + \mathcal{O}(\xi^3) & \frac{1}{n}\mathcal{O}(\xi^3) & \frac{\sin(n\hat{\mathcal{T}}) + \mathcal{O}(\xi^3)}{n} \\ -n \sin(n\hat{\mathcal{T}}) + n\mathcal{O}(\xi^3) & n\mathcal{O}(\xi^3) & \cos(n\hat{\mathcal{T}}) + \mathcal{O}(\xi^3) & \mathcal{O}(\xi^3) \\ n\mathcal{O}(\xi^3) & -n \sin(n\hat{\mathcal{T}}) + n\mathcal{O}(\xi^3) & \mathcal{O}(\xi^3) & \cos(n\hat{\mathcal{T}}) + \mathcal{O}(\xi^3) \end{pmatrix},$$

741 *and its inverse matrix as*

$$X^{-1}(\hat{\mathcal{T}}) = \begin{pmatrix} \cos(n\hat{\mathcal{T}}) + \mathcal{O}(\xi^3) & \mathcal{O}(\xi^3) & \frac{-\sin(n\hat{\mathcal{T}}) + \mathcal{O}(\xi^3)}{n} & \frac{1}{n}\mathcal{O}(\xi^3) \\ \mathcal{O}(\xi^3) & \cos(n\hat{\mathcal{T}}) + \mathcal{O}(\xi^3) & \frac{1}{n}\mathcal{O}(\xi^3) & \frac{-\sin(n\hat{\mathcal{T}}) + \mathcal{O}(\xi^3)}{n} \\ n \sin(n\hat{\mathcal{T}}) + n\mathcal{O}(\xi^3) & n\mathcal{O}(\xi^3) & \cos(n\hat{\mathcal{T}}) + \mathcal{O}(\xi^3) & \mathcal{O}(\xi^3) \\ n\mathcal{O}(\xi^3) & n \sin(n\hat{\mathcal{T}}) + n\mathcal{O}(\xi^3) & \mathcal{O}(\xi^3) & \cos(n\hat{\mathcal{T}}) + \mathcal{O}(\xi^3) \end{pmatrix}.$$

742 *Proof.* Consider the general solution \mathbf{u}_0 of system (58a) given by (64), (65) and (66), we can express
743 the fundamental matrix of the system

$$\dot{\mathbf{u}}_1 = D\mathcal{F}_0(\mathbf{u}_0)\mathbf{u}_1,$$

744 as

$$X = RA,$$

745 where

$$R = \begin{pmatrix} \cos(-t/2) & -\sin(-t/2) & 0 & 0 \\ \sin(-t/2) & \cos(-t/2) & 0 & 0 \\ 0 & 0 & \cos(-t/2) & -\sin(-t/2) \\ 0 & 0 & \sin(-t/2) & \cos(-t/2) \end{pmatrix}, \quad (86)$$

746 and A is the matrix with rows

$$\begin{aligned} \mathbf{A}_1(\hat{\mathcal{T}}) &= \left[\frac{\partial \bar{\mathcal{U}}_0}{\partial \mathbf{u}_0(0)} + \frac{\bar{\mathcal{V}}_0}{2} \frac{\partial t}{\partial \mathbf{u}_0(0)} \right] (\hat{\mathcal{T}}), \\ \mathbf{A}_2(\hat{\mathcal{T}}) &= \left[\frac{\partial \bar{\mathcal{V}}_0}{\partial \mathbf{u}_0(0)} - \frac{\bar{\mathcal{U}}_0}{2} \frac{\partial t}{\partial \mathbf{u}_0(0)} \right] (\hat{\mathcal{T}}), \\ \mathbf{A}_3(\hat{\mathcal{T}}) &= \left[\frac{\partial \dot{\bar{\mathcal{U}}}_0}{\partial \mathbf{u}_0(0)} + 2(\bar{\mathcal{U}}_0^2 + 3\bar{\mathcal{V}}_0^2) \xi^3 \frac{\partial \bar{\mathcal{V}}_0}{\partial \mathbf{u}_0(0)} + 4\bar{\mathcal{U}}_0 \bar{\mathcal{V}}_0 \xi^3 \frac{\partial \bar{\mathcal{U}}_0}{\partial \mathbf{u}_0(0)} + \frac{\dot{\bar{\mathcal{V}}}_0 - 2(\bar{\mathcal{U}}_0^2 + \bar{\mathcal{V}}_0^2)\bar{\mathcal{U}}_0 \xi^3}{2} \frac{\partial t}{\partial \mathbf{u}_0(0)} \right] (\hat{\mathcal{T}}), \\ \mathbf{A}_4(\hat{\mathcal{T}}) &= \left[\frac{\partial \dot{\bar{\mathcal{V}}}_0}{\partial \mathbf{u}_0(0)} - 2(3\bar{\mathcal{U}}_0^2 + \bar{\mathcal{V}}_0^2) \xi^3 \frac{\partial \bar{\mathcal{U}}_0}{\partial \mathbf{u}_0(0)} - 4\bar{\mathcal{U}}_0 \bar{\mathcal{V}}_0 \xi^3 \frac{\partial \bar{\mathcal{V}}_0}{\partial \mathbf{u}_0(0)} - \frac{\dot{\bar{\mathcal{U}}}_0 + 2(\bar{\mathcal{U}}_0^2 + \bar{\mathcal{V}}_0^2)\bar{\mathcal{V}}_0 \xi^3}{2} \frac{\partial t}{\partial \mathbf{u}_0(0)} \right] (\hat{\mathcal{T}}), \end{aligned} \quad (87)$$

747 where $\bar{\mathbf{u}}_0$ is given by (64).

748 Note that we are interested in solving equations (76), which correspond to the ejection orbits \mathbf{u}_0^e ,
749 that have initial conditions $(0, 0, n \cos \theta_0, n \sin \theta_0)$. So we must compute the fundamental matrix X
750 with $\mathbf{u}_0(\hat{\mathcal{T}}) = \mathbf{u}_0^e(\hat{\mathcal{T}})$. We denote by A^e and R^e the corresponding matrices. Recall also that the
751 expression of t is given by (70) and the explicit elements of A^e are provided in Appendix C.

752 In this way, we can express A^e and R^e as

$$A^e = \begin{pmatrix} \cos(n\hat{\mathcal{T}}) + \mathcal{O}(\xi^3) & \mathcal{O}(\xi^3) & \frac{\sin(n\hat{\mathcal{T}}) + \mathcal{O}(\xi^3)}{n} & \frac{1}{n}\mathcal{O}(\xi^3) \\ \mathcal{O}(\xi^3) & \cos(n\hat{\mathcal{T}}) + \mathcal{O}(\xi^3) & \frac{1}{n}\mathcal{O}(\xi^3) & \frac{\sin(n\hat{\mathcal{T}}) + \mathcal{O}(\xi^3)}{n} \\ -n\sin(n\hat{\mathcal{T}}) + n\mathcal{O}(\xi^3) & n\mathcal{O}(\xi^3) & \cos(n\hat{\mathcal{T}}) + \mathcal{O}(\xi^3) & \mathcal{O}(\xi^3) \\ n\mathcal{O}(\xi^3) & -n\sin(n\hat{\mathcal{T}}) + n\mathcal{O}(\xi^3) & \mathcal{O}(\xi^3) & \cos(n\hat{\mathcal{T}}) + \mathcal{O}(\xi^3) \end{pmatrix},$$

$$R^e = Id + \begin{pmatrix} \mathcal{O}(\xi^6) & \mathcal{O}(\xi^3) & 0 & 0 \\ \mathcal{O}(\xi^3) & \mathcal{O}(\xi^6) & 0 & 0 \\ 0 & 0 & \mathcal{O}(\xi^6) & \mathcal{O}(\xi^3) \\ 0 & 0 & \mathcal{O}(\xi^3) & \mathcal{O}(\xi^6) \end{pmatrix},$$

753 and therefore,

$$X(\hat{\mathcal{T}}) = \begin{pmatrix} \cos(n\hat{\mathcal{T}}) + \mathcal{O}(\xi^3) & \mathcal{O}(\xi^3) & \frac{\sin(n\hat{\mathcal{T}}) + \mathcal{O}(\xi^3)}{n} & \frac{1}{n}\mathcal{O}(\xi^3) \\ \mathcal{O}(\xi^3) & \cos(n\hat{\mathcal{T}}) + \mathcal{O}(\xi^3) & \frac{1}{n}\mathcal{O}(\xi^3) & \frac{\sin(n\hat{\mathcal{T}}) + \mathcal{O}(\xi^3)}{n} \\ -n\sin(n\hat{\mathcal{T}}) + n\mathcal{O}(\xi^3) & n\mathcal{O}(\xi^3) & \cos(n\hat{\mathcal{T}}) + \mathcal{O}(\xi^3) & \mathcal{O}(\xi^3) \\ n\mathcal{O}(\xi^3) & -n\sin(n\hat{\mathcal{T}}) + n\mathcal{O}(\xi^3) & \mathcal{O}(\xi^3) & \cos(n\hat{\mathcal{T}}) + \mathcal{O}(\xi^3) \end{pmatrix}.$$

754 The expression for $X^{-1}(\hat{\mathcal{T}})$ can be found in a similar way.

755

□

756 B.1 Proof of Lemma 2

757 From (73) and (75) we have

$$\mathcal{H}\{\mathbf{0}\}(\hat{\mathcal{T}}) = X(\hat{\mathcal{T}}) \int_0^{\hat{\mathcal{T}}} X^{-1}(\hat{\mathcal{T}}) \mathcal{G}(\mathbf{0}) d\hat{\mathcal{T}} = \mu X(\hat{\mathcal{T}}) \int_0^{\hat{\mathcal{T}}} X^{-1}(\hat{\mathcal{T}}) \mathcal{F}_1(\mathcal{U}_0^e(\hat{\mathcal{T}})) d\hat{\mathcal{T}}, \quad (88)$$

758 so, the first step is to bound the components of $\mathcal{F}_1(\mathcal{U}_0^e)$ (see (57)).

759 Concerning the expansions involving r_2 in (55), we have

$$\begin{aligned} \left(\frac{1}{r_2} - 1\right) &= -\frac{2(1-\mu)^{1/3}(\mathcal{U}^2 - \mathcal{V}^2)}{n^{2/3}} \xi^2 + \frac{4(1-\mu)^{2/3}(\mathcal{U}^4 - 4\mathcal{U}^2\mathcal{V}^2 + \mathcal{V}^4)}{n^{4/3}} \xi^4 + \frac{1}{n^2} \mathcal{O}(\xi^6), \\ \frac{1}{r_2^3} &= 1 - \frac{6(1-\mu)^{1/3}(\mathcal{U}^2 - \mathcal{V}^2)}{n^{2/3}} \xi^2 + \frac{1}{n^{4/3}} \mathcal{O}(\xi^4), \end{aligned} \quad (89)$$

760 where the symbol \mathcal{O} refers to terms bounded for bounded \mathcal{U} and any $\mu \in (0, 1)$ and $n \in \mathbb{N}$. Thus, we
761 obtain

$$\mathcal{F}_1(\mathcal{U}, \mathcal{V}) = \begin{pmatrix} 0 \\ 0 \\ 24(\mathcal{U}^4 - 2\mathcal{U}^2\mathcal{V}^2 - \mathcal{V}^4) \mathcal{U} \xi^6 + \frac{1}{n^{2/3}} \mathcal{O}(\xi^8) \\ 24(\mathcal{V}^4 - 2\mathcal{U}^2\mathcal{V}^2 - \mathcal{U}^4) \mathcal{V} \xi^6 + \frac{1}{n^{2/3}} \mathcal{O}(\xi^8) \end{pmatrix}. \quad (90)$$

762 Let us bound $|\mathcal{F}_1(\mathcal{U}_0^e, \mathcal{V}_0^e)|$. Recall that (see (69)) we have that,

$$\mathcal{U}_0^{e2}(\theta_0, \hat{\mathcal{T}}) + \mathcal{V}_0^{e2}(\theta_0, \hat{\mathcal{T}}) = \sin^2(n\hat{\mathcal{T}}) \leq 1,$$

763 Therefore, $|\mathcal{U}_0^e| \leq 1$, $|\mathcal{V}_0^e| \leq 1$ are bounded and consequently, for ξ small enough:

$$|\mathcal{F}_1(\mathcal{U}_0^e, \mathcal{V}_0^e)| \leq M \begin{pmatrix} 0 \\ \xi^6 + \frac{1}{n^{2/3}} \mathcal{O}(\xi^8) \\ \xi^6 + \frac{1}{n^{2/3}} \mathcal{O}(\xi^8) \end{pmatrix} = M \left[\xi^6 + \frac{1}{n^{2/3}} \mathcal{O}(\xi^8) \right] \begin{pmatrix} 0 \\ 0 \\ 1 \\ 1 \end{pmatrix} \leq M \xi^6 \begin{pmatrix} 0 \\ 0 \\ 1 \\ 1 \end{pmatrix}. \quad (91)$$

764 and the constant M is independent of μ and n .

765 By Lemma 8 we can bound $|X| \leq \mathcal{M}$ and $|X^{-1}| \leq \mathcal{M}$ where

$$\mathcal{M} = \begin{pmatrix} 1 + \mathcal{O}(\xi^3) & \mathcal{O}(\xi^3) & \frac{1 + \mathcal{O}(\xi^3)}{n} & \frac{1}{n} \mathcal{O}(\xi^3) \\ \mathcal{O}(\xi^3) & 1 + \mathcal{O}(\xi^3) & \frac{1}{n} \mathcal{O}(\xi^3) & \frac{1 + \mathcal{O}(\xi^3)}{n} \\ n + n \mathcal{O}(\xi^3) & n \mathcal{O}(\xi^3) & 1 + \mathcal{O}(\xi^3) & \mathcal{O}(\xi^3) \\ n \mathcal{O}(\xi^3) & n + n \mathcal{O}(\xi^3) & \mathcal{O}(\xi^3) & 1 + \mathcal{O}(\xi^3) \end{pmatrix}. \quad (92)$$

766 In this way, we have

$$\begin{aligned} |X^{-1}(\hat{T}) \mathcal{F}_1(\mathcal{U}_0^e(\hat{T}), \mathcal{V}_0^e(\hat{T}))| &\leq |X^{-1}(\hat{T})| |\mathcal{F}_1(\mathcal{U}_0^e(\hat{T}), \mathcal{V}_0^e(\hat{T}))| \\ &\leq \mathcal{M} |\mathcal{F}_1(\mathcal{U}_0^e(\hat{T}), \mathcal{V}_0^e(\hat{T}))| \\ &\leq M \xi^6 \begin{pmatrix} 1/n \\ 1/n \\ 1 \\ 1 \end{pmatrix}. \end{aligned} \quad (93)$$

767 And, therefore, as we have taken $T = 2\pi$:

$$\int_0^T |X^{-1}(\hat{T}) \mathcal{F}_1(\mathcal{U}_0^e(\hat{T}), \mathcal{V}_0^e(\hat{T}))| d\hat{T} \leq M \xi^6 \begin{pmatrix} 1/n \\ 1/n \\ 1 \\ 1 \end{pmatrix}. \quad (94)$$

768 Finally, multiplying by μX we have

$$|\mathcal{H}\{\mathbf{0}\}| \leq M \mu \xi^6 \begin{pmatrix} 1/n \\ 1/n \\ 1 \\ 1 \end{pmatrix}. \quad (95)$$

769 and using the definition of the norm in (77) and renaming $M_1 = M$ we obtain the desired result:

$$\|\mathcal{H}\{\mathbf{0}\}\| \leq M \mu \xi^6. \quad (96)$$

770 B.2 Proof of Lemma 3

771 In order to bound $\mathcal{H}(\mathbf{U}_\oplus) - \mathcal{H}(\mathbf{U}_\ominus)$ (see (75)), first we need to bound $\mathcal{G}(\mathbf{U}_\oplus) - \mathcal{G}(\mathbf{U}_\ominus)$, for $\mathbf{U}_\oplus,$
772 $\mathbf{U}_\ominus \in B_R(\mathbf{0})$, where $R = 2M_1 \mu \xi^6$. In order to ease the computations, let us introduce

$$\mathcal{G}(\mathbf{U}_1) = \mathcal{G}_0(\mathbf{U}_1) + \mathcal{G}_1(\mathbf{U}_1), \quad (97)$$

773 with

$$\begin{aligned} \mathcal{G}_0(\mathbf{U}_1) &= \mathcal{F}_0(\mathcal{U}_0^e(\hat{T}) + \mathbf{U}_1) - \mathcal{F}_0(\mathcal{U}_0^e(\hat{T})) - D\mathcal{F}_0(\mathcal{U}_0^e(\hat{T}))\mathbf{U}_1, \\ \mathcal{G}_1(\mathbf{U}_1) &= \mu \mathcal{F}_1(\mathcal{U}_0^e(\hat{T}) + \mathbf{U}_1, \mathcal{V}_0^e(\hat{T}) + \mathcal{V}_1). \end{aligned} \quad (98)$$

774 We will bound separately the term $\mathcal{G}_0(\mathbf{U}_\oplus) - \mathcal{G}_0(\mathbf{U}_\ominus)$ in Lemma 9 and $\mathcal{G}_1(\mathbf{U}_\oplus) - \mathcal{G}_1(\mathbf{U}_\ominus)$ in Lemma
775 10.

776 **Lemma 9.** Take $\mathbf{u}_\oplus, \mathbf{u}_\ominus \in B_R(\mathbf{0})$. Then for $0 < \xi$ small enough we have that:

$$\|\mathcal{G}_0(\mathbf{u}_\oplus) - \mathcal{G}_0(\mathbf{u}_\ominus)\| \leq \frac{M\mu}{n} \xi^9 \|\mathbf{u}_\oplus - \mathbf{u}_\ominus\|.$$

777 *Proof.* First, we observe that $\mathcal{G}_0(\mathbf{u}) = (\mathcal{G}_0^1, \mathcal{G}_0^2, \mathcal{G}_0^3, \mathcal{G}_0^4)(\mathbf{u}) = (0, 0, \mathcal{G}_0^3, \mathcal{G}_0^4)(\mathbf{u})$. Therefore we will
 778 consider the last two components. We will do the computations for \mathcal{G}_0^3 , the ones for \mathcal{G}_0^4 are analogous.
 779 Using the Mean Value Theorem we have:

$$\begin{aligned} \mathcal{G}_0^3(\mathbf{u}_\oplus) - \mathcal{G}_0^3(\mathbf{u}_\ominus) &= \mathcal{F}_0^3(\mathbf{u}_0 + \mathbf{u}_\oplus) - \mathcal{F}_0^3(\mathbf{u}_0 + \mathbf{u}_\ominus) - D\mathcal{F}_0^3(\mathbf{u}_0)(\mathbf{u}_\oplus - \mathbf{u}_\ominus) \\ &= \int_0^1 [D\mathcal{F}_0^3(\mathbf{u}_0 + s\mathbf{u}_\oplus + (1-s)\mathbf{u}_\ominus)(\mathbf{u}_\oplus - \mathbf{u}_\ominus)] ds - D\mathcal{F}_0^3(\mathbf{u}_0)(\mathbf{u}_\oplus - \mathbf{u}_\ominus) \\ &= \left\{ \int_0^1 [D\mathcal{F}_0^3(\mathbf{u}_0 + s\mathbf{u}_\oplus + (1-s)\mathbf{u}_\ominus) - D\mathcal{F}_0^3(\mathbf{u}_0)] ds \right\} (\mathbf{u}_\oplus - \mathbf{u}_\ominus) \\ &= \left\{ \int_0^1 \int_0^1 (s\mathbf{u}_\oplus + (1-s)\mathbf{u}_\ominus)^t D^2\mathcal{F}_0^3(\mathbf{u}_0 + z[s\mathbf{u}_\oplus + (1-s)\mathbf{u}_\ominus]) dz ds \right\} (\mathbf{u}_\oplus - \mathbf{u}_\ominus). \end{aligned} \tag{99}$$

780 Now we want to bound the expression appearing in the previous double integral. Notice that $D^2\mathcal{F}_0^3$
 781 (see (57)) is given by:

$$D^2\mathcal{F}_0^3 = \begin{pmatrix} 16 [\dot{\nu} + 3(5\mathcal{U}^2 + 3\mathcal{V}^2)\mathcal{U}\xi^3] \xi^3 & 48(3\mathcal{U}^2 + \mathcal{V}^2)\mathcal{V}\xi^6 & 0 & 16\mathcal{U}\xi^3 \\ 48(3\mathcal{U}^2 + \mathcal{V}^2)\mathcal{V}\xi^6 & 16 [\dot{\nu} + 3(\mathcal{U}^2 + 3\mathcal{V}^2)\mathcal{U}\xi^3] \xi^3 & 0 & 16\mathcal{V}\xi^3 \\ 0 & 0 & 0 & 0 \\ 16\mathcal{U}\xi^3 & 16\mathcal{V}\xi^3 & 0 & 0 \end{pmatrix},$$

782 and thus, as (see (69)):

$$|\mathcal{U}_0^e| \leq 1, |\mathcal{V}_0^e| \leq 1, |\dot{\mathcal{U}}_0^e| \leq n, |\dot{\mathcal{V}}_0^e| \leq n, \quad \|\mathbf{u}_\otimes\| \leq 2M_1\mu\xi^6,$$

783 we have that:

$$|D^2\mathcal{F}_0^3(\mathbf{u}_0^e + \mathbf{u}_\otimes)| \leq M\xi^3 \begin{pmatrix} n & \xi^3 & 0 & 1 \\ \xi^3 & n & 0 & 1 \\ 0 & 0 & 0 & 0 \\ 1 & 1 & 0 & 0 \end{pmatrix}. \tag{100}$$

784 Now, as $\|\mathbf{u}_\ominus\| \leq 2M_1\mu\xi^6$:

$$\begin{aligned} |\mathbf{u}_\ominus^t D^2\mathcal{F}_0^3(\mathbf{u}_0^e + \mathbf{u}_\otimes)| &\leq |\mathbf{u}_\ominus^t| |D^2\mathcal{F}_0^3(\mathbf{u}_0^e + \mathbf{u}_\otimes)| \\ &\leq 2M_1\mu\xi^6 (1/n, 1/n, 1, 1) M\xi^3 \begin{pmatrix} n & \xi^3 & 0 & 1 \\ \xi^3 & n & 0 & 1 \\ 0 & 0 & 0 & 0 \\ 1 & 1 & 0 & 0 \end{pmatrix} \\ &\leq 2MM_1\mu\xi^9 (1, 1, 0, 1/n). \end{aligned} \tag{101}$$

785 Taking into account the integral expression in (99) we obtain

$$|\mathcal{G}_0^3(\mathbf{u}_\oplus) - \mathcal{G}_0^3(\mathbf{u}_\ominus)| \leq 2MM_1\mu\xi^9 (1, 1, 0, 1/n) \|\mathbf{u}_\oplus - \mathbf{u}_\ominus\| \leq \frac{1}{n} 2MM_1\mu\xi^9 \|\mathbf{u}_\oplus - \mathbf{u}_\ominus\|.$$

786 We get a similar bound for the fourth components and using that the first and the second are identically
 787 zero and the definition of the norm we get the result of the lemma. \square

788 The next goal is to bound $\mathcal{G}_1(\mathbf{u}_\oplus) - \mathcal{G}_1(\mathbf{u}_\ominus)$. To do so, we apply the same trick:

789 **Lemma 10.** Given $\mathbf{u}_\oplus, \mathbf{u}_\ominus \in B_R(\mathbf{0})$. Then for $\xi > 0$ small enough we have that

$$\|\mathcal{G}_1(\mathbf{u}_\oplus) - \mathcal{G}_1(\mathbf{u}_\ominus)\| \leq \frac{M\mu\xi^6}{n} \|\mathbf{u}_\oplus - \mathbf{u}_\ominus\|.$$

790 *Proof.* Using again the Main Value Theorem we obtain:

$$\mathcal{G}_1(\mathbf{u}_\oplus) - \mathcal{G}_1(\mathbf{u}_\ominus) = \int_0^1 D\mathcal{G}_1(s\mathbf{u}_\oplus + (1-s)\mathbf{u}_\ominus) (\mathbf{u}_\oplus - \mathbf{u}_\ominus) ds. \quad (102)$$

791 So we only need to bound $|D\mathcal{G}_1(\mathbf{u}_\ominus)|$ where $\mathbf{u}_\ominus \in B_R(\mathbf{0})$, $= 2M_1\mu\xi^6$

792 Let us recall that

$$D\mathcal{G}_1(\mathbf{u}_\ominus) = \mu D\mathcal{F}_1(\mathcal{U}_0^e + \mathcal{U}_\ominus, \mathcal{V}_0^e + \mathcal{V}_\ominus),$$

793 and \mathcal{F}_1 is given in (57). Proceeding similarly as to bound \mathcal{F}_1 we can differentiate (89) to obtain:

$$\begin{aligned} D\mathcal{F}_1(\mathcal{U}, \mathcal{V}) &= \begin{pmatrix} 0 & 0 & 0 & 0 \\ 0 & 0 & 0 & 0 \\ 24(5\mathcal{U}^4 - 6\mathcal{U}^2\mathcal{V}^2 - \mathcal{V}^4)\xi^6 + \frac{1}{n^{2/3}}\mathcal{O}(\xi^8) & -96(\mathcal{U}^2 + \mathcal{V}^2)\mathcal{U}\mathcal{V}\xi^6 + \frac{1}{n^{2/3}}\mathcal{O}(\xi^8) & 0 & 0 \\ -96(\mathcal{U}^2 + \mathcal{V}^2)\mathcal{U}\mathcal{V}\xi^6 + \frac{1}{n^{2/3}}\mathcal{O}(\xi^8) & 24(5\mathcal{V}^4 - 6\mathcal{U}^2\mathcal{V}^2 - \mathcal{U}^4)\xi^6 + \frac{1}{n^{2/3}}\mathcal{O}(\xi^8) & 0 & 0 \end{pmatrix} \\ &= 24\xi^6 \begin{pmatrix} 0 & 0 & 0 & 0 \\ 0 & 0 & 0 & 0 \\ 5\mathcal{U}^4 - 6\mathcal{U}^2\mathcal{V}^2 - \mathcal{V}^4 + \frac{1}{n^{2/3}}\mathcal{O}(\xi^2) & -4(\mathcal{U}^2 + \mathcal{V}^2)\mathcal{U}\mathcal{V} + \frac{1}{n^{2/3}}\mathcal{O}(\xi^2) & 0 & 0 \\ -4(\mathcal{U}^2 + \mathcal{V}^2)\mathcal{U}\mathcal{V} + \frac{1}{n^{2/3}}\mathcal{O}(\xi^2) & 5\mathcal{V}^4 - 6\mathcal{U}^2\mathcal{V}^2 - \mathcal{U}^4 + \frac{1}{n^{2/3}}\mathcal{O}(\xi^2) & 0 & 0 \end{pmatrix}. \end{aligned}$$

794 So, using again that (see (69)):

$$|\mathcal{U}_0^e| \leq 1, |\mathcal{V}_0^e| \leq 1, \quad \|\mathbf{u}_\ominus\| \leq 2M_1\mu\xi^6,$$

795

$$|D\mathcal{F}_1(\mathcal{U}_0^e + \mathcal{U}_\ominus, \mathcal{V}_0^e + \mathcal{V}_\ominus)| \leq [120\xi^6 + \frac{1}{n^{2/3}}\mathcal{O}(\xi^8)] \begin{pmatrix} 0 & 0 & 0 & 0 \\ 0 & 0 & 0 & 0 \\ 1 & 1 & 0 & 0 \\ 1 & 1 & 0 & 0 \end{pmatrix},$$

796 and therefore

$$|D\mathcal{G}_1(\mathbf{u}_\ominus)| \leq M\mu\xi^6 \begin{pmatrix} 0 & 0 & 0 & 0 \\ 0 & 0 & 0 & 0 \\ 1 & 1 & 0 & 0 \\ 1 & 1 & 0 & 0 \end{pmatrix}.$$

797 And using the integral equation (102) and the fact that the first two rows of the previous matrix are

798 zero we get:

$$|\mathcal{G}_1(\mathbf{u}_\oplus) - \mathcal{G}_1(\mathbf{u}_\ominus)| \leq M\mu\xi^6 \begin{pmatrix} 0 \\ 0 \\ |\mathbf{u}_\oplus - \mathbf{v}_\oplus| \\ |\mathbf{u}_\oplus - \mathbf{v}_\oplus| \end{pmatrix} \leq \frac{M\mu\xi^6}{n} \|\mathbf{u}_\oplus - \mathbf{u}_\ominus\| \begin{pmatrix} 0 \\ 0 \\ 1 \\ 1 \end{pmatrix}.$$

799 Now, using the definition of the norm we get the result.

800

□

801 From the results of lemmas 9 and 10 we have:

$$\|\mathcal{G}(\mathbf{u}_\oplus) - \mathcal{G}(\mathbf{u}_\ominus)\| \leq \frac{M\mu\xi^6}{n} \|\mathbf{u}_\oplus - \mathbf{u}_\ominus\|.$$

802 Now, proceeding as we did in the proof of Lemma 2, we multiply $\mathcal{G}(\mathbf{u}_\oplus) - \mathcal{G}(\mathbf{u}_\ominus)$ by X^{-1} , integrate
803 for a finite time and multiply the resulting expression by X . We use that $|X| \leq \mathcal{M}$ and $|X^{-1}| \leq \mathcal{M}$
804 where \mathcal{M} is given in (92) and proceed to bound the expression which gives $\mathcal{H}\{\mathbf{u}_\oplus\} - \mathcal{H}\{\mathbf{u}_\ominus\}$ as we
805 did for $\mathcal{H}\{\mathbf{0}\}$ in (93), (94), (95), (96), to obtain

$$\|\mathcal{H}\{\mathbf{u}_\oplus\} - \mathcal{H}\{\mathbf{u}_\ominus\}\| \leq M_2\mu\xi^6 \|\mathbf{u}_\oplus - \mathbf{u}_\ominus\|. \quad (103)$$

806 This finishes the proof of Lemma 3.

807 B.3 Proof of Lemma 5

808 In order to compute $\mathcal{H}\{\mathbf{0}\}(\hat{\mathcal{T}}_0^*)$ let us recall its expression:

$$\mathcal{H}\{\mathbf{0}\}(\hat{\mathcal{T}}_0^*) = X(\hat{\mathcal{T}}_0^*) \int_0^{\hat{\mathcal{T}}_0^*} X^{-1}(\hat{\mathcal{T}}) \mathcal{G}(\mathbf{0}) d\hat{\mathcal{T}} = \mu X(\hat{\mathcal{T}}_0^*) \int_0^{\hat{\mathcal{T}}_0^*} X^{-1}(\hat{\mathcal{T}}) \mathcal{F}_1(\mathbf{u}_0^e(\hat{\mathcal{T}})) d\hat{\mathcal{T}}.$$

809 From (90), substituting (69) we have

$$\mathcal{F}_1(\mathbf{u}_0^e, \mathbf{v}_0^e) = \begin{pmatrix} 0 \\ 0 \\ 24 \sin^5(n\hat{\mathcal{T}}) \cos \theta_0 (2 \cos^4 \theta_0 - 1) \xi^6 + \mathcal{O}(\xi^8) \\ 24 \sin^5(n\hat{\mathcal{T}}) \sin \theta_0 (2 \sin^4 \theta_0 - 1) \xi^6 + \mathcal{O}(\xi^8) \end{pmatrix}, \quad (104)$$

810 Multiplying (104) by X^{-1} using the expression provided in Lemma 8 we obtain:

$$X^{-1} \mathcal{F}_1(\mathbf{u}_0^e, \mathbf{v}_0^e) = \begin{pmatrix} -\frac{24 \sin^6(n\hat{\mathcal{T}}) \cos \theta_0 (2 \cos^4 \theta_0 - 1)}{n} \xi^6 + \frac{1}{n} \mathcal{O}(\xi^8) \\ -\frac{24 \sin^6(n\hat{\mathcal{T}}) \sin \theta_0 (2 \sin^4 \theta_0 - 1)}{n} \xi^6 + \frac{1}{n} \mathcal{O}(\xi^8) \\ 24 \cos(n\hat{\mathcal{T}}) \sin^5(n\hat{\mathcal{T}}) \cos \theta_0 (2 \cos^4 \theta_0 - 1) \xi^6 + \mathcal{O}(\xi^8) \\ 24 \cos(n\hat{\mathcal{T}}) \sin^5(n\hat{\mathcal{T}}) \sin \theta_0 (2 \sin^4 \theta_0 - 1) \xi^6 + \mathcal{O}(\xi^8) \end{pmatrix}.$$

811 Finally, integrating and multiplying by μX using the expression of X provided in Lemma 8 we have:

$$\mathcal{H}_1\{\mathbf{0}\} = -\frac{\mu \cos \theta_0 (2 \cos^4 \theta_0 - 1) (60n\hat{\mathcal{T}} - 16 \sin(2n\hat{\mathcal{T}}) + \sin(4n\hat{\mathcal{T}})) \cos(n\hat{\mathcal{T}})}{8n^2} + \frac{\mu}{n} \mathcal{O}(\xi^8),$$

$$\mathcal{H}_2\{\mathbf{0}\} = -\frac{\mu \sin \theta_0 (2 \sin^4 \theta_0 - 1) (60n\hat{\mathcal{T}} - 16 \sin(2n\hat{\mathcal{T}}) + \sin(4n\hat{\mathcal{T}})) \cos(n\hat{\mathcal{T}})}{8n^2} + \frac{\mu}{n} \mathcal{O}(\xi^8).$$

812 Note that the values of $\mathcal{H}_3\{\mathbf{0}\}$ and $\mathcal{H}_4\{\mathbf{0}\}$ can be obtained directly by differentiating $\mathcal{H}_1\{\mathbf{0}\}$ and
813 $\mathcal{H}_2\{\mathbf{0}\}$ respectively. This finishes the proof of Lemma 5.

814 C Value of the auxiliary matrix A^e

The values of the terms $(A_{i,j}^e)$ are given by

$$A_{11}^e = \cos(n\hat{\mathcal{T}}) - \sin(2\theta_0) \left[\hat{\mathcal{T}} \cos(n\hat{\mathcal{T}}) - \sin(n\hat{\mathcal{T}}) \frac{1 + \sin^2(n\hat{\mathcal{T}})}{n} \right] \xi^3$$

$$\begin{aligned}
& + \frac{2 \sin^2 \theta_0}{n} \left[\hat{\mathcal{T}} \left(1 + 2 \cos^2(n\hat{\mathcal{T}}) \right) - \frac{3 \cos(n\hat{\mathcal{T}}) \sin(n\hat{\mathcal{T}})}{n} \right] \sin(n\hat{\mathcal{T}}) \xi^6, \\
A_{12}^e &= 2 \left[\cos^2 \theta_0 \hat{\mathcal{T}} \cos(n\hat{\mathcal{T}}) - \frac{\sin(n\hat{\mathcal{T}}) \left(\cos^2 \theta_0 - \sin^2 \theta_0 \sin^2(n\hat{\mathcal{T}}) \right)}{n} \right] \xi^3 \\
& - \frac{\sin(2\theta_0)}{n} \left[\hat{\mathcal{T}} \left(1 + 2 \cos^2(n\hat{\mathcal{T}}) \right) - \frac{3 \cos(n\hat{\mathcal{T}}) \sin(n\hat{\mathcal{T}})}{n} \right] \sin(n\hat{\mathcal{T}}) \xi^6, \\
A_{13}^e &= \frac{\sin(n\hat{\mathcal{T}})}{n} + \frac{2 \sin^2 \theta_0}{n} \left[\hat{\mathcal{T}} - \frac{\cos(n\hat{\mathcal{T}}) \sin(n\hat{\mathcal{T}})}{n} \right] \sin(n\hat{\mathcal{T}}) \xi^3, \\
A_{14}^e &= \frac{\sin(2\theta_0)}{n} \left[\hat{\mathcal{T}} - \frac{\cos(n\hat{\mathcal{T}}) \sin(n\hat{\mathcal{T}})}{n} \right] \sin(n\hat{\mathcal{T}}) \xi^3, \\
A_{21}^e &= -2 \left[\sin^2 \theta_0 \hat{\mathcal{T}} \cos(n\hat{\mathcal{T}}) + \frac{\sin(n\hat{\mathcal{T}}) \left(\sin^2 \theta_0 - \cos^2 \theta_0 \sin^2(n\hat{\mathcal{T}}) \right)}{n} \right] \xi^3 \\
& - \frac{\sin(2\theta_0)}{n} \left[\hat{\mathcal{T}} \left(1 + 2 \cos^2(n\hat{\mathcal{T}}) \right) - \frac{3 \cos(n\hat{\mathcal{T}}) \sin(n\hat{\mathcal{T}})}{n} \right] \sin(n\hat{\mathcal{T}}) \xi^6, \\
A_{22}^e &= \cos(n\hat{\mathcal{T}}) + \sin(2\theta_0) \left[\hat{\mathcal{T}} \cos(n\hat{\mathcal{T}}) - \sin(n\hat{\mathcal{T}}) \frac{1 + \sin^2(n\hat{\mathcal{T}})}{n} \right] \xi^3 \\
& + \frac{2 \cos^2 \theta_0}{n} \left[\hat{\mathcal{T}} \left(1 + 2 \cos^2(n\hat{\mathcal{T}}) \right) - \frac{3 \cos(n\hat{\mathcal{T}}) \sin(n\hat{\mathcal{T}})}{n} \right] \sin(n\hat{\mathcal{T}}) \xi^6, \\
A_{23}^e &= -\frac{2 \cos^2 \theta_0}{n} \left[\hat{\mathcal{T}} - \frac{\cos(n\hat{\mathcal{T}}) \sin(n\hat{\mathcal{T}})}{n} \right] \sin(n\hat{\mathcal{T}}) \xi^3, \\
A_{24}^e &= \frac{\sin(n\hat{\mathcal{T}})}{n} - \frac{\sin(2\theta_0)}{n} \left[\hat{\mathcal{T}} - \frac{\cos(n\hat{\mathcal{T}}) \sin(n\hat{\mathcal{T}})}{n} \right] \sin(n\hat{\mathcal{T}}) \xi^3, \\
A_{31}^e &= -n \sin(n\hat{\mathcal{T}}) + \sin(2\theta_0) \sin(n\hat{\mathcal{T}}) \left(n\hat{\mathcal{T}} + 3 \cos(n\hat{\mathcal{T}}) \sin(n\hat{\mathcal{T}}) \right) \xi^3 \\
& + 2 \left[\sin^2 \theta_0 \hat{\mathcal{T}} \left(5 - 8 \cos^2(n\hat{\mathcal{T}}) \right) \cos(n\hat{\mathcal{T}}) \right. \\
& \quad \left. - \frac{\sin(n\hat{\mathcal{T}})}{n} \left(\cos^2 \theta_0 \left(8 - 13 \cos^2(n\hat{\mathcal{T}}) + 2 \cos^4(n\hat{\mathcal{T}}) \right) + 9 \cos^2(n\hat{\mathcal{T}}) - 6 \right) \right] \xi^6 \\
& - \frac{2 \sin(2\theta_0)}{n} \left[\hat{\mathcal{T}} \left(1 + 2 \cos^2(n\hat{\mathcal{T}}) \right) - \frac{3 \cos(n\hat{\mathcal{T}}) \sin(n\hat{\mathcal{T}})}{n} \right] \sin^3(n\hat{\mathcal{T}}) \xi^9,
\end{aligned}$$

$$\begin{aligned}
A_{32}^e &= -2 \left[n \cos^2 \theta_0 \hat{\mathcal{T}} - (1 + 3 \sin^2 \theta_0) \cos(n\hat{\mathcal{T}}) \sin(n\hat{\mathcal{T}}) \right] \sin(n\hat{\mathcal{T}}) \xi^3 \\
&\quad + \sin(2\theta_0) \left[\hat{\mathcal{T}} \left(5 - 8 \cos^2(n\hat{\mathcal{T}}) \right) - \frac{8 - 13 \cos^2(n\hat{\mathcal{T}}) + 2 \cos^4(n\hat{\mathcal{T}})}{n} \sin(n\hat{\mathcal{T}}) \right] \xi^6 \\
&\quad + \frac{4 \cos^2 \theta_0}{n} \left[\hat{\mathcal{T}} \left(1 + 2 \cos^2(n\hat{\mathcal{T}}) \right) - \frac{3 \cos(n\hat{\mathcal{T}}) \sin(n\hat{\mathcal{T}})}{n} \right] \sin^3(n\hat{\mathcal{T}}) \xi^9,
\end{aligned}$$

$$\begin{aligned}
A_{33}^e &= \cos(n\hat{\mathcal{T}}) + \sin(2\theta_0) \left[\hat{\mathcal{T}} \cos(n\hat{\mathcal{T}}) + \frac{2 - 3 \cos^2(n\hat{\mathcal{T}})}{n} \sin(n\hat{\mathcal{T}}) \right] \xi^3 \\
&\quad - \frac{4 \cos^2 \theta_0}{n} \left[\hat{\mathcal{T}} - \frac{\cos(n\hat{\mathcal{T}}) \sin(n\hat{\mathcal{T}})}{n} \right] \sin^3(n\hat{\mathcal{T}}) \xi^6,
\end{aligned}$$

$$\begin{aligned}
A_{34}^e &= 2 \left[\sin^2 \theta_0 \left(\hat{\mathcal{T}} - \frac{\cos(n\hat{\mathcal{T}}) \sin(n\hat{\mathcal{T}})}{n} \right) \cos(n\hat{\mathcal{T}}) + \frac{2 \sin^2 \theta_0 + 1}{n} \sin^3(n\hat{\mathcal{T}}) \right] \xi^3 \\
&\quad - \frac{2 \sin(2\theta_0)}{n} \left[\hat{\mathcal{T}} - \frac{\cos(n\hat{\mathcal{T}}) \sin(n\hat{\mathcal{T}})}{n} \right] \sin^3(n\hat{\mathcal{T}}) \xi^6,
\end{aligned}$$

$$\begin{aligned}
A_{41}^e &= 2 \left[n \sin^2 \theta_0 \hat{\mathcal{T}} - (1 + 3 \cos^2 \theta_0) \cos(n\hat{\mathcal{T}}) \sin(n\hat{\mathcal{T}}) \right] \sin(n\hat{\mathcal{T}}) \xi^3 \\
&\quad + \sin(2\theta_0) \left[\hat{\mathcal{T}} \left(5 - 8 \cos^2(n\hat{\mathcal{T}}) \right) - \frac{8 - 13 \cos^2(n\hat{\mathcal{T}}) + 2 \cos^4(n\hat{\mathcal{T}})}{n} \sin(n\hat{\mathcal{T}}) \right] \xi^6 \\
&\quad - \frac{4 \sin^2 \theta_0}{n} \left[\hat{\mathcal{T}} \left(1 + 2 \cos^2(n\hat{\mathcal{T}}) \right) - \frac{3 \cos(n\hat{\mathcal{T}}) \sin(n\hat{\mathcal{T}})}{n} \right] \sin^3(n\hat{\mathcal{T}}) \xi^9,
\end{aligned}$$

$$\begin{aligned}
A_{42}^e &= -n \sin(n\hat{\mathcal{T}}) - \sin(2\theta_0) \sin(n\hat{\mathcal{T}}) \left(n\hat{\mathcal{T}} + 3 \cos(n\hat{\mathcal{T}}) \sin(n\hat{\mathcal{T}}) \right) \xi^3 \\
&\quad + 2 \left[-\cos^2 \theta_0 \hat{\mathcal{T}} \left(5 - 8 \cos^2(n\hat{\mathcal{T}}) \right) \cos(n\hat{\mathcal{T}}) \right. \\
&\quad \quad \left. - \frac{\sin(n\hat{\mathcal{T}})}{n} \left(\sin^2 \theta_0 \left(8 - 13 \cos^2(n\hat{\mathcal{T}}) + 2 \cos^4(n\hat{\mathcal{T}}) \right) + 9 \cos^2(n\hat{\mathcal{T}}) - 6 \right) \right] \xi^6 \\
&\quad + \frac{2 \sin(2\theta_0)}{n} \left[\hat{\mathcal{T}} \left(1 + 2 \cos^2(n\hat{\mathcal{T}}) \right) - \frac{3 \cos(n\hat{\mathcal{T}}) \sin(n\hat{\mathcal{T}})}{n} \right] \sin^3(n\hat{\mathcal{T}}) \xi^9,
\end{aligned}$$

$$\begin{aligned}
A_{43}^e &= -2 \left[\cos^2 \theta_0 \left(\hat{\mathcal{T}} - \frac{\cos(n\hat{\mathcal{T}}) \sin(n\hat{\mathcal{T}})}{n} \right) \cos(n\hat{\mathcal{T}}) + \frac{2 \cos^2 \theta_0 + 1}{n} \sin^3(n\hat{\mathcal{T}}) \right] \xi^3 \\
&\quad - \frac{2 \sin(2\theta_0)}{n} \left[\hat{\mathcal{T}} - \frac{\cos(n\hat{\mathcal{T}}) \sin(n\hat{\mathcal{T}})}{n} \right] \sin^3(n\hat{\mathcal{T}}) \xi^6,
\end{aligned}$$

$$\begin{aligned}
A_{44}^e &= \cos(n\hat{\mathcal{T}}) - \sin(2\theta_0) \left[\hat{\mathcal{T}} \cos(n\hat{\mathcal{T}}) + \frac{2 - 3 \cos^2(n\hat{\mathcal{T}})}{n} \sin(n\hat{\mathcal{T}}) \right] \xi^3 \\
&\quad - \frac{4 \sin^2 \theta_0}{n} \left[\hat{\mathcal{T}} - \frac{\cos(n\hat{\mathcal{T}}) \sin(n\hat{\mathcal{T}})}{n} \right] \sin^3(n\hat{\mathcal{T}}) \xi^6.
\end{aligned}$$